

Highlights of the **COOL05** Conference

K.Beard, TJNAF

with support from

Muons, Inc.



Thomas Jefferson National Accelerator Facility



<http://conferences.fnal.gov/cool05/Presentations/>



Topics

- overview
- stochastic cooling
- muon cooling
- electrostatic rings
- low energy electron cooling
- high energy electron cooling
- laser cooling



Thomas Jefferson National Accelerator Facility



Overviews



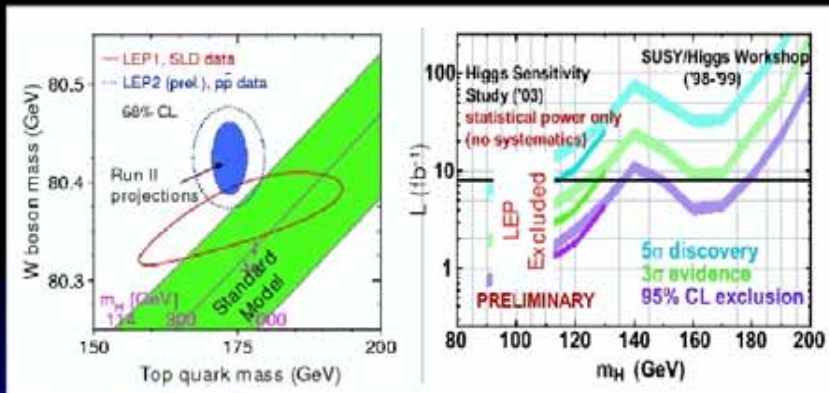
Thomas Jefferson National Accelerator Facility



M01 general introduction

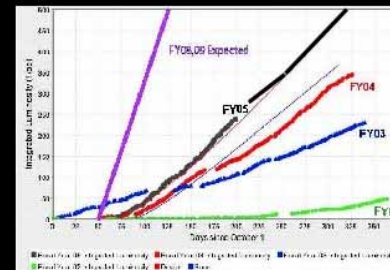
It's tough to make predictions,
especially about the future. - *Yogi Berra*

Closing in on the the SM Higgs

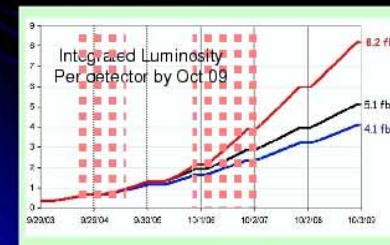


- Sensitivity to low mass Higgs, or
- Severely constrain mass

Tevatron: key is luminosity



Luminosity history
for each fiscal year



Integrated luminosity
for different assumptions

Top Line: all run II upgrades work

Bottom line: none work

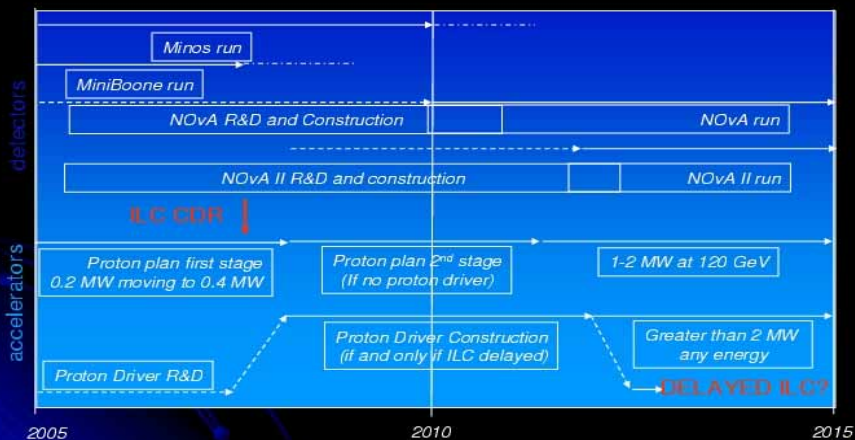
(pink/white bands show the
doubling times for the top line)



Thomas Jefferson National Accelerator Facility



Neutrino Program (delayed ILC)



Strategic context: U.S. contribution

Domestic accelerator program with new and redirected investment



= leading

X = secondary

Neutrino
Frontier

Flavor
frontier

Energy
Frontier

2015



2010



2005



10



Thomas Jefferson National Accelerator Facility



Operated by the Southeastern Universities Research Association for the U.S. Department of Energy

M02 Einstein

A.Sessler,
LBNL



"The state has become a modern idol whose suggestive power few men are able to escape."

~~"If we knew what we are~~

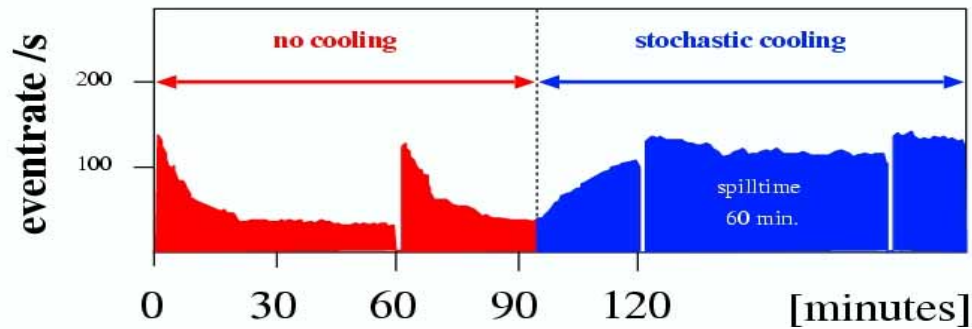
doing it would not be called research, would it?"



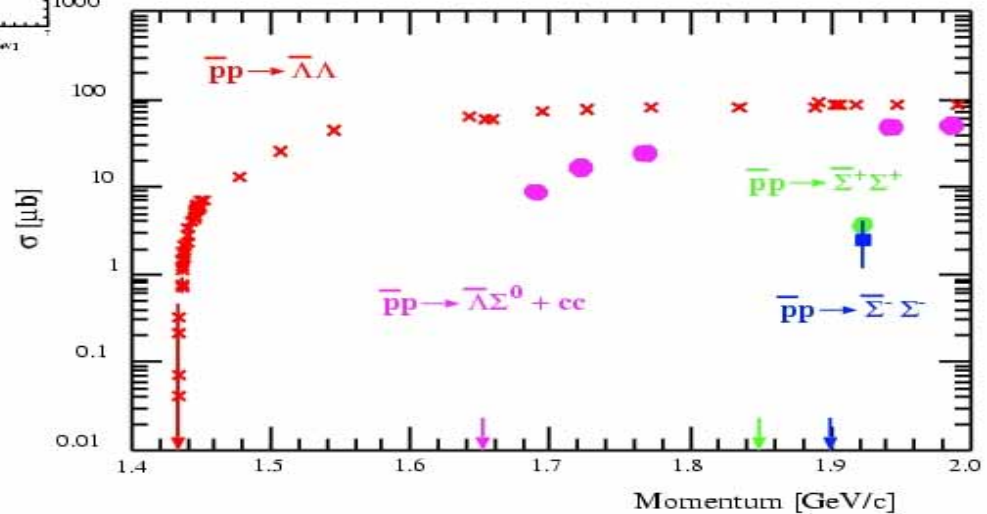
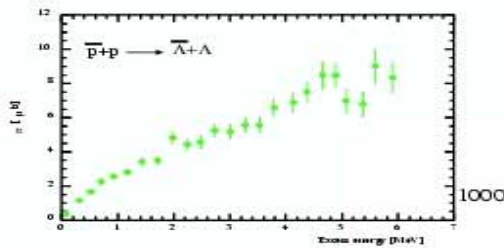
Thomas Jefferson National Accelerator Facility



M03 Why cool?

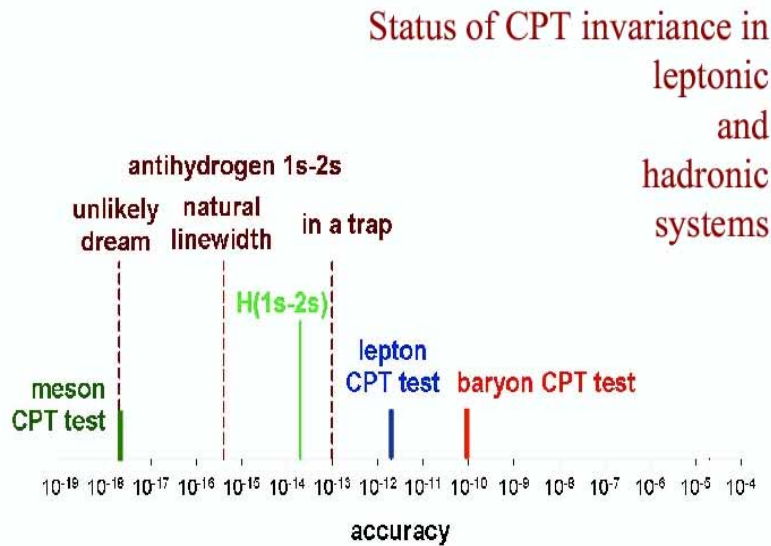


W.Oelert, FZI

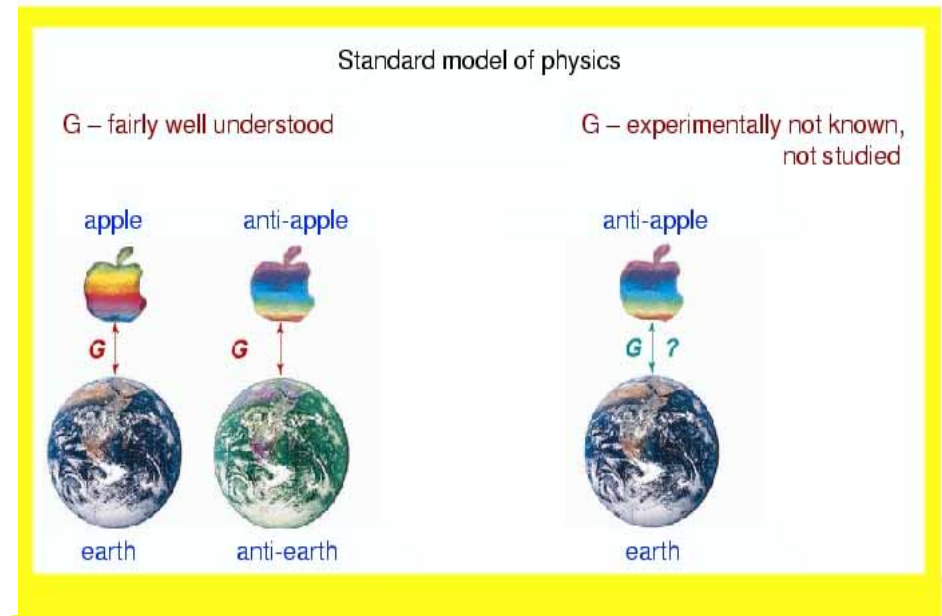


antihydrogen

W.Oelert, FZI, *cont.*



$$\frac{R_\infty[\bar{H}]}{R_\infty[H]} = \frac{m[e^+](\frac{q[e^+]}{q[e^-]})^2}{m[e^-](\frac{q[e^-]}{q[e^+]})^2} \left(\frac{q[\bar{p}]}{q[p]} \right)^2 \frac{1+m[e^+]/M[\bar{p}]}{1+m[e^-]/M[p]}$$



Overview of recent trends in beam cooling methods and technology

Igor Meshkov and Dieter Möhl
(JINR, Dubna) (CERN, Geneva)

Menu

1. Introduction: What's new since COOL'03 ?
2. Cooling by electrons
3. Stochastic cooling
4. Stability of electron cooled beams
5. Theory and numerical simulations
6. Muon cooling
7. Beam Ordering
- Conclusion



Trends in beam cooling

COOL'05

D. Möhl, I. Meshkov

September 2005 Galena, IL, USA



1

1. Introduction: What's new since COOL'03 ?

Demonstration of the first electron cooling at intermediate energy :
8 GeV antiprotons in the FERMILAB recycler! **CONGRATULATIONS!**

Commissioning of three state-of-the-art low energy electron coolers
(LANZHOU & LEIR) built in Budker INP.

Commissioning of LEPTA at JINR (Dubna) \Rightarrow under way to e-cooling
of positrons and e-cooling with circulating electron beam.

Construction of a special "dispersionless" ring for laser cooling/beam
ordering started (Kyoto University).

International effort and great **progress** in the conception,

1. Introduction: What's new since COOL'03 ?

Approval of Muon Ionisation Cooling Experiment (**MICE**) at Rutherford
Appleton Lab.

Start of elaboration of International **FAIR** project at GSI, where
cooling methods will play a key role.

New proposals for very small aperture
machines for m (applications).

The hot news in brief



Bad news: Shutdowns of CELSIUS and CRYRING.



Good news: CRYRING will be used as a cooler storage ring
in FLAIR - subproject of FAIR.



Trends in beam cooling

COOL'05

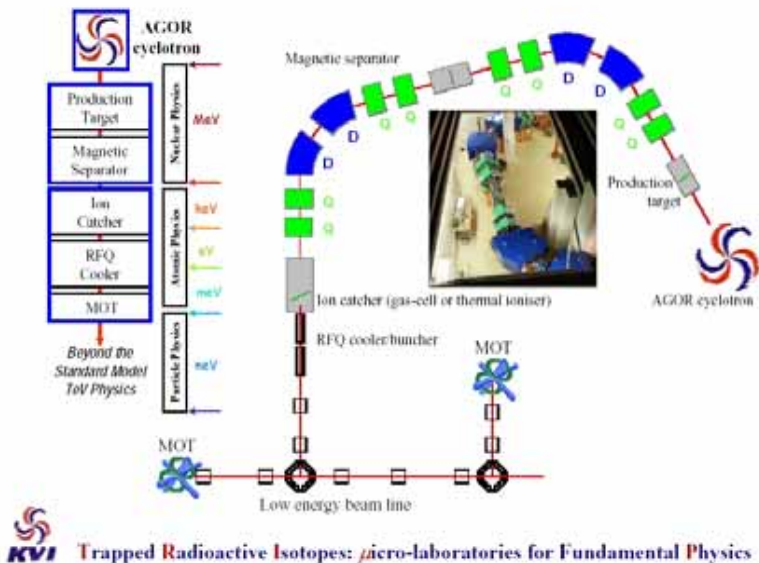
D. Möhl, I. Meshkov

September 2005 Galena, IL, USA



Thomas Jefferson N

F06 RFQ cooler/buncher for TRImP L.Willmann KVI

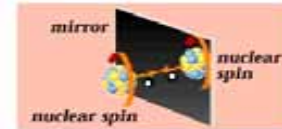


Experimental Program of **TRI μ P** group

Investigating discrete symmetry violations *C, P, and T*.

• Origin of Parity Violation in Weak Interactions

- ⇒ details of β -decays
Na, Ne isotopes



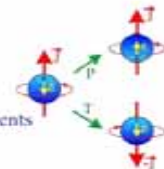
• Dominance of Matter over Antimatter



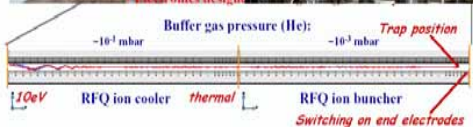
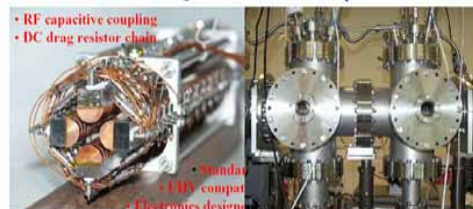
CP - Violation
Time Reversal Symmetry
Parity Violation

⇒ permanent electric dipole moments

Ra isotopes

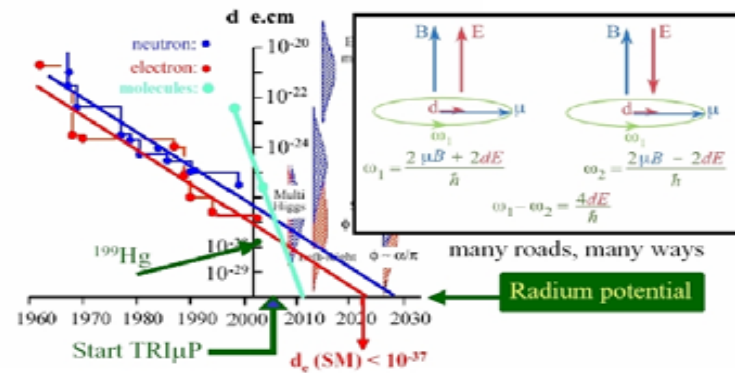


Our RFQ cooler/buncher concept



KVI Trapped Radioactive Isotopes: μ icro-laboratories for Fundamental Physics

The race for a nonzero EDM...



M05 Future Directions

D.Sutter, DOE (retired)

Where Next? – What are the Real Physics Needs?

Proposed but Not Approved The realm of Near Term and Some Mid Term R&D

<u>Facility</u>	<u>Status</u>	<u>Issues</u>
ILC @ .5 to 1 TeV	R&D – GDE In place.	Location! Politics!
Super \square Beams @ Fermi	R&D – Hope!	Funding, Timing & the ILC
CLIC @ 2 to 4 TeV	R&D – A Prayer	The ILC, Energy needs of
HEP		
Japanese Super \square	Unclear	ILC in Japan?

Wish You Were Here! The realm of Advanced & Some Mid Term R&D

<u>Facility</u>	<u>Status</u>	<u>Issues</u>
Muon Storage Ring et al	R&D - Targets & Cooling	Funding & HEP priority
LHC Upgrades – L and E \square	R&D – LARP (In U.S.)	Priority versus LHC Start
Linear Collider @ >100 MeV/m	U.S. High Gradient R&D	Funding & HEP priority
VLHC	No Activity	LHC & ILC in U.S.
“Other” Facilities	No Activity	Unidentified Physics needs!

Facilities Available for HEP Research

Fermilab Tevatron	Shut down in 2008 – 2010?
Fermilab Neutrino Beam	Upgrades? In --- ?
SLAC B-factory	Shut down in 2008
SLAC 50 GeV linac	Off in 2006. LCLS { 10 GeV }, SABER @ 30 GeV > 2008?
KEK B-factory	Upgrade to Super B?
RHIC	Shut down or continue? { NSAC Study! }
LHC	First operation in 2007 – 2008



Thomas Jefferson National Accelerator Facility



Advanced R&D – To give Access to New Research Ability

The Principal Thrusts:

- Plasma Accelerators – Particle and laser driven
- Very high gradient structures – for warm and cold radio frequency systems
- Beam Cooling – beyond stochastic and radiation means
- Space charge dominated Beams – There is life after $\square \square < \square$!
- Super conducting Magnets – The future is A15 & other compounds {Nb₃Sn, MgB₂}
- Accelerator Theory – Advanced simulation & the merging of particle & plasma physics

The above areas of R&D are by no means the only ones supported by the DOE And NSF. They are the principal ones addressing new approaches to facilities.

There is a lot of R&D in our Future!

PBW SMLWA RF Structures:
A IFEL SC, Warm LWFA
Come Join the Fun
Think Out of the Box!



Uncertainty isn't just a physics principle!



We start the ILC when?



muon cooling

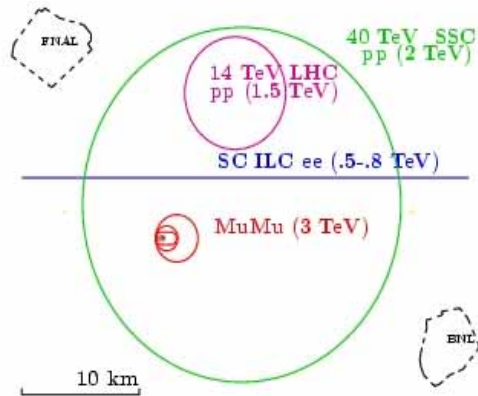


Thomas Jefferson National Accelerator Facility



Review of Muon Cooling R.Palmer BNL

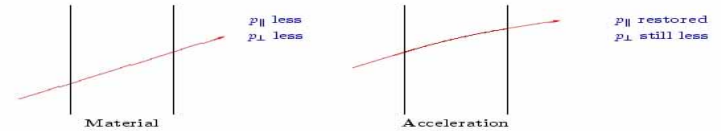
Why a Muon Collider



- Muons are point like, similar to electrons
- Can probe the same physics, and some more
- But have 40,000 less radiation
- So Muon Colliders can be much smaller than Linear Colliders

2

Transverse Cooling



Rate of Cooling without scattering

$$\frac{d\epsilon}{\epsilon_{x,y}} = \frac{dp}{p} J_{x,y}$$

For the moment the "partition functions" **Explanation later**

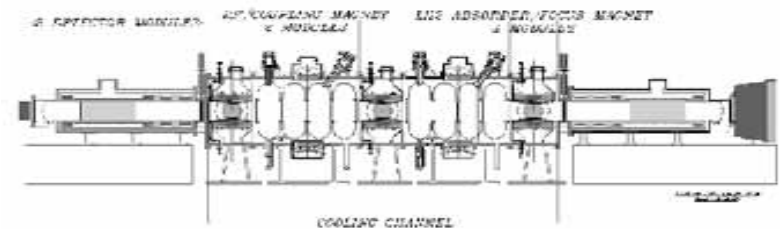
$$J_{x,y} = 1$$

•

SFOFO used in Study 2 and Cooling Experiment

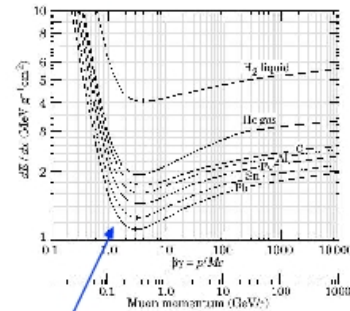
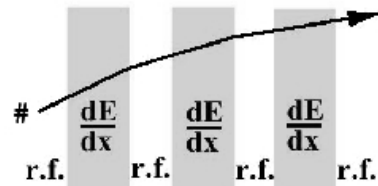
Muon Ionization Cooling Experiment MICE

- International Collaboration: (US, Europe, Japan)
- Proposal Approved at RAL
- Funding for phase I NSF (NSF, DOE, Europe, Japan)



47

Ionization Cooling

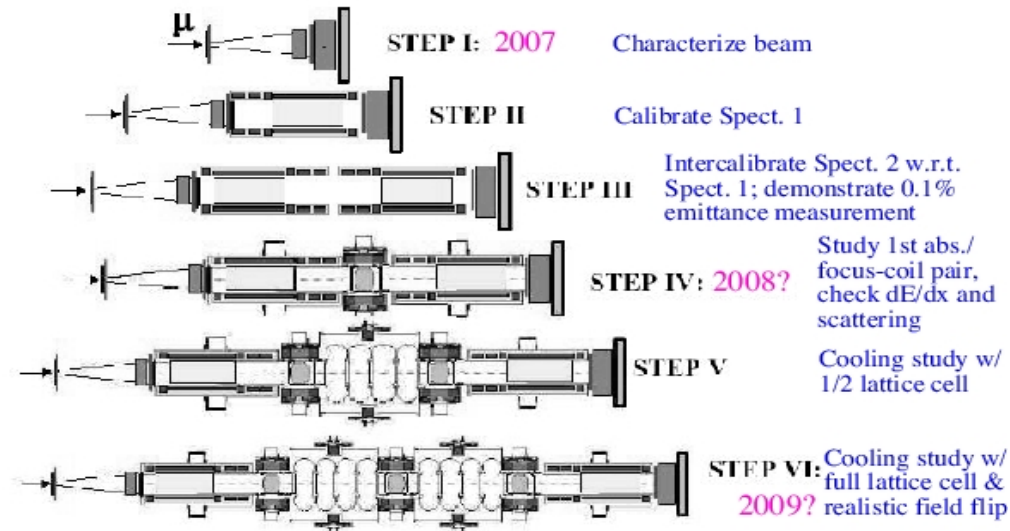


- Absorbers: $\exists E \forall E \# \left\langle \frac{dE}{dx} \right\rangle (s)$
 $\& \% \& \forall) !)$ rms space
 ionization energy loss
 multiple Coulomb scattering
- RF cavities between absorbers replace (E
- Net effect: reduction in p_x w.r.t. p_y i.e., transverse cooling

Note: The physics is not in doubt
 + in principle, ionization cooling **has** to work!
 ... but in practice it is subtle and complicated...

Avatars of MICE

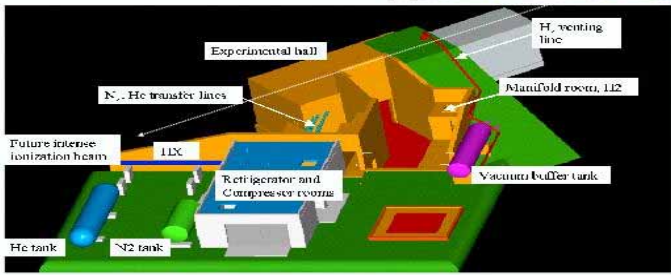
- Measurement precision relies crucially on precise calibration & thorough study of systematics:



Mucool Hydrogen Absorber R&D, M.Cummings NIU

Mucool Test Area

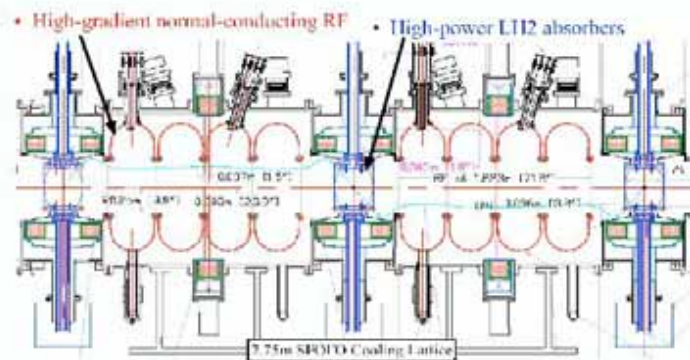
- The MTA is becoming our focus of Mucool activity
 - ➔ LH₂ Absorber tests
 - ➔ RF testing (805 and 201 MHz)
 - ➔ Finish cryo infrastructure
 - ➔ High pressure H₂ gas absorbers
 - ➔ High intensity beam design



M. A. C. Cummings, Cool 05
September 20, 2005

MuCool: cooling channel R & D

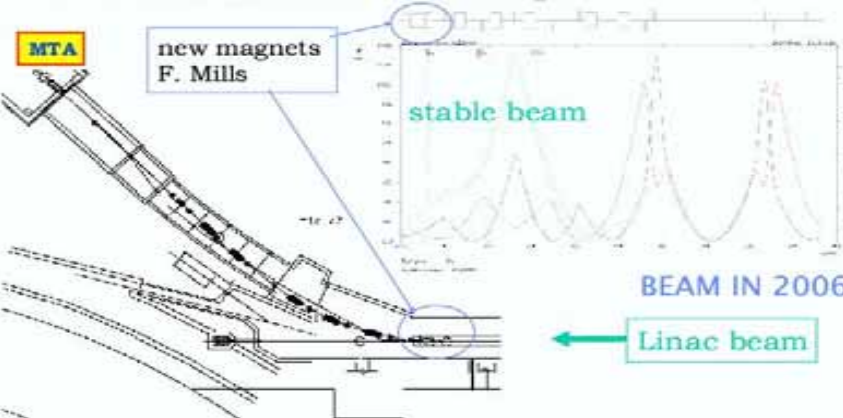
- **MuCool:** MC subset based at FNAL and charged with the development of muon ionization cooling channels
 - ➔ **Goal: Cooling cell test in high-powered beam (MTA)**
- SFOFO Cooling Lattice – **transverse** cooling for ν factories



M. A. C. Cummings, Cool 05
September 20, 2005

MTA High Intensity Beam

Beamline designed and costed by C. Johnstone for the MTA.
Part of the Linac Instrumentation Test Program



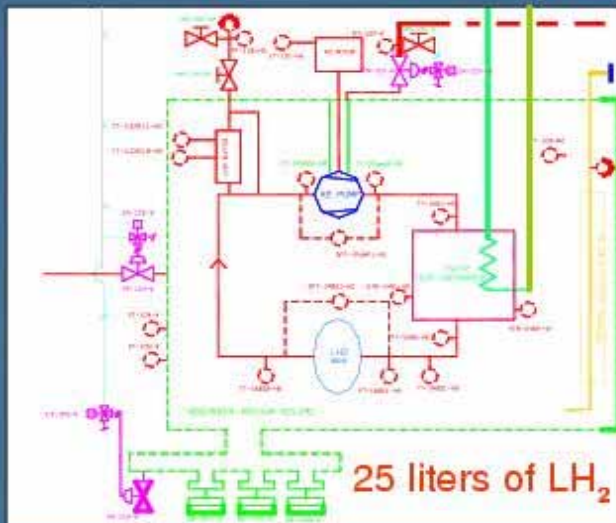
M. A. C. Cummings, Cool 05
September 20, 2005

T16: MTA Cryogenics C.Darve FNAL



Cryogenic Department

Application 3: Forced-flow LH_2 absorber Process and Instrumentation Proposal



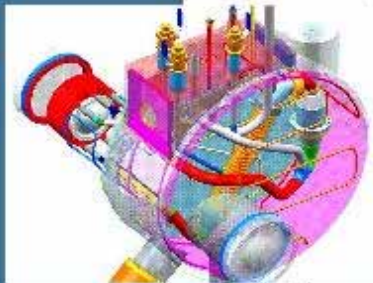
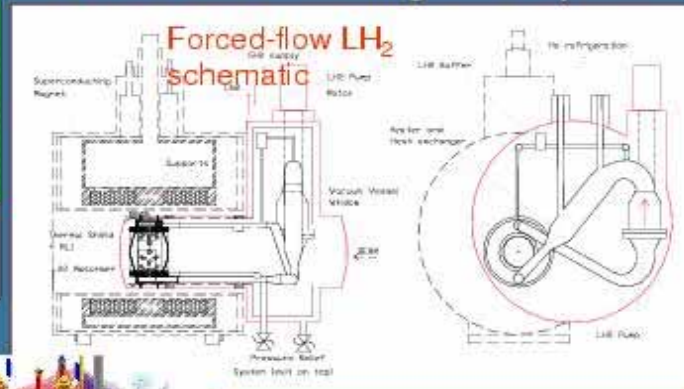
Safety issue:

25 liters of LH_2 released into the air and ignited with only a 10 % yield the energy equivalent to 4 kg of TNT

Total heat load estimation

Heat load (W)	80 K	17 K
Mechanical Supports	67	6
Superinsulation	1.5	0.2
Cryostat windows	-	17
LH2 pump	-	-
Total	68.5	73.2

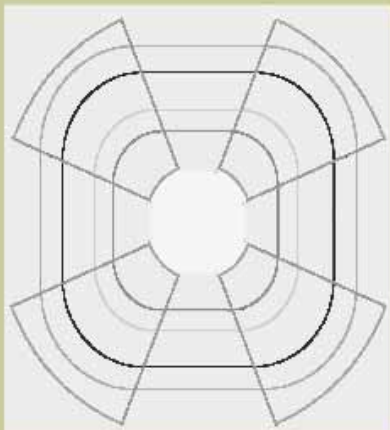
vs. 500 W for total refrigeration system



T10. 6D cooling of a circulating muon beam

A.Garren UCLA

1.8T Dipoles and 200 MHz Closed Orbits for 4 Cell Demonstration Ring



Fix the closed orbits for a 1.8T dipole ring such that the total path length is a harmonic of 200 MHz.

Then:

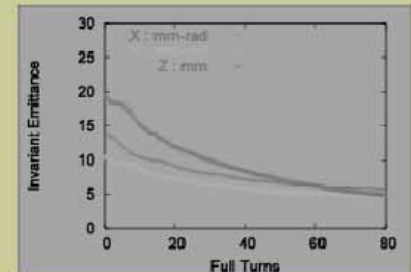
- Harmonic 2
 - Circumference = 1.76 m
 - $P_0 = 77 \text{ MeV/c}$
- Harmonic 3
 - Circumference = 3.76 m
 - $P_0 = 165 \text{ MeV/c}$
- Harmonic 4
 - Circumference = 5.45 m
 - $P_0 = 240 \text{ MeV/c}$

UCLA

Al. Garren

00/30/2005

4 Sector Ring, 1.8 T Dipoles



- Harmonic 3
- 40 Atmosphere H_2
- Total Merit without decay is 20

UCLA

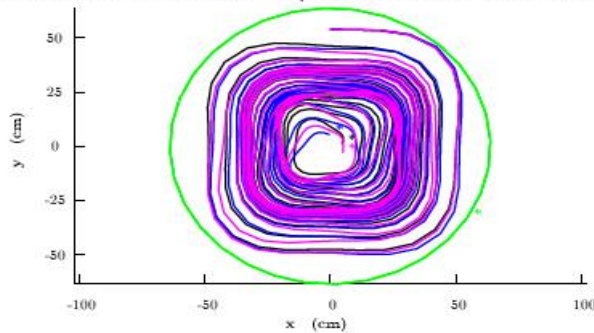
Al. Garren

00/30/2005

inverse cyclotron - Y.Yorin ITT

Single Turn Energy Loss Injection

- Four Magnet (1.8T) Sector Cyclotron. Soft edged fields, ICOOL simulation. Multiple scattering and straggling on. Radial LiH wedges surrounded by hydrogen. Matter decreases adiabatically with radius. 3 identical 172 MeV/c muons are injected.



- ± 5 cm vertical motion along the 70 m spiral
- Injection scaling relation: $\Delta p = .3 B \Delta r$.

14

Emittance Reduction Goals

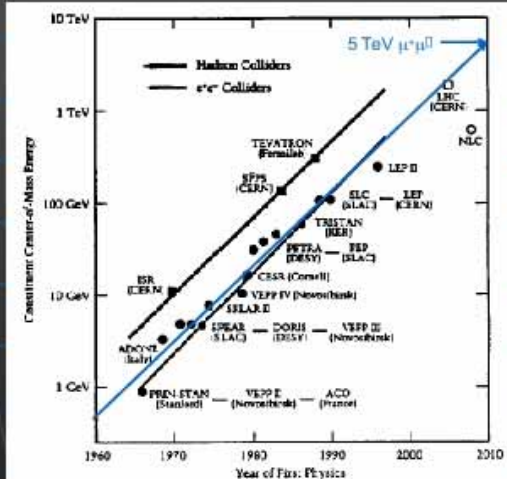
- A muon collider needs 10^6 cooling.
- $\epsilon = (\Delta p_x \Delta x) (\Delta p_y \Delta y) (\Delta p_z \Delta z)$
- Δp_x : 30 MeV/c \rightarrow 0.3 MeV/c
- Δp_y : 30 MeV/c \rightarrow 0.3 MeV/c
- Δp_z : 30 MeV/c \rightarrow 0.3 MeV/c
- Δx : 70 mm \rightarrow 50 mm
- Δy : 70 mm \rightarrow 50 mm
- Δz : 10000 mm \rightarrow 50 mm
- In: $10\times$ transverse cooler, physics/0411123.
- Out: "Frictional μ cooling,"
H. Abramowicz, A. Caldwell, R. Galea, and S. Schlenstedt, NIM A546 (2005) 356.

15

T09 Innovations in Muon Beam Cooling

R.Johnson, Muons Inc.

Muon Colliders: Back to the Livingston Plot



Modified Livingston Plot taken from: W. K. H. Panofsky and M. Breidenbach, Rev. Mod. Phys. 71, s121-s132 (1999)

Eight New Ideas for Bright Beams for High Luminosity Muon Colliders

supported by SBIR/STTR grants

- H₂-Pressurized RF Cavities
- Continuous Absorber for Emittance Exchange
- Helical Cooling Channel
- Z-dependent HCC
- MANX 6d Cooling Demo
- Parametric-resonance Ionization Cooling
- Reverse Emittance Exchange
- RF capture, phase rotation, cooling in HP RF Cavities

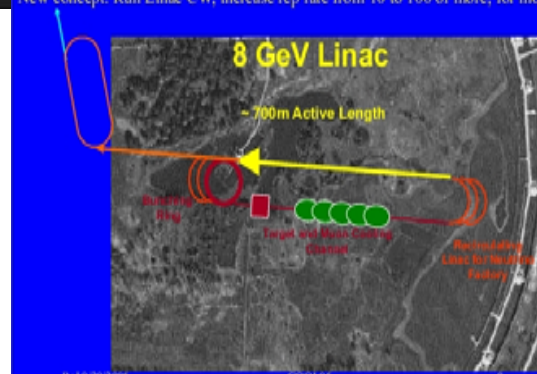
Roll 9/20/2005

COOL05

10

Neutrinos from an 8 GeV SC Linac

Muon cooling to reduce costs of a neutrino factory based on a storage ring. Cooling must be 6D to fit in 1.3 GHz SC RF, where the last 6.8 GeV of 8 GeV are $\gamma \approx 1$. New concept: Run Linac CW, increase rep rate from 10 to 100 or more, for more γ .



Roll 9/20/2005

COOL05

11

Muons Inc. Funding History

Year	Project Title	Expected Funds	Research Partner
2002	Company Founded		
2002-5	High Pressure RF Cavities	\$600,000	IFT
2003-6	Helical Cooling Channel	\$850,000	SLAC
2004-5	MANX demo experiment	\$ 95,000	FNAL TD
2004-7	Phase Ionization Cooling	\$745,000	SLAC
2004-7	Hydrogen Cryostat	\$795,000	FNAL TD
2005-6*	Reverse Emittance Exch.	\$100,000	SLAC
2005-6*	Capture, phi. rotation	\$100,000	FNAL AD
* Can be extended to phase II for +\$170,000 and +2 years -\$1,300,000 spent of \$1,285,000 granted so far			
SBIR/STTR funding: Solicitation September, Phase I proposal due December, Winners in May, get \$100,000 for 9 months, Phase II proposal due April, Winners June, get \$750,000 for 2 years			
Thanks to Dave Butler, Jerry Peters, Bruce Strauss, UK Lenz			

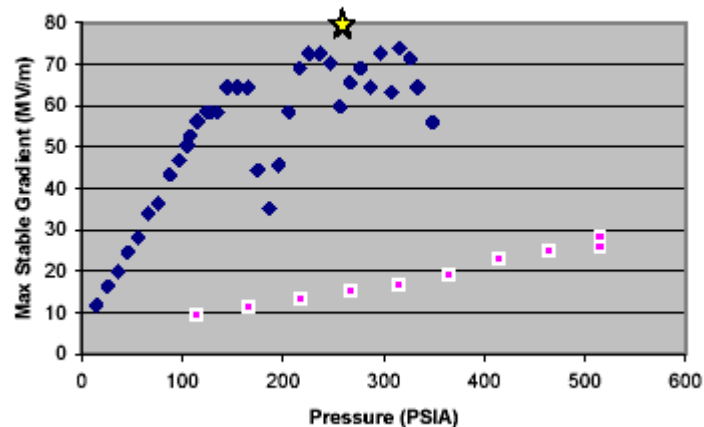


Thomas Jefferson National Accelerator Facility



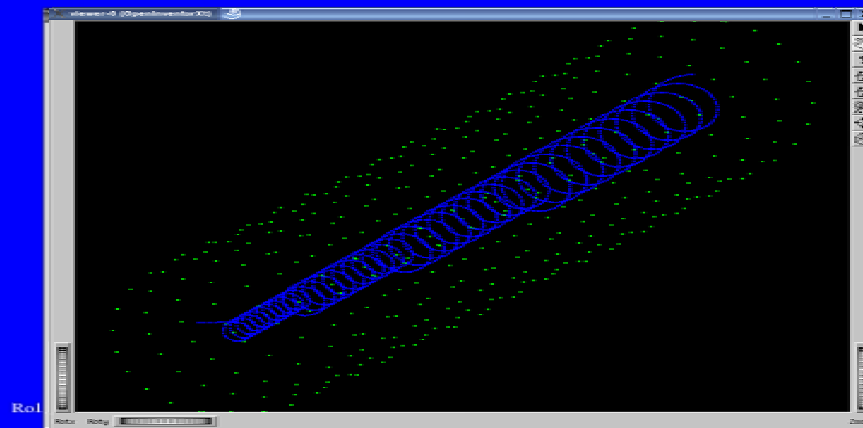
Lab G Results, Molybdenum Electrode

H2 vs He RF breakdown at 77K, 800MHz



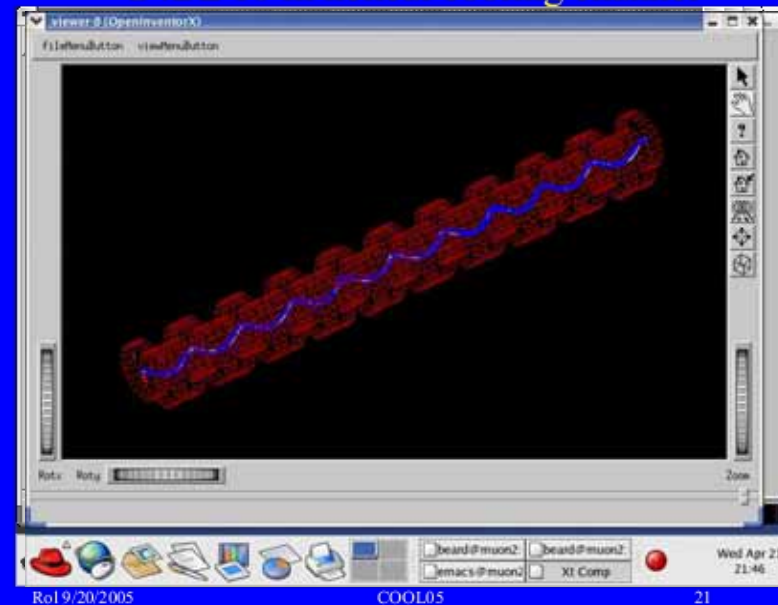
RoI 9/20/2005

Reference orbit in series of HCCs

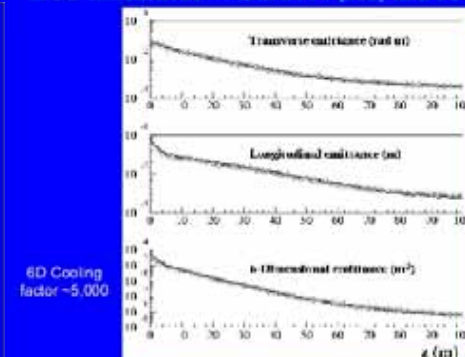


RoI

G4BL 10 m helical cooling channel



HCC simulations w/ GEANT4 (red) and ICOOL (blue)



Katsuya Yonehara, et al., Simulations of a Gas-Filled Helical Cooling Channel, PAC05
RoI 9/20/2005 COOL05 21

Muon Trajectories in 3-m MANX



The design of the coils and cryostat are the next steps for MANX, as seen in the next slides on the technology of the HCC.

Ro19/20/2005

COOL05

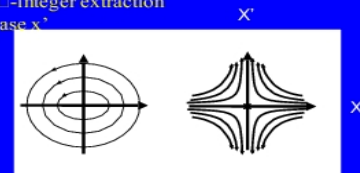
33

Idea #7: Parametric-Resonance Ionization Cooling (PIC)

Derbenev Talk to Follow (theory)!

See Beard poster P24 tomorrow (simulations)!

- Derbenev: 6D cooling allows new IC technique
- PIC Idea:
 - Excite parametric resonance (in linac or ring)
 - Like vertical rigid pendulum or π -integer extraction
 - Use $xx' = \text{const}$ to reduce x , increase x'
 - Use IC to reduce x'
 - Detuning issues being addressed
 - chromatic aberration example



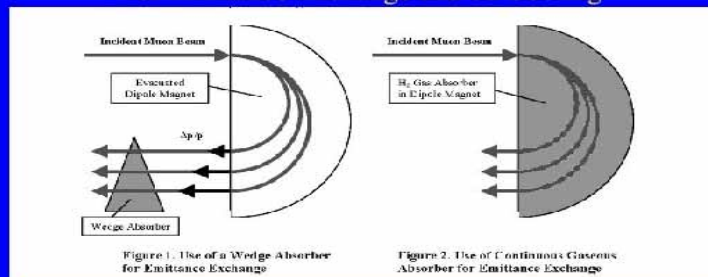
Yaroslav Derbenev et al., Ionization Cooling Using a Parametric Resonance, PAC05
Kevin Beard et al., Simulations of Parametric-resonance IC..., PAC05

Ro19/20/2005

COOL05

37

Idea #2: Continuous Energy Absorber for Emittance Exchange and 6d Cooling



Ionization Cooling is only transverse. To get 6D cooling, emittance exchange between transverse and longitudinal coordinates is needed. In figure 2, positive dispersion gives higher energy muons larger energy loss due to their longer path length in a low-Z absorber.

Ro19/20/2005

COOL05

17

Idea #8: Simultaneous RF Capture, Bunch Rotation and Cooling in HP RF Cavities

- Proton bunches have ~ 1 ns such that produced pion bunches do too.
- Placing RF cavities close to the production target allows 1/4 synchrotron period rotation to get longer pion bunches with smaller momentum spread.
- Subject of new STTR grant to use HP RF (see Dave Neuffer & Kevin Paul)

Ro19/20/2005

COOL05

40

T14: Muon Cooling R&D Y.Torun, IIT



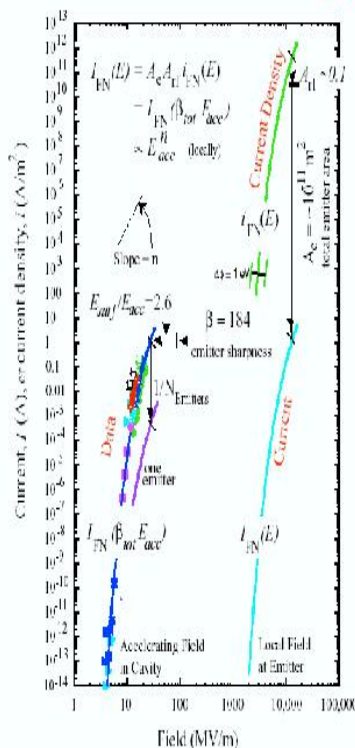
Dark Currents



- Precursor to breakdown
- Electrons tunnel through work function of metal
- Current rises very steeply with field (hard to make measurements)

$$j_{FN}(E) = \frac{A}{\phi} (\beta E)^2 \exp\left(-\frac{B\phi^{3/2}}{\beta E}\right)$$

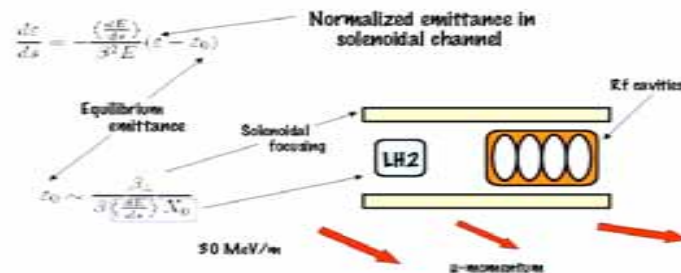
$$n = \frac{E}{j} \frac{dj}{dE} \simeq 2 + \frac{67.4 \text{ GV/m}}{\beta E}$$



Ionization Cooling



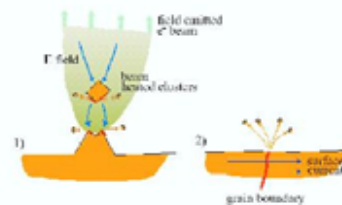
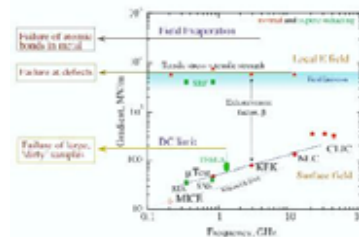
- Muon lifetime is 2.2 μs , traditional beam cooling techniques not applicable
- Ionization cooling works “at the speed of the muon”



Rf R&D Directions



- Many problems are common to
 - DC and rf breakdown
 - Normal and superconducting rf (CLIC, ILC)
- We need help from materials science and surface chemistry
- Surface physics initiative (J. Norum, ANL + D. Seidman, Northwestern) for understanding breakdown processes using atom probe tomography and molecular cluster simulations



P23: Helical Muon Beam Cooling Channels K.Yonehara IIT



Muons, Inc.



A abstract

A helical cooling channel (HCC) has been proposed to quickly cool the six-dimensional phase space of muon beams for muon colliders, hadron colliders, and other muon sources. The simulation study for the HCC has been done, and simulated the cooling mechanism in the HCC. The HCC design concept has been extended to have a maximum of parallel length for a helical length for a muon application, which is a 3D Helical Collimator. And the first Helical muon beam cooling channel has been proposed (HMC). The simulation study for the HMC has been done, and it shows the improvement of muon quality. This is a helical channel where the cooling is done in the HMC system.

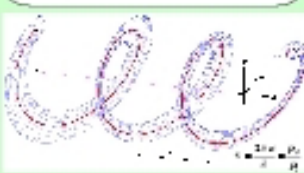


Figure 1. Particle trajectory in the HCC. The helical path is shown by using 3D plot. The helical path is shown by using 3D plot. The helical path is shown by using 3D plot.

INDEX CHANNEL

Helical muon beam cooling channel has been proposed to quickly cool the six-dimensional phase space of muon beams for muon colliders, hadron colliders, and other muon sources. The simulation study for the HCC has been done, and simulated the cooling mechanism in the HCC. The HCC design concept has been extended to have a maximum of parallel length for a helical length for a muon application, which is a 3D Helical Collimator. And the first Helical muon beam cooling channel has been proposed (HMC). The simulation study for the HMC has been done, and it shows the improvement of muon quality. This is a helical channel where the cooling is done in the HMC system.



Work supported by the U.S. Department of Energy.
DE-SC-0001401 and DE-SC-0001402

Simulations of A Helical Muon Beam Cooling Channel

Katsuya Yonehara, Dan Kaplan (Illinois Institute of Technology, Chicago, Illinois, USA),
Kevin B. Beard, S. Alex Bogacz, Yaroslav Derbenev (Jefferson Lab, Newport News, Virginia, USA),
Roland P. Johnson, Kevin Paul, Thomas J. Roberts (Muons, Inc, Batavia, Illinois, USA)

INDEX CHANNEL SIMULATION RESULTS

A simulation study for the HCC has been done, and simulated the cooling mechanism in the HCC. The HCC design concept has been extended to have a maximum of parallel length for a helical length for a muon application, which is a 3D Helical Collimator. And the first Helical muon beam cooling channel has been proposed (HMC). The simulation study for the HMC has been done, and it shows the improvement of muon quality. This is a helical channel where the cooling is done in the HMC system.



Figure 2. Simulation results for the HCC. The helical path is shown by using 3D plot. The helical path is shown by using 3D plot.

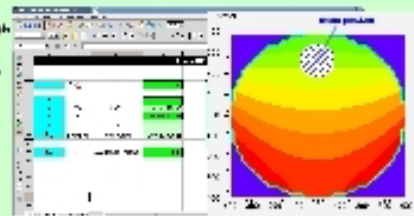


Figure 3. The parameters of the helical path for the HCC. The helical path is shown by using 3D plot. The helical path is shown by using 3D plot.

PRactical INDEX CHANNEL DESIGN CONCEPT

1. The HCC is used as the helical path of the HCC. The helical path is shown by using 3D plot. The helical path is shown by using 3D plot.
2. The helical path is shown by using 3D plot. The helical path is shown by using 3D plot.
3. The helical path is shown by using 3D plot. The helical path is shown by using 3D plot.
4. The helical path is shown by using 3D plot. The helical path is shown by using 3D plot.

Finally, the helical path is shown by using 3D plot. The helical path is shown by using 3D plot.



ILLINOIS INSTITUTE OF TECHNOLOGY
Batavia, Illinois, USA

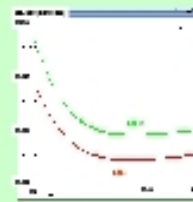


Figure 4. Simulation results for the HCC. The helical path is shown by using 3D plot. The helical path is shown by using 3D plot.

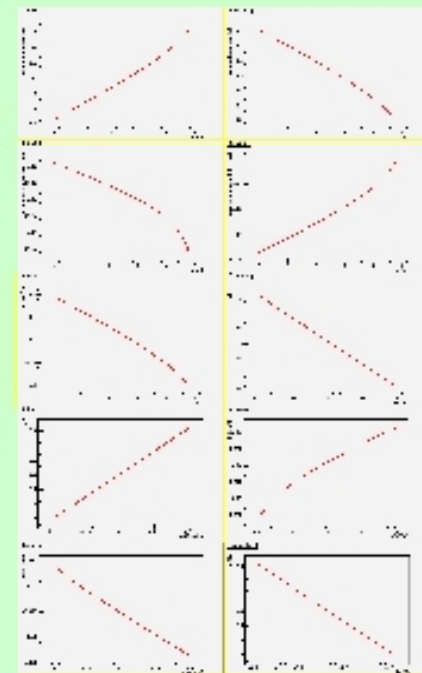


Figure 5. Simulation results for the HCC. The helical path is shown by using 3D plot. The helical path is shown by using 3D plot.

Work supported by the U.S. Department of Energy.



Thomas Jefferson National Accelerator Facility



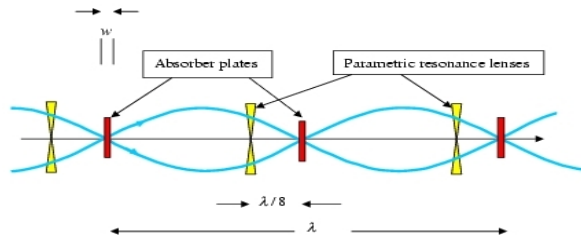
T11: Parametric Resonance Ionization Cooling and Reverse Emittance exchange, Ya.Derbenev, TJNAF

Basic principles of PIC

- Assume initially the tune spread for a beam in a focusing channel to be smaller than the cooling decrement
- Weak lenses installed every half oscillation period drive a half-integer parametric resonance that creates a hyperbolic beam evolution at the absorber plates:

$$\begin{pmatrix} x \\ x' \end{pmatrix}_{n+1} = - \begin{pmatrix} k^{-1} & 0 \\ 0 & k \end{pmatrix} \begin{pmatrix} x \\ x' \end{pmatrix}_n; \quad k = \exp(\Lambda_d \lambda / 2)$$

$$0 < \Lambda_d \lambda \ll 1$$



The lattice magnets and RF cavities to replace energy loss are not shown.

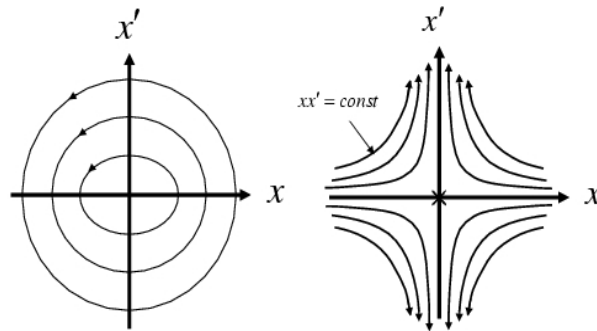
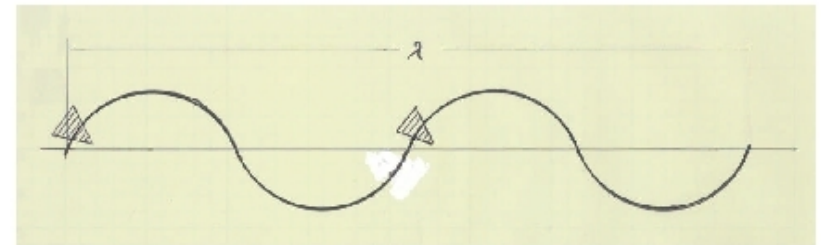


Fig. 1 Comparison of particle motion at periodic locations along the beam trajectory in transverse phase space for: LEFT ordinary oscillations and RIGHT hyperbolic motion induced by perturbations at a harmonic of the betatron frequency.

Achromatic channel for PIC

- Compensation for chromaticity requires relatively large orbit dispersion – which is a constraint to PIC because of increase of energy straggling impact on transverse emittance
- A resolution of this constraint is:** design a dispersion function that follows the beam envelope at PR

Scheme: **Achromatic wiggler**



- Field index $n = 1/2$ (symmetric focusing, $f \equiv (\lambda / 2\pi) = R\sqrt{2}$)
- Betatron phase advance $\pi/2$ per bend segment (bend angle $\pi/\sqrt{2}$)
- Dispersion then oscillates with period equal to half of the betatron oscillation period
- Sextupole alternates in tact with the beam bend
- Orbit plane interchanges

However, compensation for chromaticity leads to a revival of the angle aberration. This seems possible to compensate by superimposing octupole field in combination with solenoid one (both relatively weak) /under study/

P24: G4Beamline simulations of Parametric Resonance Ionization Cooling

K.Beard, TJNAF



Muons, Inc.

Abstract

The technique of using a parametric resonance to allow better ionization cooling is being developed to create small emittance beams so that high collider luminosity can be achieved with fewer muons. While parametric resonance ionization (PRI) cooling of muons has been shown to work in matrix-based simulations when the system is properly tuned, doing the same using a much more detailed GEANT-based **g4beamline** simulation has been more difficult.

The starting point for this work is a linear channel; a half integer resonance is induced such that the normal elliptical motion of particles in $x-x'$ phase space becomes hyperbolic, with particles moving to smaller x and larger x' as they pass down the channel. Thus absorbers placed at the focal points of the channel then cool the angular divergence of the beam by the usual ionization cooling mechanism where each absorber is followed by RF cavities to replenish the energy. Thus the phase space of the beam is compressed in transverse position by the dynamics of the resonance and its angular divergence is compressed by the ionization cooling mechanism.

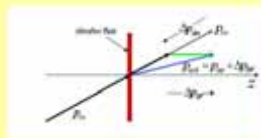
The **g4beamline** and **OptiM** simulations show the importance of synchrotron motion as averaging mechanism for chromatic detuning. Multiple scattering and energy straggling play a significant role that must be addressed via further optimizations and additional compensation solutions.



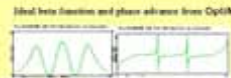
Work supported by the U.S. Department of Energy,
HSCC grants DE-FG02-03ER40124 and DE-FG02-03ER40124.

g4beamline Simulations of Parametric Resonance Ionization Cooling of Muon Beams

Kevin B. Beard, S. Alex Bogacz, Yaroslav Derbenev (Jefferson Lab, Newport News, Virginia, USA),
Katsuya Yonehara (Illinois Institute of Technology, Chicago, Illinois, USA),
Rolland P. Johnson, Kevin Paul, Thomas J. Roberts (Muons, Inc, Batavia, Illinois, USA)



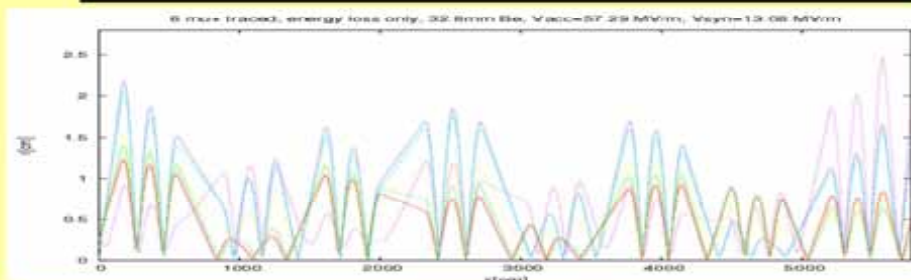
Schematic of angular divergence cooling



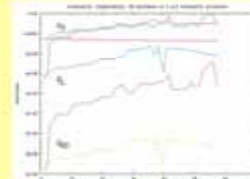
typical values:

KE= 200 MeV μ^+ $\epsilon_{x,y} = 30$ mm-mrad $\epsilon_L = 0.8$ mm $L_{eff} = 7.2$ m absorber: 32.8 mm Be
90° off-crest (Vsyn) RF: 13.08 MV/m on-crest RF (Vacc): 57.28 MV/m
-100% transmission w/o stochastic processes, -65% w/ stochastic processes

PIC beam line with 8 cells



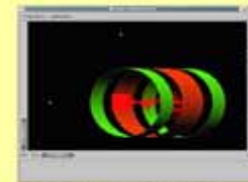
Particle tracking by g4beamline, solved by retrack.



As a first step, all energy straggling, multiple scattering, and muon decay was disabled to enable a comparison with the previous **OptiM** work. The improvement due to induced synchrotron motion is in qualitative agreement with the earlier work. **ECALC9** is used to calculate the emittances. The Be absorbers are 32.8mm thick in these examples.

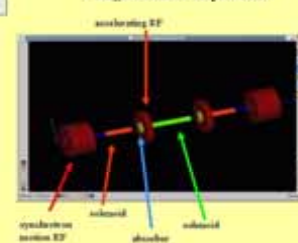
The figure immediately to the right shows the improvement in emittance due to synchrotron motion **when only energy loss is enabled**.

One can note two orders of magnitude better cooling in the case of synchrotron motion averaging.



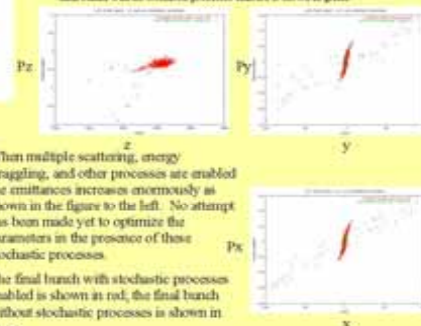
Solenoid triplet and muon beam as viewed in g4beamline with no RF present.

Single Solenoid Triplet Cell



One solenoid triplet cell with absorber with 4E-20 RF and off-crest RF to induce synchrotron motion

The final bunch with all stochastic processes enabled is shown in red, while the final bunch with no stochastic processes enabled is shown in green.



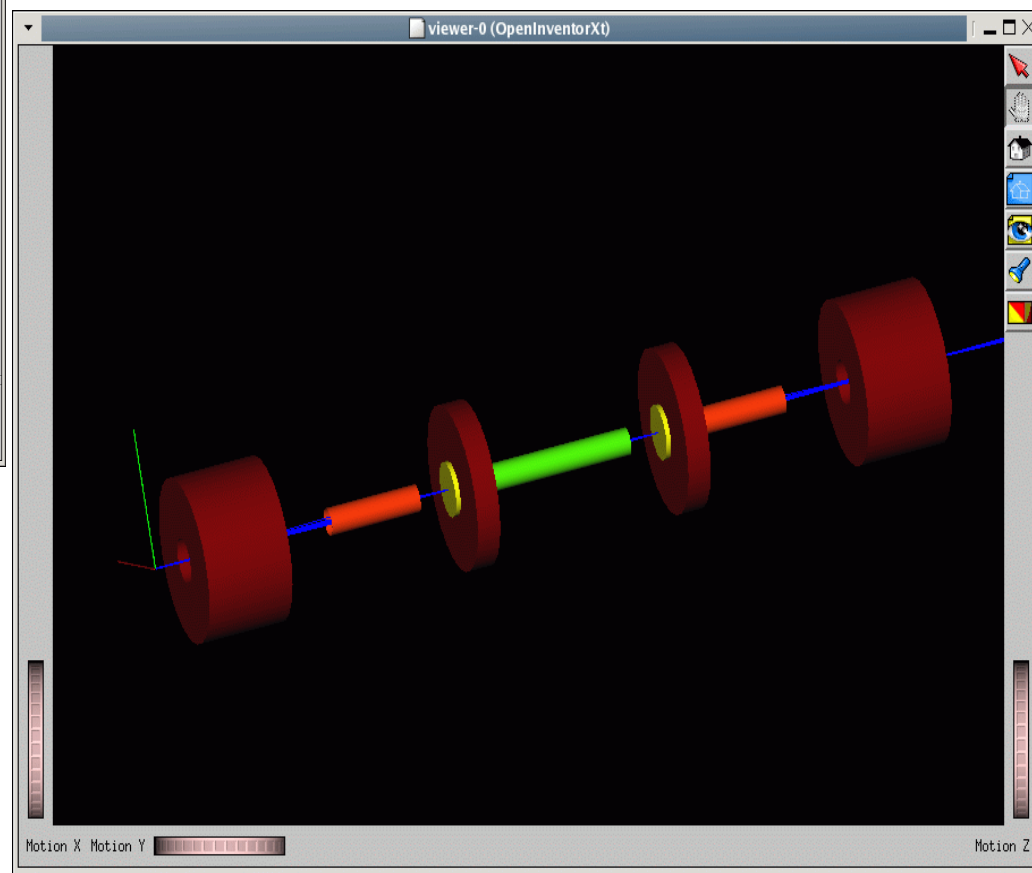
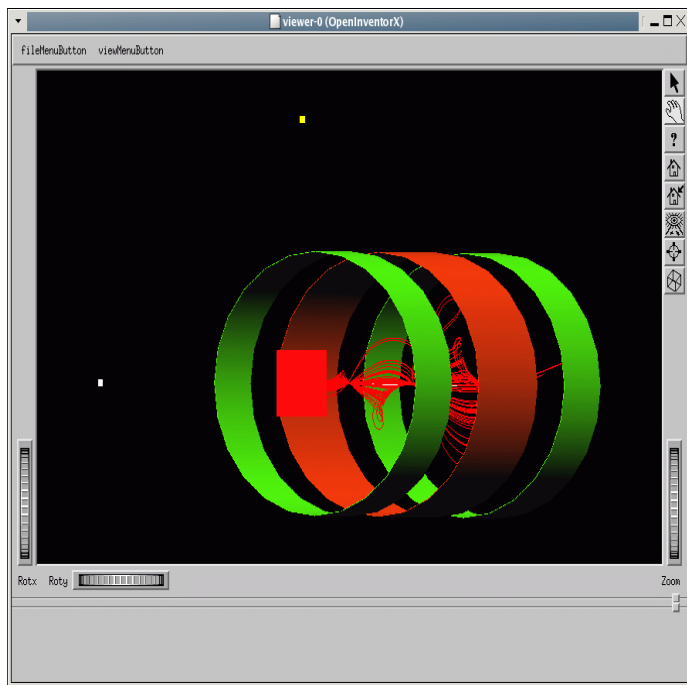
When multiple scattering, energy straggling, and other processes are enabled the emittances increase enormously as shown in the figure to the left. No attempt has been made yet to optimize the parameters in the presence of these stochastic processes.

The final bunch with stochastic processes enabled is shown in red; the final bunch without stochastic processes is shown in green.



Thomas Jefferson National Accelerator Facility





Thomas Jefferson National Accelerator Facility



stochastic cooling



Thomas Jefferson National Accelerator Facility

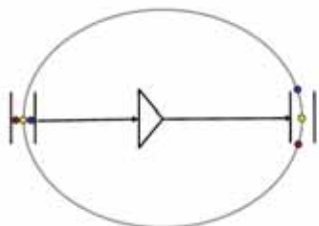


T01 Stochastic Cooling at GSI, F.Nolden GSI

Stochastic Cooling Slip Factor

$$\eta_{\text{sl}} = \frac{1}{\gamma^2} - \alpha_p = \frac{1}{\gamma^2} - \frac{1}{\gamma_{tr}^2}$$

$$\alpha_p = \frac{1}{s_k - s_p} \int_{s_p}^{s_k} \frac{D(s)}{\rho(s)} ds$$



GSI

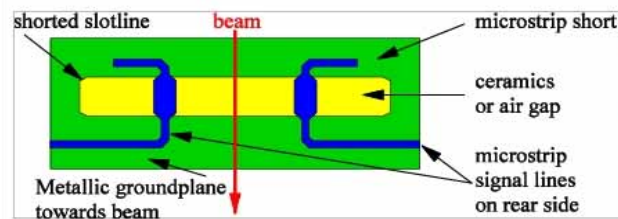
Overview of the FAIR Complex



F. Nolden, Cool05, September 20, 2005

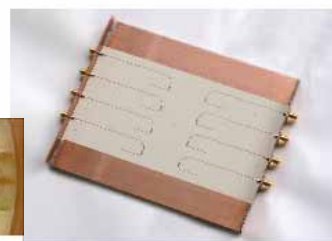
GSI

Stochastic Cooling Electrode Development



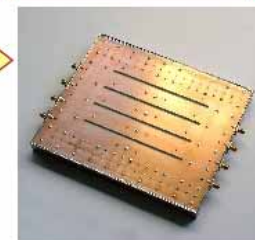
3D field calculations:
L. Thorndahl (CERN)

Prototype design:
C. Peschke (GSI)
See his poster
on Wednesday!



Front side
(towards beam)

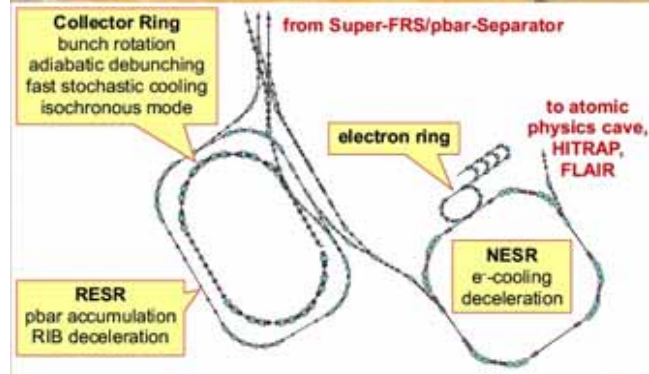
Rear side



Nolden, Cool05, September 20, 2005

GSI

The Small Storage Rings



F. Nolden, Cool05, September 20, 2005

GSI



Thomas Jefferson National Accelerator Facility



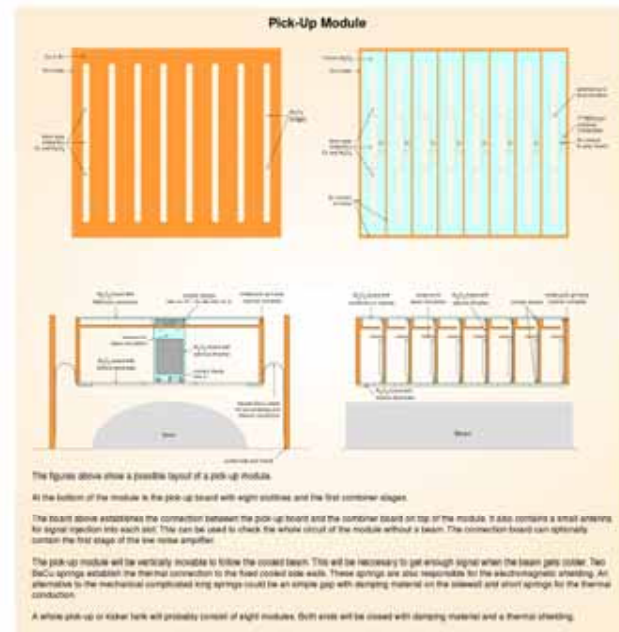
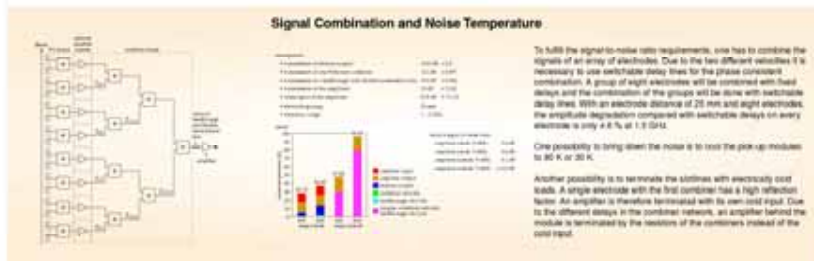
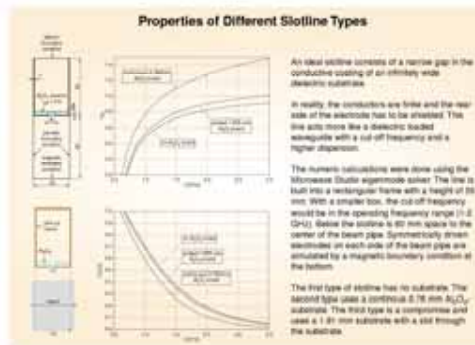
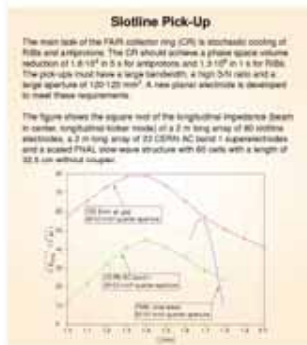
P26: Pick-Up and Kicker Electrodes for Stochastic Cooling

C.Peschke GSI



Investigations on Pick-Up and Kicker Electrodes for Stochastic Cooling

Claudius Peschke, Fritz Nolden (GSI, Darmstadt); Lars Thorndahl (CERN, Geneva)

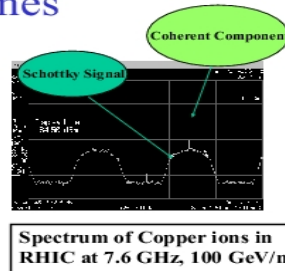


T03 bunched beam stochastic cooling at RHIC

M.Brennan - BNL

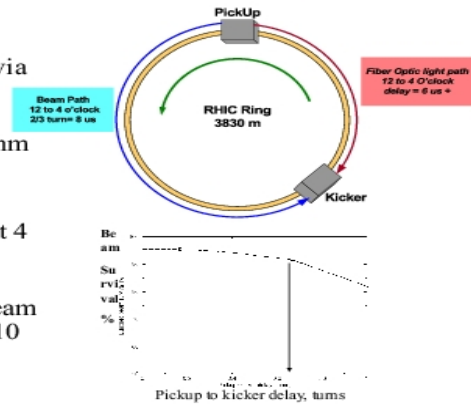
Coherent Lines

- This has been Nemesis of bunched-beam cooling.
- Not as severe for ions as for protons.
- Nevertheless, can cause saturation and disable the electronics. The problem is high peak voltages in the time domain.



PickUp to Kicker Delay

- Fiber optic link runs via the tunnel against the beam
- $V_{\text{light}} = c/1.47$ @ 1550nm
- Effectively 2/3 turn delay
- Mixing factor is about 4 turns
- Simulations (J. Wei) indicate that >90% beam is still bunched after 10 hours



Origin of the Coherent Lines

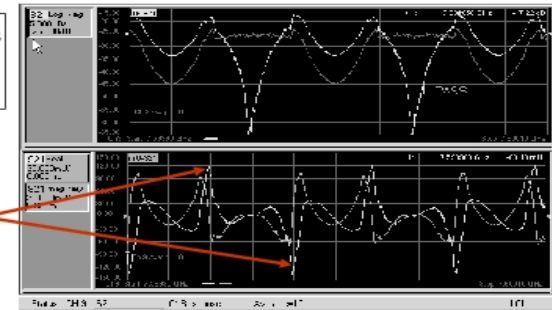
- M. Blaskiewicz has a talk at this conference on our studies of the coherent lines.
- We believe the origin is different for **ions** and **protons** in RHIC.
 - The key difference is that ions are stored in completely **filled buckets** (large synchrotron frequency spread) and protons are **short bunches** in long buckets (28 MHz, $\square f_s$ small)
 - For protons, the coherent signals come from the motion of the bunch.
 - For ions, they come from the shape of the bunch.
- The ion bunches have very high frequency structure because of the satellite bunches
 - The Fourier transform of the bunch shape is not negligible at 8 GHz
 - All bunches have the same shape so they contribute coherently to the spectrum
 - The low frequency spectrum envelope reflects the bunch fill pattern
 - As does the high frequency spectrum

Beam Transfer Function

- The BTF measures the entire loop
 - Calibrates kickers (corrected for duty factor)
 - Obtains beam response
 - Determines loop phase (stability)
 - Reveals filter response
- The filter flips the sign of the real part at each Frev
- The phase is stable on the 10-minute time scale
- Run-time BTFs will be used to correct drifts

Magnitude: red is no filter, yellow is with 2-turn filter

Real (yellow) and Imaginary parts. Real part changes sign at Frev



T06 Stochastic Cooling and Coherent Lines

M.Blaskiewicz BNL

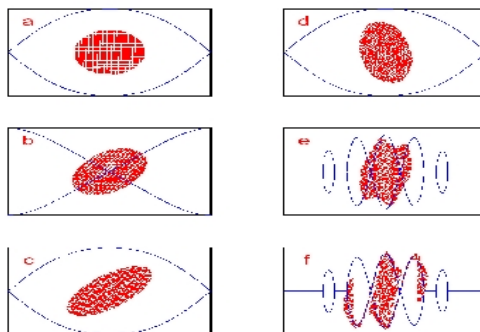
Coherence in Heavy Ion Beams

Two distinct types:

- 2) Strong revolution lines
- 3) Strong signals associated with synchrotron motion

We see the first type with heavy ions and both with protons.

Heavy ions are “rebucketed”
to shorten the bunch and
combat IBS

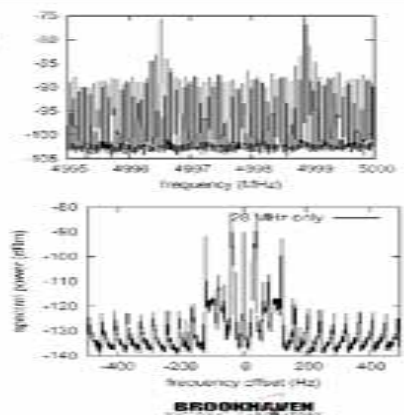


Mike Blaskiewicz C-AD

BROOKHAVEN
NATIONAL LABORATORY

Coherence in Proton Beams

Wide band (top) observed with
28 bunches in 30 bunch fill pattern.
 $h=360$. Similar to what would be
expected due to hard edge bunch.
Zoom of the strong right peak (bottom).
90% of the power in dipole lines (40
Hz)
10% in rev and ± 120 Hz.
<1% Schottky.

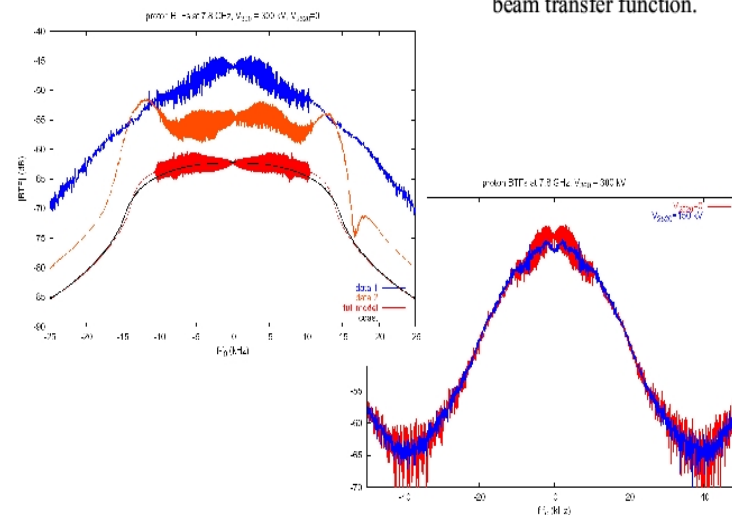


Mike Blaskiewicz C-AD

BROOKHAVEN
NATIONAL LABORATORY

General features look good

Generic features are well
modeled by a coasting
beam transfer function.



Mike Blaskiewicz C-AD

BROOKHAVEN
NATIONAL LABORATORY

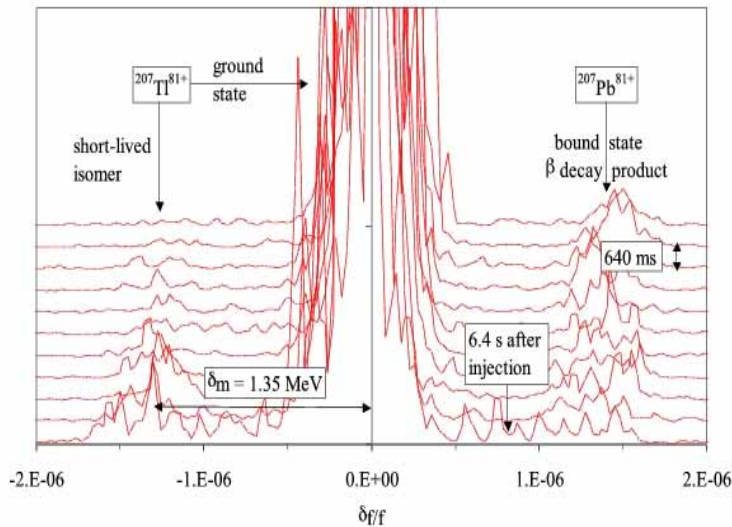


Thomas Jefferson National Accelerator Facility



T07: Schottky Spectroscopy, F.Nolden GSI

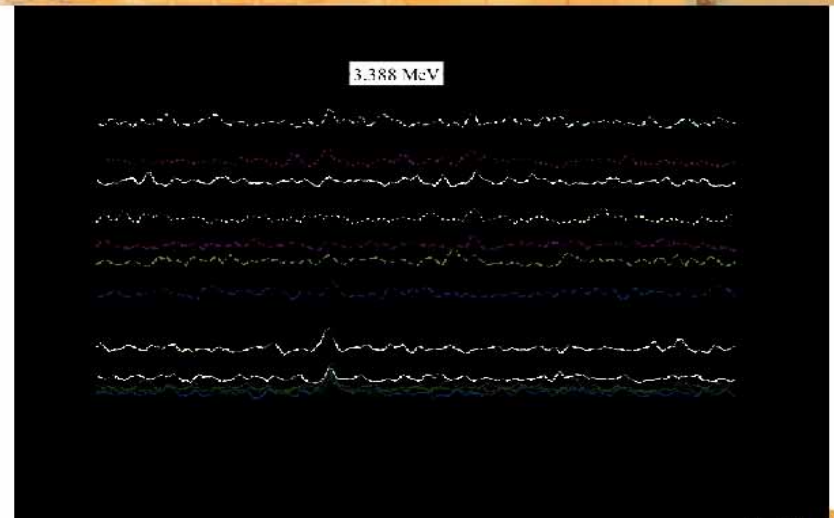
$^{207}\text{Tl}^{81+}$ Decay Spectra with Isomer



F. Nolden, Coal05, September 20, 2005



Decay of one Ion out of Two



F. Nolden, Coal05, September 20, 2005



Thomas Jefferson National Accelerator Facility



electron cooling



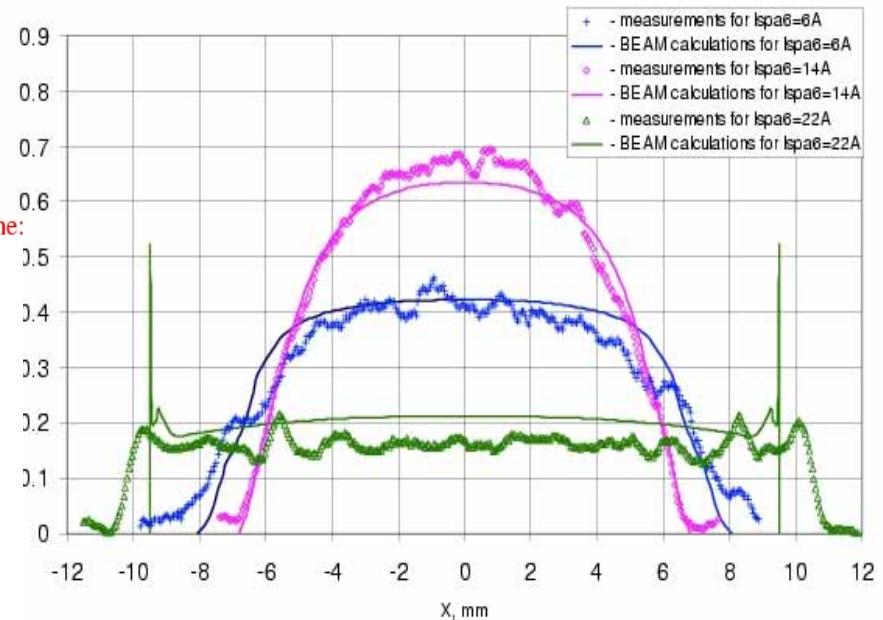
Thomas Jefferson National Accelerator Facility



M12 Optics of Electron Beam in Recycler: A.Burov, FNAL

OTR profiles: Measurements & UltraSam-Beam Simulations (Sep 14)

Current density distribution on TRA07 for Upulse = 4.5 kV
(Ibeam = 0.56A)



Electron cooling beam line:

Acceleration section

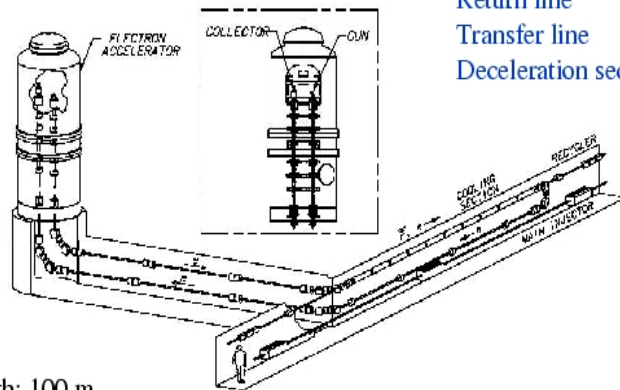
Supply line

Cooling Section

Return line

Transfer line

Deceleration section



Total length: 100 m

Cooler length: 20 m

Kinetic energy: 4.35 MeV

Phase advance: ~30 rad

Alexey Burov

15

high-quality electron beam @ FNAL's 4.3MV cooler

A.Shemyakin FNAL

Setup

Recirculation

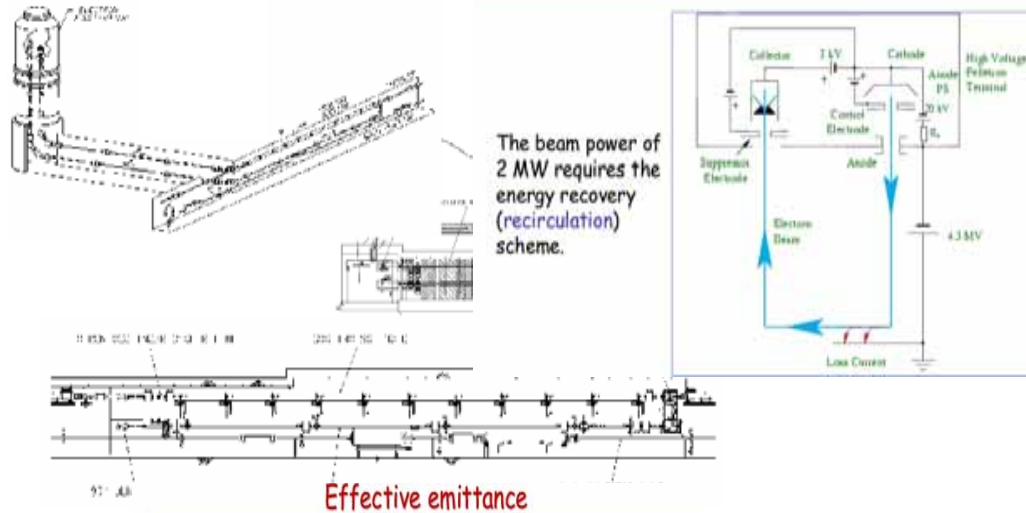
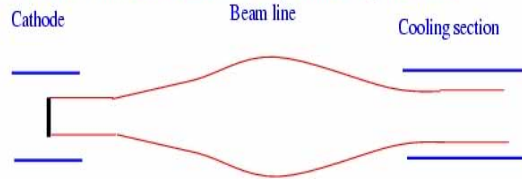


Figure of merit: magnetic flux inside the beam in the cooling section = effective emittance outside the longitudinal magnetic field



$$\begin{aligned}
 B_{cz} &= 90 \text{ G} & B_z &= 0 & B_{cz} &= 105 \text{ G} \\
 R_{cath} &= 3.8 \text{ mm} & R &= 2 - 10 \text{ mm} & R_{beam} &= 3.5 \text{ mm} \\
 \epsilon_i &= R_{cath} \sqrt{\frac{T}{mc^2}} & \epsilon_{eff} &= B_{cz} R_{cath}^2 \frac{e}{2mc^2} & \epsilon_{cs} &< 7 \mu\text{m} \\
 &= 2 \mu\text{m (normalized)} & &= 38 \mu\text{m (normalized)} & & \text{(normalized)}
 \end{aligned}$$

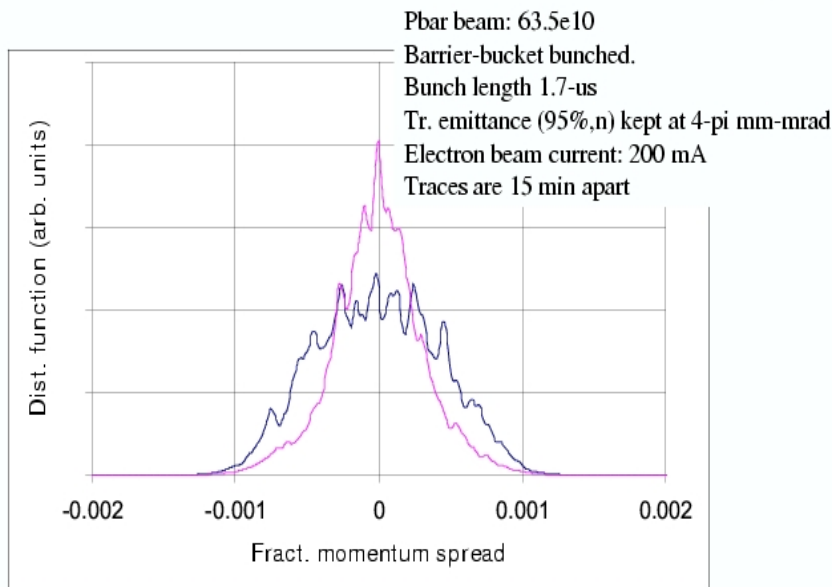
Low energy portions of the acceleration and deceleration tubes have to be immersed into a longitudinal magnetic field.

A 3D beam line has to provide an axially symmetrical beam transformation.

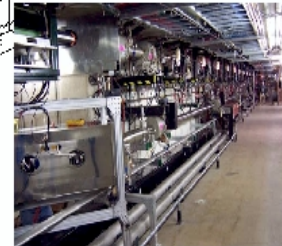
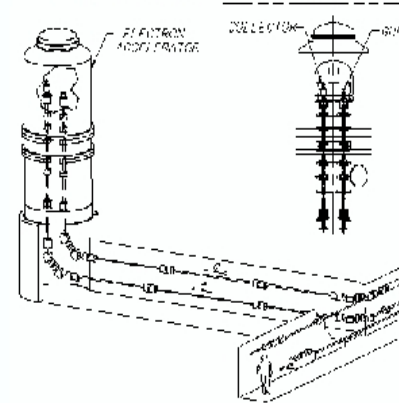
See report of A. Burov et al.

Setup parameters

Parameter	Unit	Value (for cooling)	Value (maximum)
Electron energy	MeV	4.338	5
Beam current used for cooling	A	0.05 - 0.2	0.6
Magnetic field in the cooling section	G	105	190
Beam radius in the cooling section	mm	3 - 5	
Pressure	nTorr	0.2 - 1	
Total length of the beam line	m	80	



- The maximum antiproton stack size in the Recycler is limited by
 - Stacking Rate in the Debuncher-Accumulator at large stacks
 - Longitudinal cooling in the Recycler
- Longitudinal stochastic cooling of 8 GeV antiprotons in the Recycler is being replaced by Electron Cooling
 - Electron beam: 4.34 MeV - 0.5 Amps DC - $200 \mu\text{rad}$ angular spread



Recycler-Only Operations

- Recycler has been participating in Collider Operations in the Combined Shot mode because the Recycler Stack size has been limited to $\sim 120 \times 10^{10}$ pbars
 - Longitudinal Cooling
 - Transverse Stability
- With Electron Cooling operational and the transverse dampers commissioned, the Recycler stack size can now be increased to over 200×10^{10} pbars
- The Collider complex is now transitioning from Combined Shot mode to Recycler-Only mode
 - Faster average stacking.
 - Smaller pbar emittances in the TEV

28



Electron beam parameters

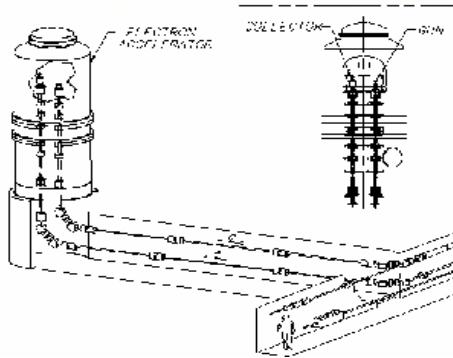
- | | |
|--|-------------------------|
| ▪ Electron kinetic energy | 4.34 MeV |
| ▪ Uncertainty in electron beam energy | 0.3 % |
| ▪ Energy ripple | $\leq 10^{-4}$ |
| ▪ Beam current (max) | 0.5 A DC |
| ▪ Duty factor (averaged over 8 h) | 95 % |
| ▪ Electron angles in the cooling section (averaged over time, beam cross section, and cooling section length), rms | $\leq 0.2 \text{ mrad}$ |

22

T02 antiproton rate increase D.McGinnis - FNAL



Recycler Electron Cooling

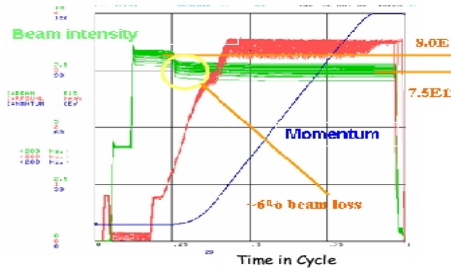
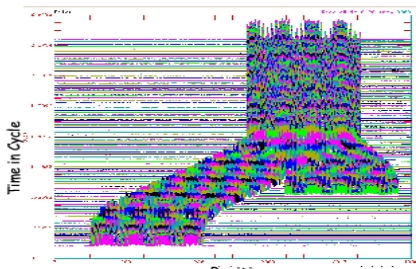


- The maximum antiproton stack size in the Recycler is limited by
 - Stacking Rate in the Debuncher-Accumulator at large stacks
 - Longitudinal cooling in the Recycler
- Longitudinal stochastic cooling of 8 GeV antiprotons in the Recycler is being replaced by Electron Cooling
 - Electron beam: 4.34 MeV - 0.5 Amp DC - 200 μ rad beam spread - 99% recirculation efficiency

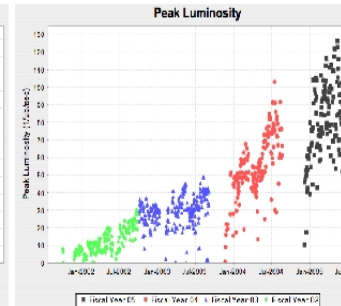
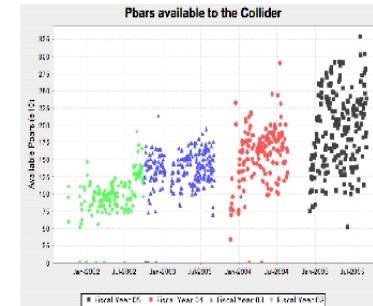


Antiproton Production - Slip Stacking

- Slip Stacking is the process of combining two Booster batches at injection into in the Main Injector to effectively double the amount of protons on the antiproton production target



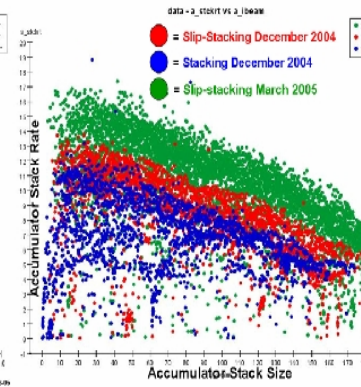
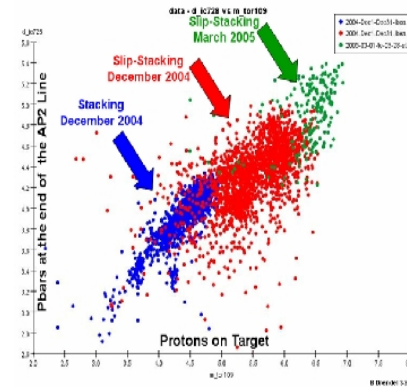
Antiprotons and Luminosity



- The strategy for increasing luminosity in the Tevatron is to increase the number of antiprotons
 - Increase the antiproton production rate (Run 2 Upgrades)
 - Provide a third stage of antiproton cooling with the Recycler
 - Increase the transfer efficiency of antiprotons to low beta in the Tevatron



Antiproton Production - Slip Stacking



Thomas Jefferson National Accelerator Facility



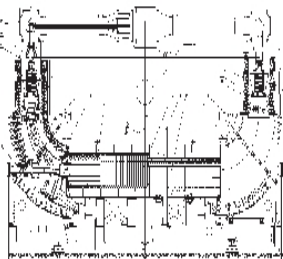
P03 Recuperation of electron beam in coolers with electrostatic bending V.Parkhomchuk BINP



Recuperation electron beam in the coolers with electrostatic bending

M. Bryzgunov, V. Parasyuk, V. Parkhomchuk, V. Reva, M. Vedenev

EC-300



Electron cooler EC-300 with the electrostatic bending

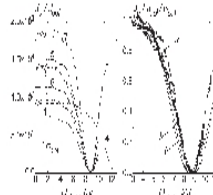
Collector



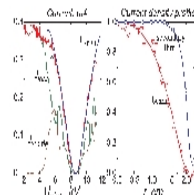
1. Last decelerator electrode
2. Collector input
3. Input collector electrode
4. Suppressor
5. Collector aperture plate
6. Magnetic flux concentrator
7. Collector surface
8. Cooling system

Profile of the secondary beam flux

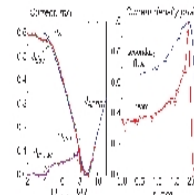
The initial profile of the fibre of the secondary system was estimated in this experiment after straightening from a product by modification of the longitudinal and circumferential. Circumferential and radial distance, using the primary system, were measured to the cell wall. Surface volume is defined as the horizontal diameter depending on the angle between the shear field on circumferential and radial distance of the secondary system. Figure 10 shows the loading sequence. Circumferential is an unusual replacement as the large loading system is observed. The initial profile of the fibre of the secondary system is obtained.



Before we can answer the question of why we have not found the expected pattern



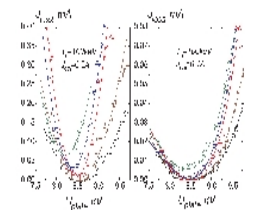
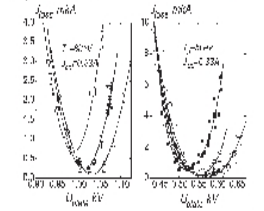
Measuring 7 in Table



Metering 6 in Table

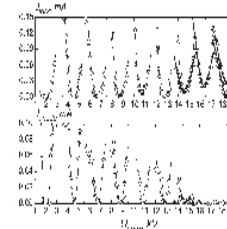
Optimal voltage on the electrostatic plates

Suppressor voltage

[illegible]

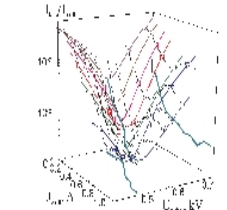
ECM. In fact, significant differences of the amount of collagen in the ECM were observed between the two groups. In the control group, the amount of ECM was 1.00 \pm 0.05 mg, while in the experimental group, it was 0.55 \pm 0.05 mg ($P < 0.001$). The amount of ECM in the control group was 100%, while in the experimental group, it was 55% of the control group. The difference in the amount of ECM between the two groups was 45% ($P < 0.001$).

Electron energy

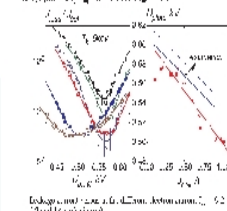


Let us now turn to the question of the form of the \mathcal{L} function. We shall assume that the \mathcal{L} function is of the form

Current



because of the lack of precise definition, the term is used in a variety of ways. In this paper, the term is used to refer to the



Excerpt from the 2000 Census, American Indian, Alaska Native, and Native Hawaiian population

Summary

The electron energy is fixed at a temperature of 300 eV (Fig. 2). The main part of the secondary electrons is returning and is collected on the collector and on the inner cone of the collector. There is much less their degree of axial efficiency (0.02–0.03). The energy profile of secondary electron flux depends on beam density profile width. The flux density in outer layer is equal on outer layer first inside. The important detail is presence of returning secondary electrons in small gap (0.25 mm) between the collector and wire and the hole.

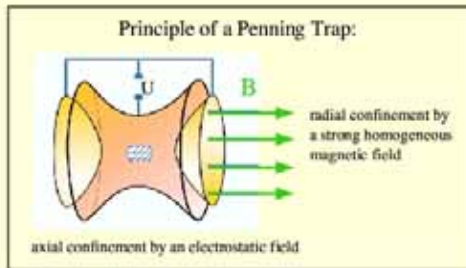
The optical plate voltage U_{opt} for helical current minimization are proportional to $1/\beta$ but the measured values U_{opt} correspond to varying of group relations which were less than the term energy U_0 , the observed energy still may be explained by current reduction of secondary electrons.

Magnetron recuperation levels at $T_{\text{rec}} = 717^{\circ}\text{K}$ change very rapidly with T_{rec} , i.e. are very sensitive to some change potential, but different recuperation levels apparently depend on the magnetic field. Optimum values $T_{\text{rec}}^{\text{opt}}$ independent of hour current $T_{\text{rec}}^{\text{opt}}$ at $T_1 = 24\text{ keV}$.

F05 electron cooling of highly charged ions in traps

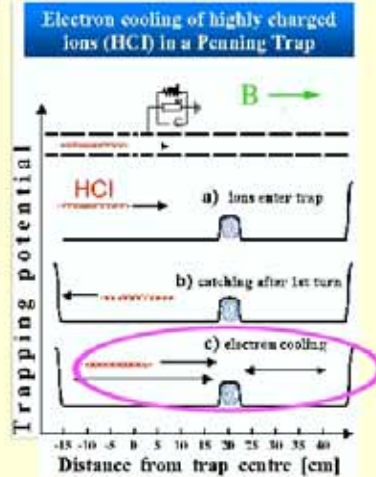
G.Zwacknagel, Erlangen U.

Electron Cooling in a Penning Trap



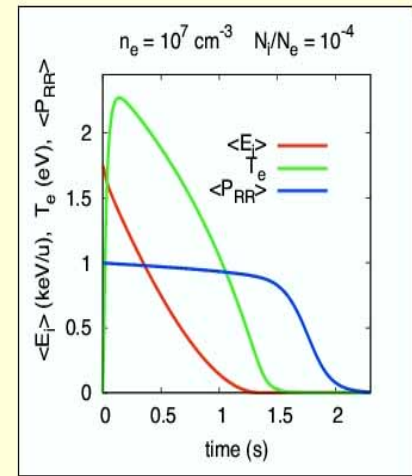
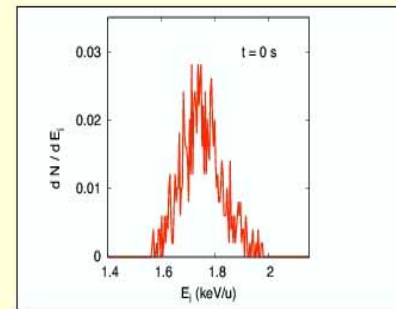
Typical parameters:

- $Z = -1, 1 \dots 92$
- $B \lesssim 6 \text{ T}$
- $T_{e,0} \approx 4 \text{ K}$
- $n_e \approx 10^7 \text{ cm}^{-3}$
- $N_e \approx 10^8 \dots 10^{10}$
- $N_i \approx 10^5$



Cooling of U^{92+} and heating of electrons

- U^{92+} , $T_e(0) = 4 \text{ K}$, $B = 6 \text{ T}$
- Initial ion distribution with $N_i = 500$ ions as obtained from ion optics simulations of the injection into the cooler trap for the HITRAP setup*



*F. Herfurth, private communications

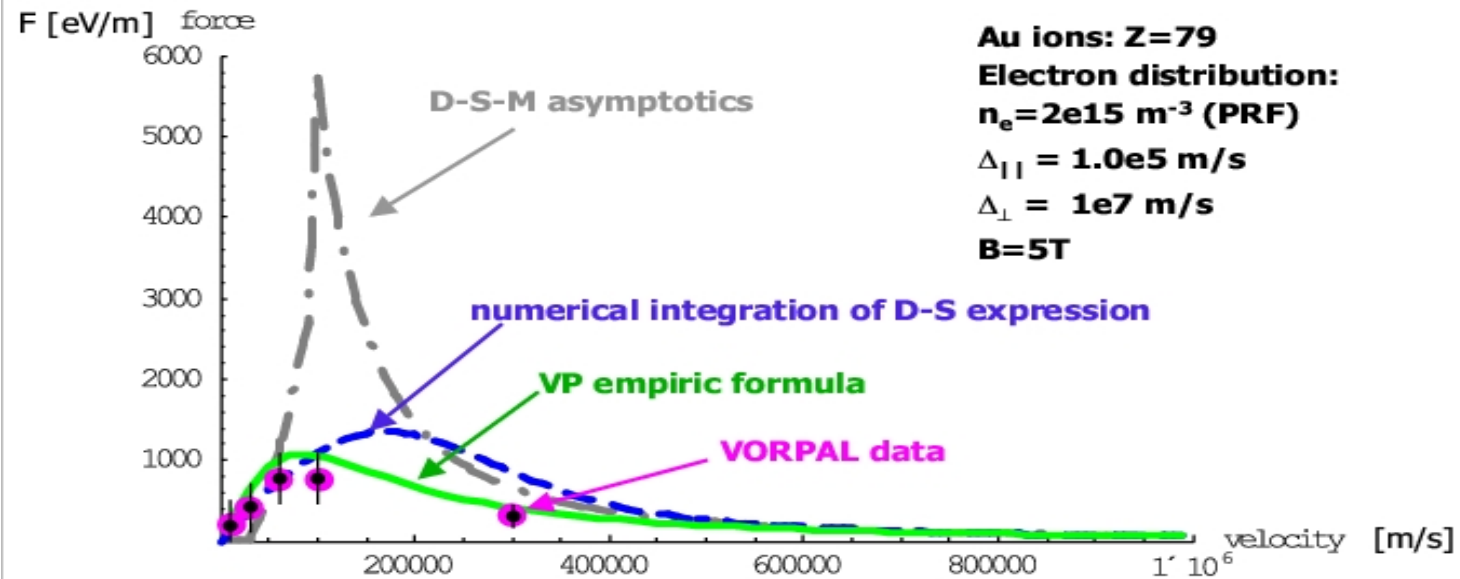
W06: Studies of electron cooling frictional force

A.Fedotov BNL

Friction force for ion velocity along magnetic field line

$$V_{\perp} = 0$$

15



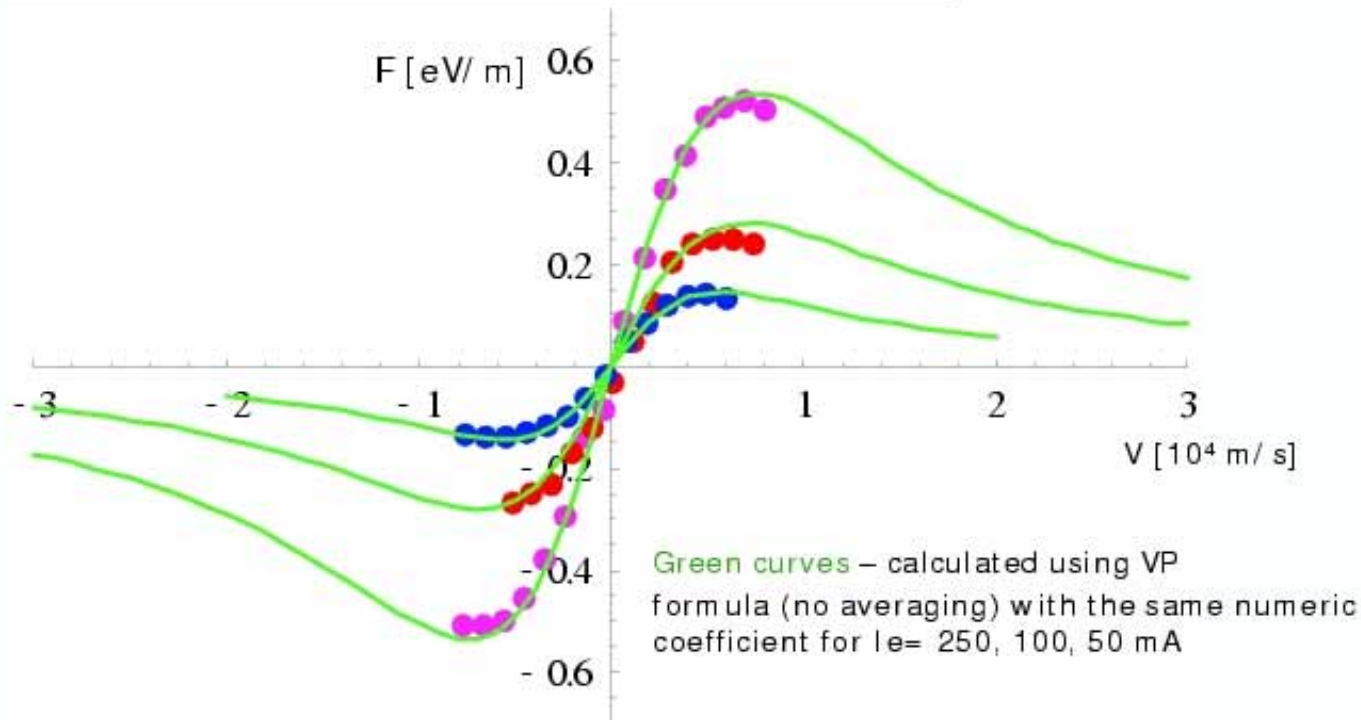
BROOKHAVEN
NATIONAL LABORATORY

COOL05, September 19-23, 2005

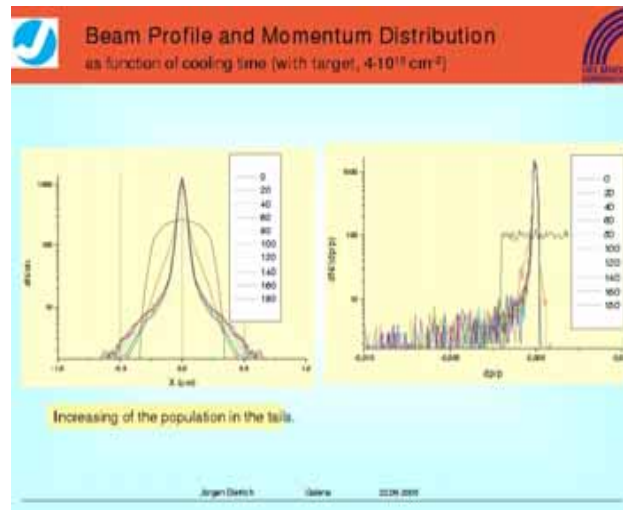
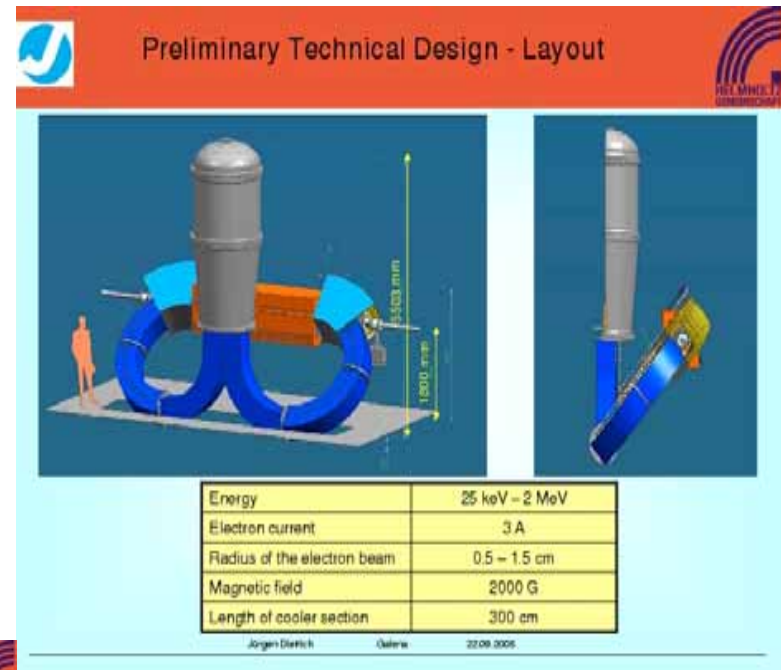
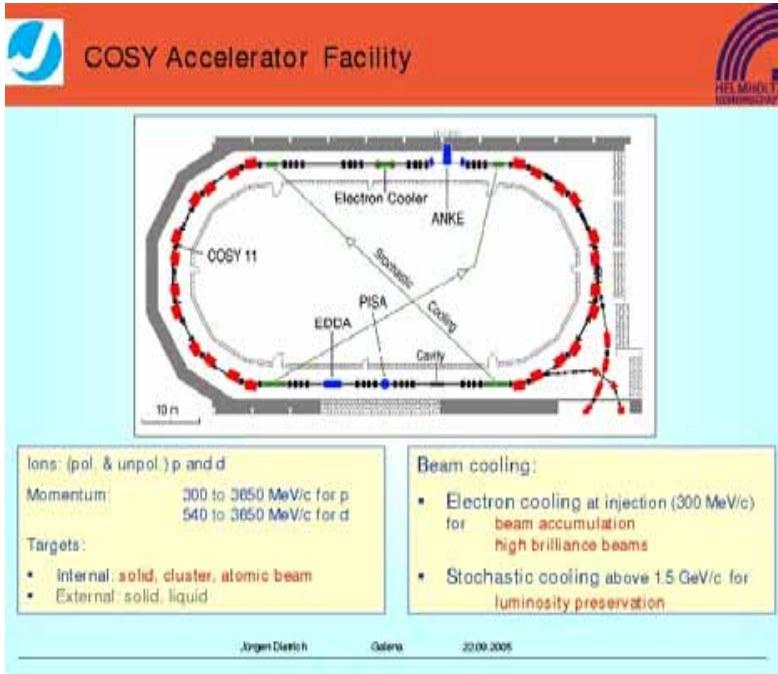


March 2 data: $B=0.1\text{T}$, electron current $I_e=250$ (pink color), 100 (red), 50 (blue) mA

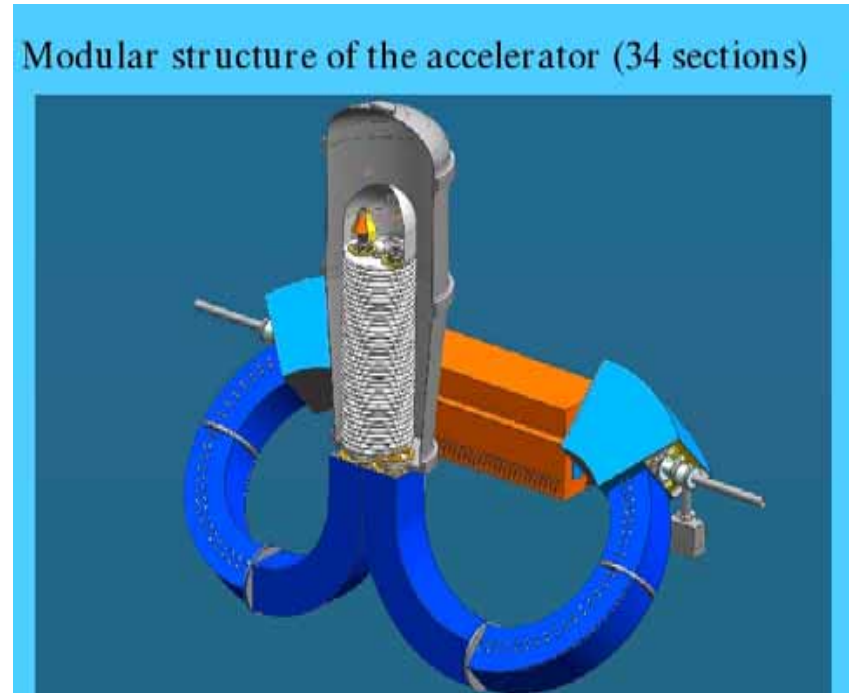
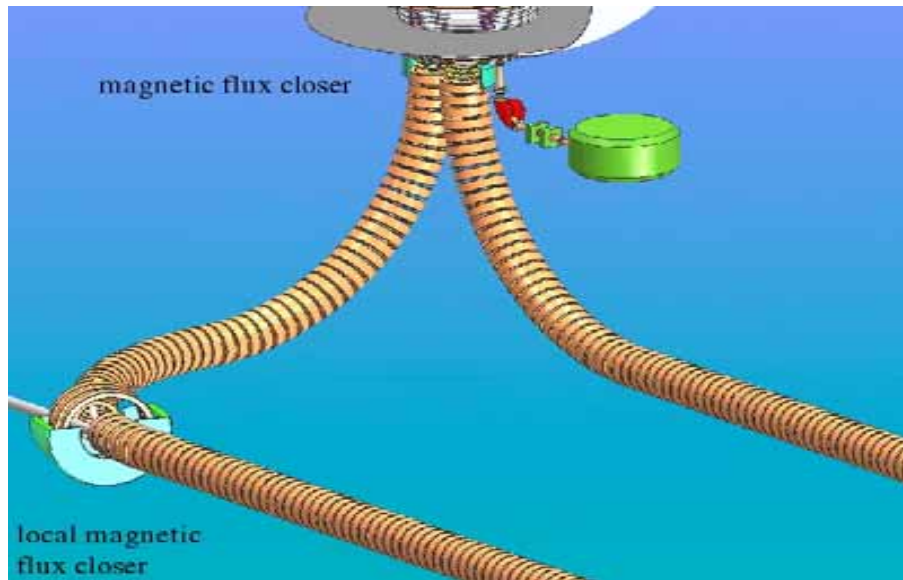
11



R10: COSY 2-MeV cooling system proposal J.Dietrich FZ/IKP

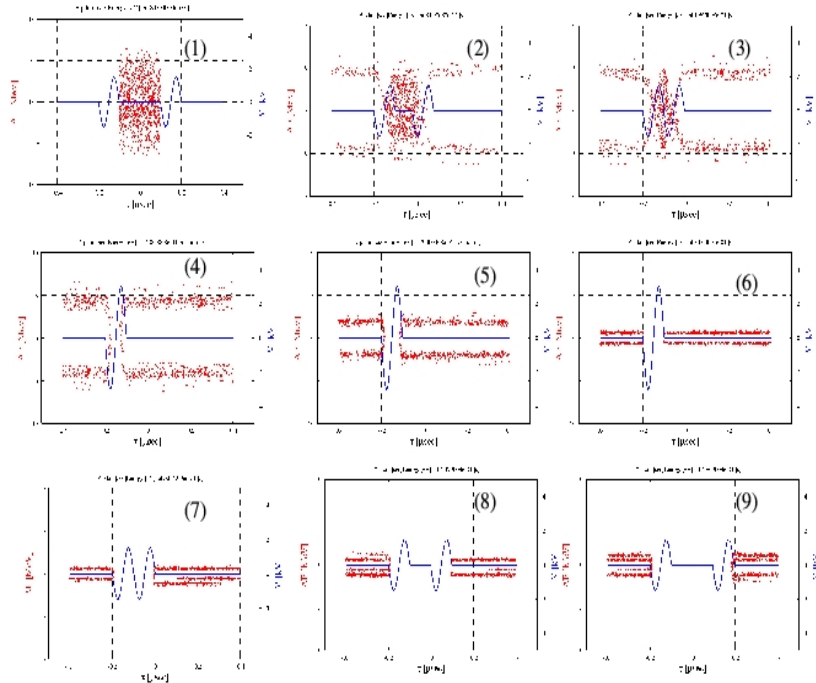


R11: Budker INP proposals for HESR and COSY electron cooling systems V.Reva BINP

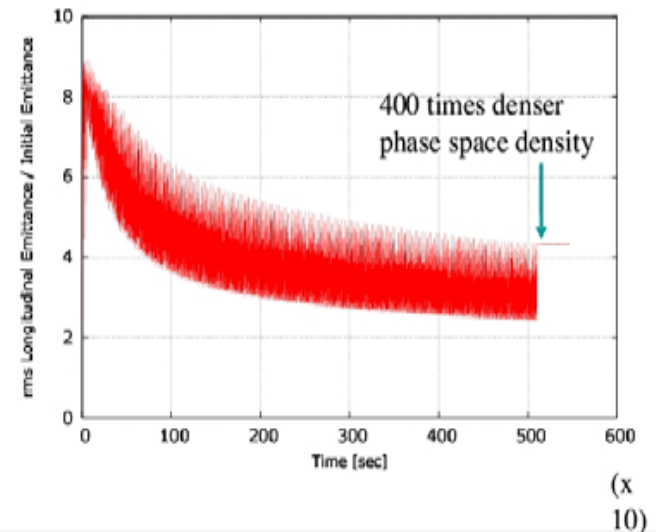


T05: Moving Barrier Bucket, T.Katayama GSI

Operational Scheme of Moving Barrier Bucket System



Variation of emittance during 1000 times injection

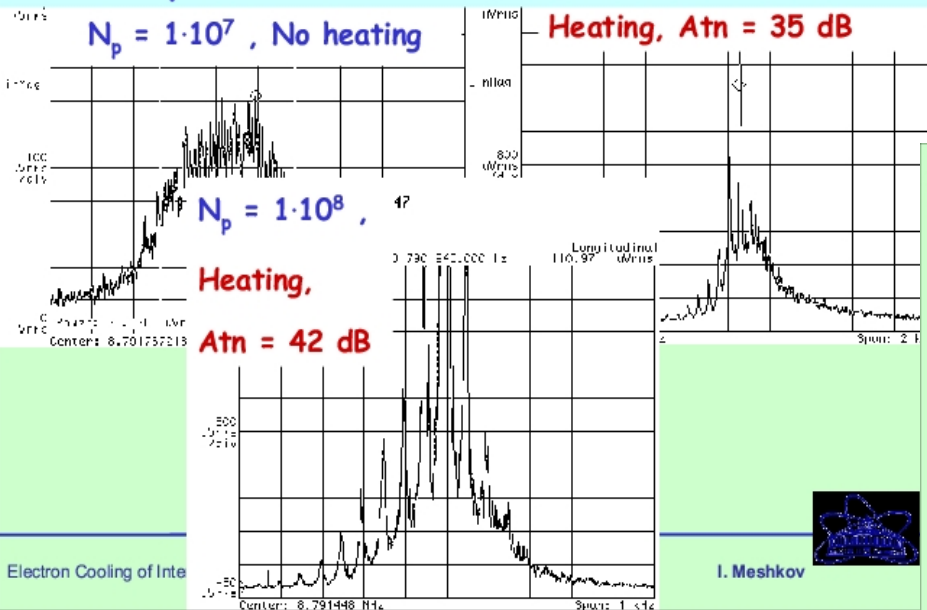


R06: electron cooling of intense ion beam I.Meshkov JINR

5.Coherent instability 5.4. IBS (?) and longitudinal modulation Influence of transverse heating

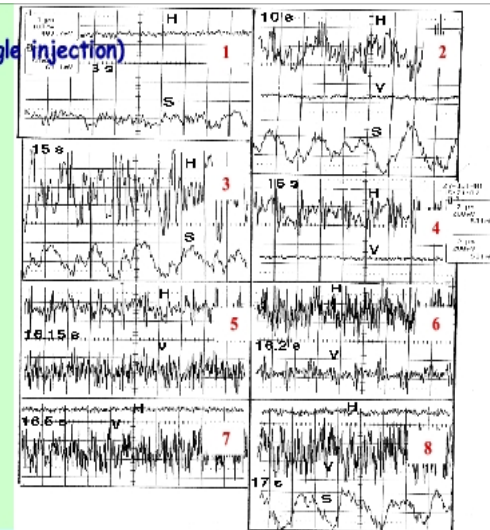
$(V_{\text{noise}})_{\text{rms}} = 6 \text{ V/Atn}$, $\Delta f = 0.1 - 2 \text{ MHz}$, $I_e = 250 \text{ mA}$
Atn = attenuation

Schottky noise: 18th harmonics, $f = 5.8 \text{ MHz}$



5.Coherent instability (single injection)

Coherent
instability
development
in COSY



Beam Position Monitor analog signals clearly demonstrating the collective oscillations of the p-beam: the signals from differential horizontal (H) and vertical (V) PU's and sum (S) PU.

Note: longitudinal oscillations (sum signal) appear together with horizontal one and present later on.

Electron Cooling of Intensive Ion Beam

COOL'05

I. Meshkov

September 2005 Galena, IL, USA

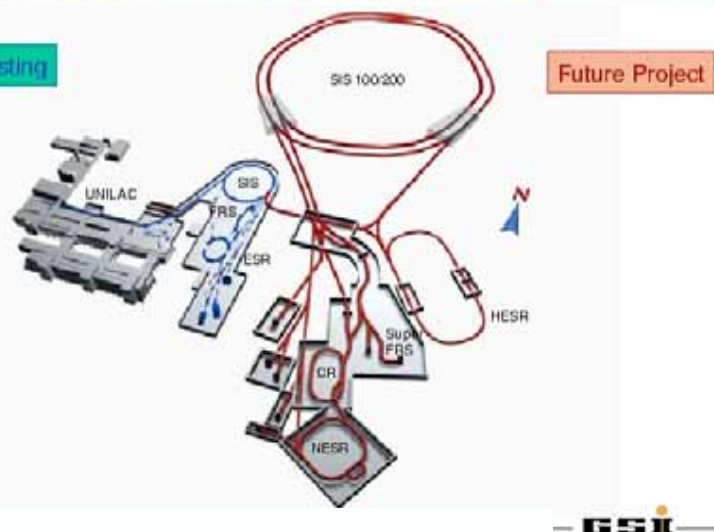


Thomas Jefferson National Accelerator Facility

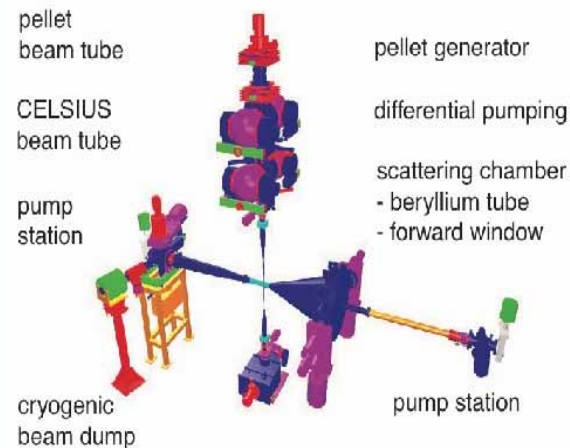


R09: HESR electron cooling proposal D.Reistad TSL

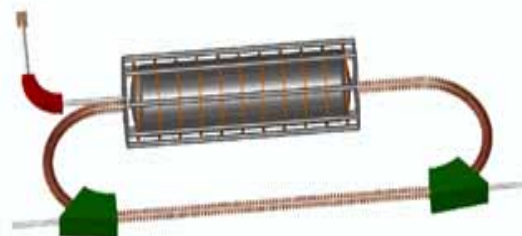
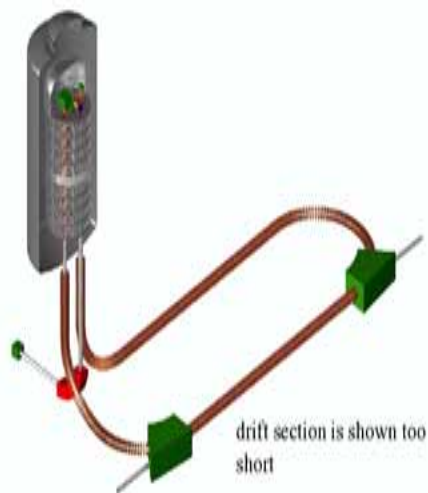
The Future International Facility at GSI:
Beams of Ions and Antiprotons



WASA Pellet Target



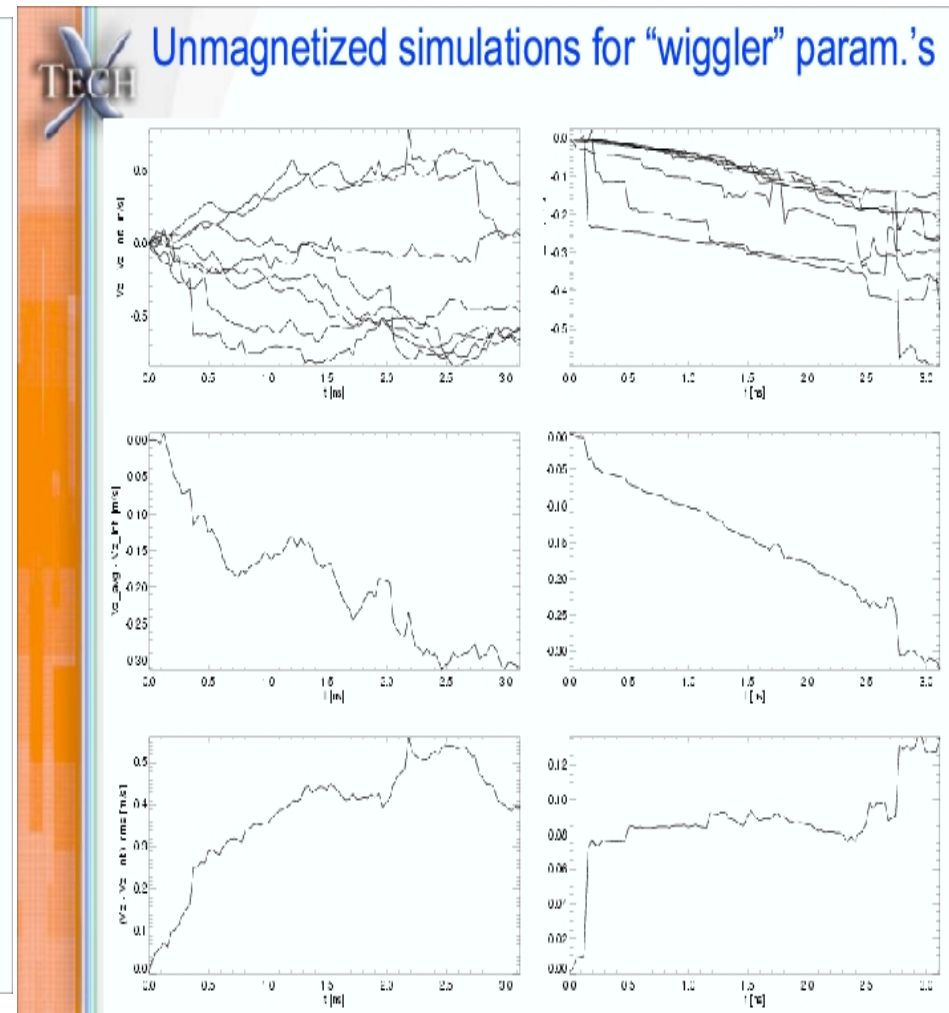
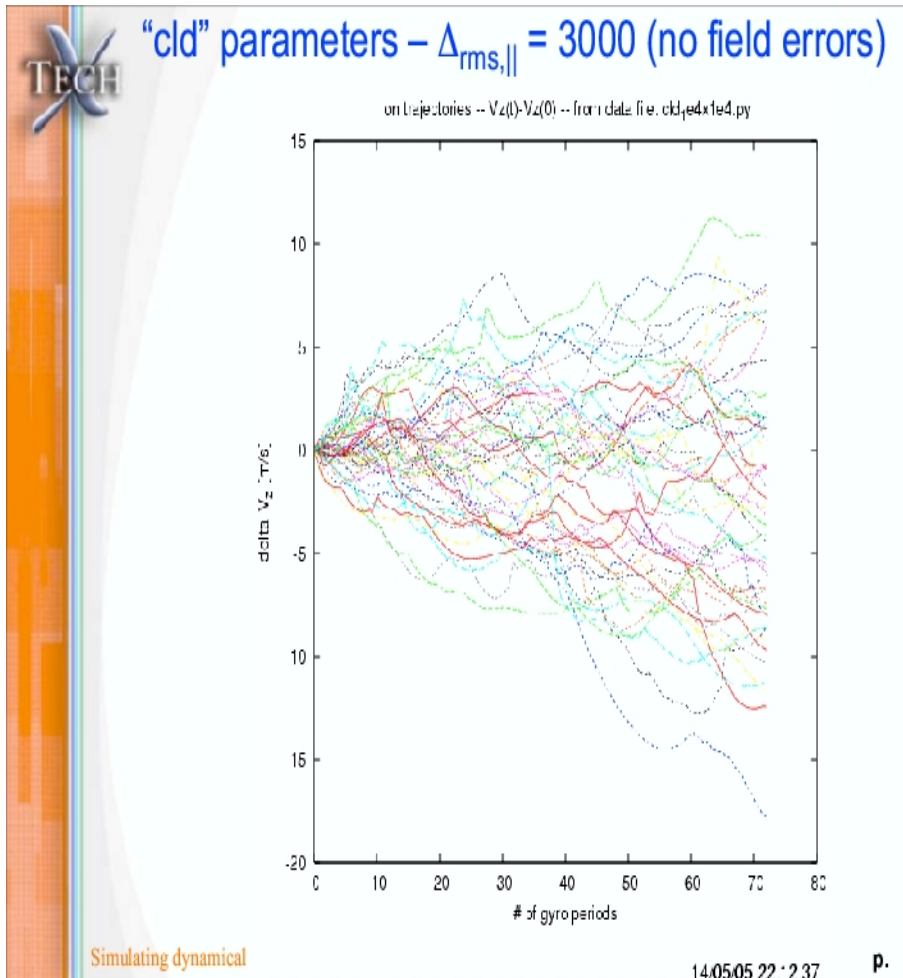
- access and availability restricted
- development of the PTS !



P18: cooling of ions & antiprotons with magnetized electrons G.Zwacknagel – Erlangen U.

[illegible]

W07: Simulationsof dynamical friction, D.Bruhweiler, Tech-X

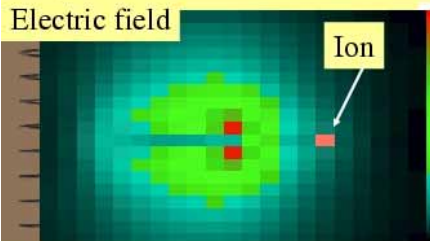


R01: Coolers with Hollow e beam & electrostatic cooling

V.Parkhomchuk BINP

Wave at electron beam by moving Bi ion

Electric field

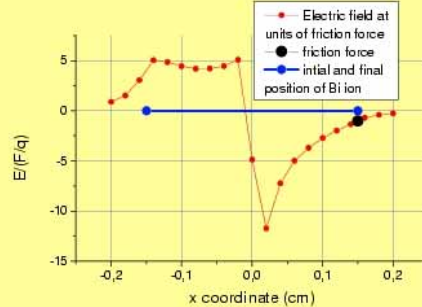


12

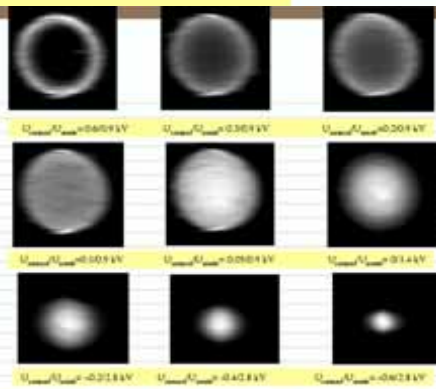
0



Red boat (as Bi ion) exit visual wave



Electric field around moving ion Bi at plane (color map) and along axis (down figure)



Electron beam distribution for different voltage on the control electrode and the anode.

How to proceed for cooling high ion beam current?

→ **Hollow electron beam!**

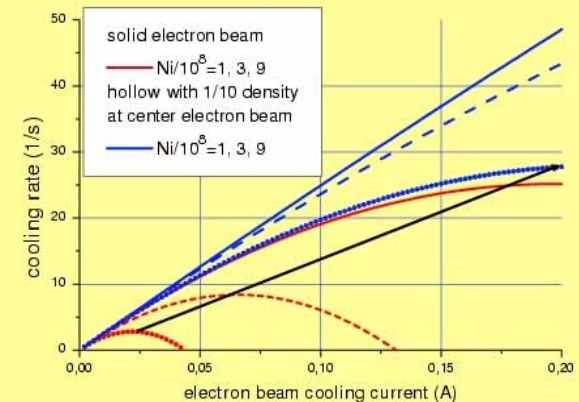
$$\lambda = \lambda_0 (1 - \omega_i^2 \omega_e^2 \tau^4 * k)$$

k=1 N=9E8 optimum cooling 0.025 A only
k=0.1 optimum 0.2 A

$$\omega_e^2 - \downarrow$$

$$\omega_i^2 - \uparrow$$

Decreasing electron beam density results to Increasing threshold ion beam density



P13: electron beam profile monitoring with OTR at the E-cooling facility A. Warner, FNAL

f

Fermi National Accelerator Laboratory

OTR MEASUREMENTS AND MODELING OF THE ELECTRON BEAM PARAMETERS AT THE E-COOLING FACILITY

A. Warner¹, A. Burov¹, K. Carlson¹, G. Kazakevich², S. Nagaitsev¹, L. Probst¹, M. Sutherland¹, and M. Tiunov²

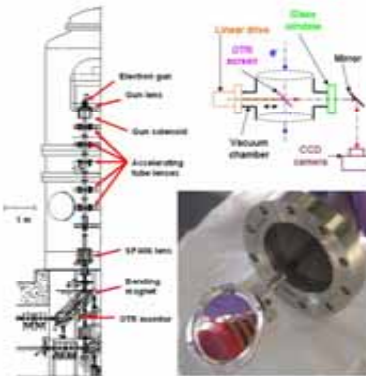
¹FNAL, Batavia IL, U.S.A., ²BINP, 630090 Novosibirsk, Russia

ABSTRACT

Parameters of the electron beams accelerated in the Pelletron, intended for the electron cooling of 5.5 GeV antiprotons in the Fermilab recycler storage ring, have been studied. The parameters were measured under the accelerating section using an Optical Transition Radiation (OTR) monitor. The monitor employs a highly-reflective 2 inch-diameter aluminum OTR-screen with a thickness of 5 μ m and a digital CCD camera allowing operation with good linearity and good space resolution. The measurements were done in a pulsed mode in the current range of 0.05-0.5 A and at pulse durations ranging from 1 μ s to 5 μ s. Modeling of the beam dynamics from the Pelletron cathodes to the OTR monitor was done on the basis of ULTRASAM [1] and BEAM [2] programs. An adjustment of the magnetic fields in the lenses of the accelerating section was done in the simulations. Simulated electron beam parameters characteristics of the accelerating section were compared with measured parameters and demonstrated good agreement.

INTRODUCTION

Optical transition radiation monitors are being used to image the transverse profiles of the 4.5 MeV electron beam in signal-pulse mode for modeling of the beam dynamics in the electron cooler at Fermilab. The linear response of OTR monitors to beam shape, the high optical resolution and the fact that the radiation is prompt has several advantages over more traditional imaging devices. The transition radiation is produced by the charged particles as they traverse the boundary between media with different dielectric constants, for example a metal or dielectric foil to vacuum [1]. For relativistic electron beams, transition radiation can be measured with readily available equipment and imaging techniques. The imaging system used in the FNAL set-up consists of digital CCD cameras connected to computers via IEEE 1394 firewire interfaces. This provides the operator with real-time beam images and tools for image analysis and measurements of the beam's dynamic properties as a function of the optics of the acceleration. The OTR diagnostic systems used at the cooler are designed to be constantly used to optimize the beam transport and to measure the transverse beam size and shape with a resolution down to 22 μ m. Very thin (7 μ m) aluminum foils are being used to reduce the background signal due to beam scattering and bremsstrahlung radiation. In this report we describe the system, measured results obtained in data and compare with results of simulation the beam dynamics in DC mode.

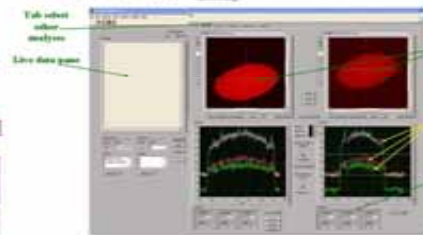


Left side: Experimental set-up.
Right side: Schematic layout of the OTR monitor and photo of the OTR screen.

The beam diagnostic studies are done with the Pelletron in pulse-signal mode with the bending magnet turned OFF. This allows accelerated beam to be passed straight on to the OTR monitor. The residual field in the bending magnet is compensated with a coil mounted in the bending magnet. The 2" in diameter OTR screen is made from a mirror-coated 3 μ m aluminum foil laminated onto a ring support. The linear drive provides insertion of the OTR screen into final position for the measurements with good accuracy. The CCD camera has an objective with focal length F=23 mm, relative apertures F=1.4.

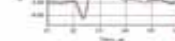
DATA ACQUISITION

The images taken from the optical monitors are digitized in the CCD camera and stored in an uncompressed format. In addition, the IEEE 1394 (fire-wire) allows control of the camera's gate and other features remotely. The images are then displayed and analyzed with proprietary software that was developed using LabView and DataGrip common utility tools. The program allows the user to display live (real-time) images of the beam and to simultaneously analyze other current level data or stored data from files. Two profiles taken with different pulse durations or optical settings can also be compared. This type of development differs from the standard application in that it incorporates image digitization, image display, as well as image analysis and system calibration in a real-time mode. These image analysis tools are used to combine techniques that compute position and measurements based on the gray-level information of the image pixels. Linear (interpolation) filters can be applied to remove unwanted background at any stage of the analysis of monitor.

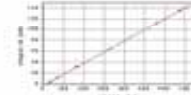


MEASUREMENTS

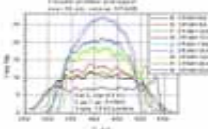
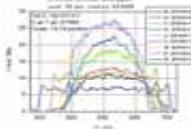
Pulsed beams with duration of 2 μ s and 1 μ s are extracted and beam size and profile are measured as a function of the Pelletron gun current which is varied by changing the pulse voltage of the gun control electrode. The subtraction is done to avoid effect of shape varying of the gun optics caused by limits of accelerating voltage.



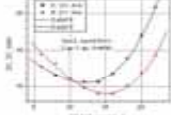
Shape of the pulse-signal beam current



OTR monitor demonstrates good linearity versus beam current and relatively weak dependence of sensitivity to the beam position over the surface area of the monitor.

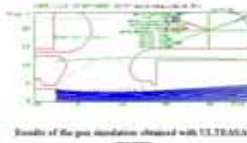
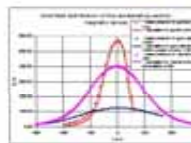


Results of the processing of measured with the OTR monitor beam profiles versus SPADs current (X and Y extracts for the beam image) is shown in these figures.



Figures show measured the X and Y beam profile size versus the SPADs lens current

SIMULATIONS

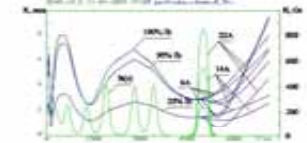


Results of the gun simulation obtained with ULTRASAM program.

Adjusted magnetic field distribution in the lenses of the accelerating section obtained using LAM program and used for simulation of the beam dynamics from the cathode to the OTR monitor.

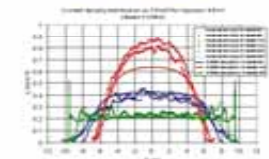
Electron trajectories are shown with blue lines; border of electrodes and the equipotentials are shown with red lines; distributions of the electric and magnetic fields are plotted with green and gray lines respectively.

In the right upper corner one can see the beam phase picture at the gun exit (20-40 mm). In this picture with blue line plotted the beam current density, red and green lines shows the axial and radial velocity distributions.



The electron beam envelope versus SPADs current for full beam current, 95% of the beam current and 25% of the beam current respectively, calculated using BEAM program. Blue lines show the envelopes, green lines show distributions of the strength of the axial magnetic field.

COMPARISON MEASUREMENTS & SIMULATIONS



Measured (dots) and calculated (solid lines) beam profiles for the SPADs current values of 4 A (blue color), 18 A (red color) and 22 A (green color). The resulting was done to transform the elliptic coordinates to axial based on the measured horizontal and vertical size of the electron beam.

SUMMARY

OTR monitoring and data acquisition systems have been developed for analysis of beam dynamics with operation of the Pelletron in the pulse-signal mode. Using these systems measurements were done of the beam profile distributions of the Pelletron accelerating section at the OTR screen location. Modeling of the beam dynamics in DC mode from the cathodes to the OTR screen was done using ULTRASAM and BEAM programs.

Measured results shows good agreement with the modeling. This demonstrates that the developed systems operating in the pulse-signal mode provides results important for the beam dynamics analysis at the E-cooling facility.

BIBLIOGRAPHY

1. M. Tiunov, *ULTRASAM - 3D code package for simulation of high-energy electron beam dynamics in the recycler storage ring*, FNAL Report, 1997.
2. A. Burov, *BEAM - 3D code package for simulation of high-energy electron beam dynamics in the recycler storage ring*, FNAL Report, 1997.
3. A. Burov, *3D code package for simulation of high-energy electron beam dynamics in the recycler storage ring*, FNAL Report, 1997.
4. A. Burov, *3D code package for simulation of high-energy electron beam dynamics in the recycler storage ring*, FNAL Report, 1997.
5. A. Burov, *3D code package for simulation of high-energy electron beam dynamics in the recycler storage ring*, FNAL Report, 1997.

electrostatic rings

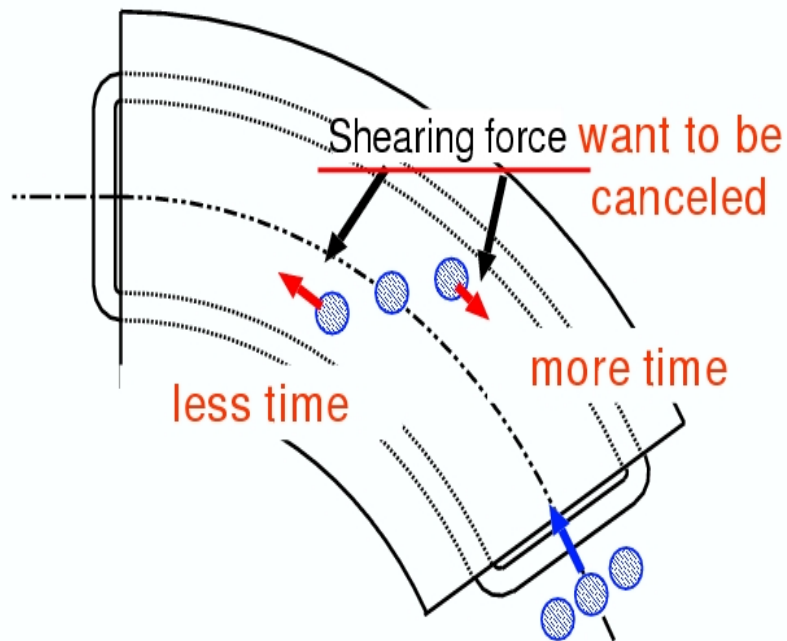


Thomas Jefferson National Accelerator Facility



M12 Dispersion Control: M. Tanabe - Kyoto

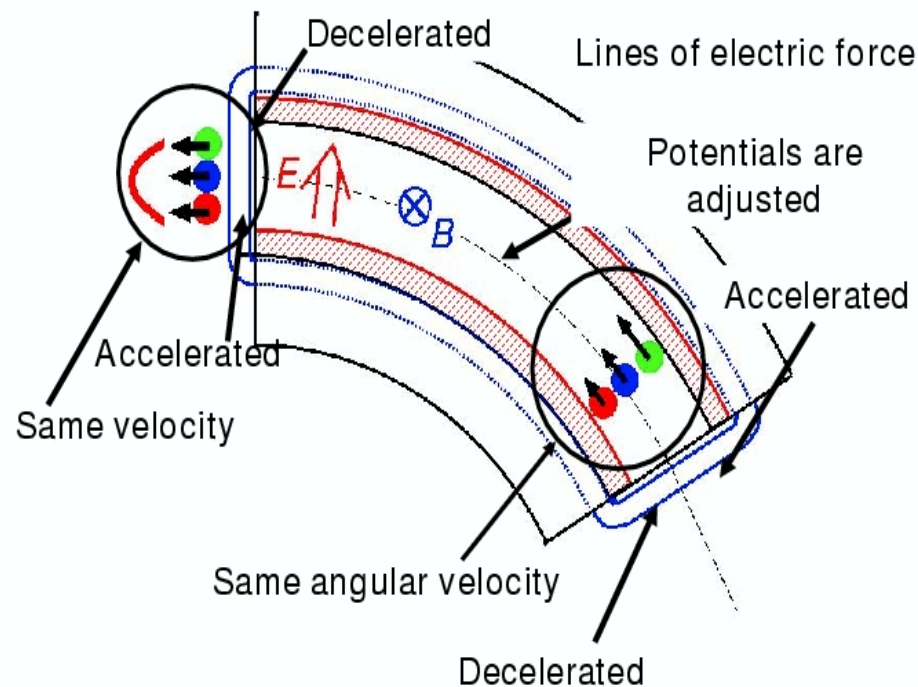
Issue in storing ordered beam



Ordering particles at a bending section

COOL05, 19-23 Sep. 2005 @Eagle Ridge Resort and Spa, Galena Illinois, The United States

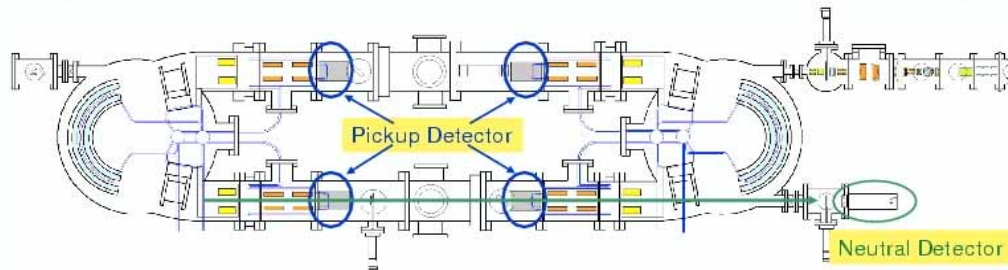
How to overcome 'Shearing force'



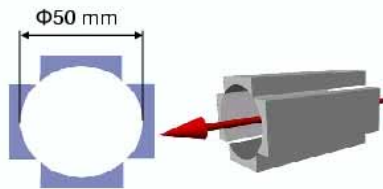
COOL05, 19-23 Sep. 2005 @Eagle Ridge Resort and Spa, Galena Illinois, The United States

W01: LN2-cooled electrostatic ring T.Azuma TMU

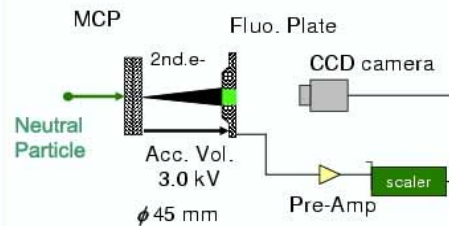
Monitor for Beam Diagnosis



Pickup Detector x 4

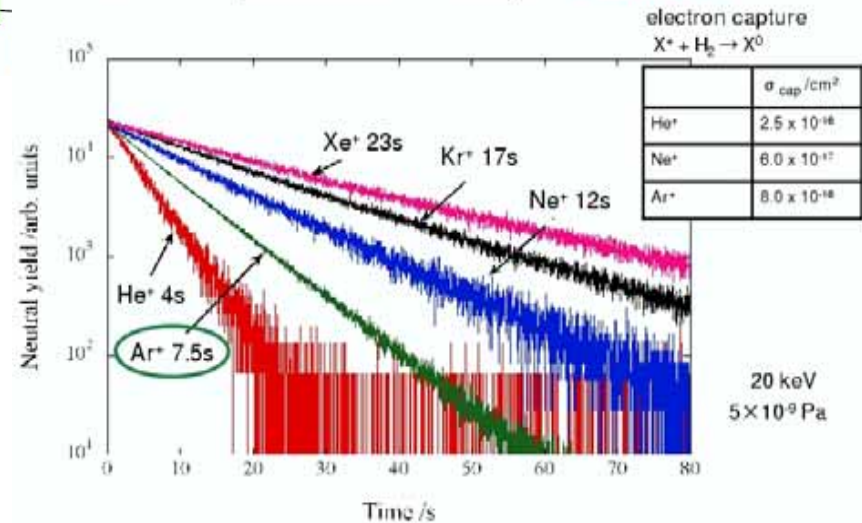


Neutral Detector x 1



Storage Time of Rare Gas Ions

$\sim 5.0 \times 10^{-9}$ Pa, observation of storage = \sim a few min.



Why Electrostatic Rings?

Using electrostatic optics, rather than magnets, in a low-energy storage ring has some advantages, and also some disadvantages.

The main issue, at least in our case, is cost. A pair of deflection plates is much cheaper than a magnet. They also take less space and are lighter, allowing a more compact overall design.

Heavy singly charged ions in a small ring are slow, and for slow particles the magnetic force, which is proportional to v , is small. This is, however, not an obvious argument as it may seem, since the only consequence is that heavy particles are slower in a magnetic ring than in an electrostatic ring.

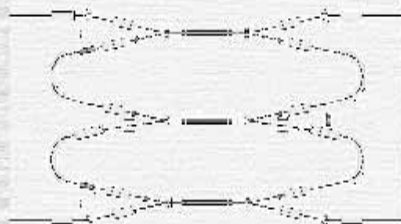
Voltages are independent of mass for a given potential, which makes selection of ions comparatively simple.

There are fewer design factors for electrostatic rings and less experience in building them. Also, electrostatic elements tend to have larger tolerances than magnetic ones.



Ring Layout

	Ring 1	Ring 2	
160° cylindrical bends	2	2	Platform voltage: $< 25/100$ kV
Quadrupole doublets	4	4	Electrode voltage: < 16 kV
10° deflections	4	2	Beam energy: $5-100$ q keV
Variable deflections	6	6	Ion mass ratio: $1-20$ ($q = \pm 1$)
Symmetries	2	1	



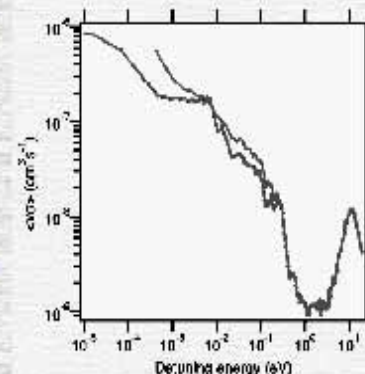
Low Temperatures

The rings will be cooled with cryogenerators to 5–10 K.

This will allow internal degrees of freedom of (infrared-active) molecular ions to cool radiatively, and ions produced in a cold ion source will stay cold. Also, the vapour pressure of all gases except H_2 and He is below 1×10^{-13} mbar at $T < 18$ K.

Development in atomic and molecular physics since 1990: Cooled ions \rightarrow cold electrons (~ 20 K) \rightarrow low quantum states. Figure shows rate for $H_3^+ + e^- \rightarrow H_2 + H$ with ions from hot plasma source/cold expansion source.

DESIREE will allow measurements as a function of temperature by controlling the cryostat temperature from room temperature and down.



McGill et al., PRA 70, 052715 (2004)

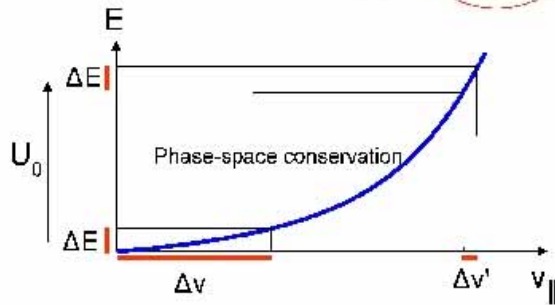
W04: Ultra-cold electron target D.Orlov, MPI-K

Electron beam formation

Acceleration

Magnetic adiabatic expansion

$$kT_{\parallel} \text{ reduction: } k_B T_{\parallel} \equiv \frac{k_B^2 T_C^2}{2eU} \left(C \frac{e^2}{4\pi\epsilon_0} n_e^{1/3} \right)$$

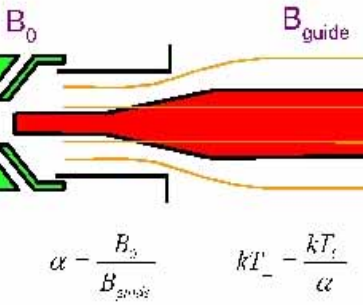


$C = 1.9$ - fast acceleration

$C < 1.9$ - slow (adiabatic) acceleration

$$kT_{\parallel} = 0.1 \text{ meV}$$

$$kT_{\parallel} \ll kT$$



Thermocathode $kT_C = 110\text{-}120 \text{ meV}$

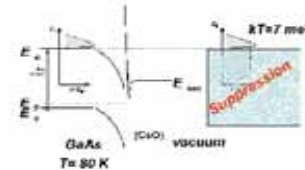
$\alpha = 20$ $kT_{\perp} = 5\text{-}6 \text{ meV}$

$\alpha = 90$ $kT_{\perp} = 2 \text{ meV (CR)}$

Photocathode $kT_C = 10 \text{ meV}$

Electron beam from photocathode

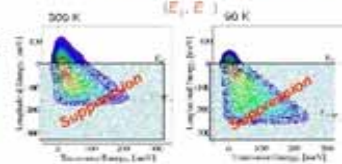
Photocathode principle



Strong energy and impulse relaxations
enlarge electron energy spreads in vacuum

Fully activated cathode: QY = 20-30%

Energy distributions of photoelectrons
2D-measurement



Suppression

Energy spreads about kT

QY = 1 %

Laser power (660 nm) for 1 mA: $< 1 \text{ W}$
Efficient heat transfer from the cathode

D. A. Orlov et al., Accel. Phys. Lett. 78 (2001) 27.

laser cooling



Thomas Jefferson National Accelerator Facility



F04: cooling techniques for trapped particles Y.Yamazaki RIKEN

Why? CPT: $p\mu^-$ vs $p\mu^+$ \bar{H} vs. H

Plank mass $M_{pl} = \sqrt{\hbar c/G} = 10^{19} \text{GeV}/c^2$

$(m_p/M_{pl}) m_p \sim \text{vibrational level } 10 \text{ KHz}$

traps



Thomas Jefferson National Accelerator Facility



F01: Laer cooling for 3D crystalline state at S-LSR

A.Noda, Kyoto ICR

• Compact Cooler Ring S-LSR

- Circumference 22.56m
- Straight Section Length 1.86m

• Two e-cooling modes

- Protons 7MeV ($E_e=3.8\text{keV}$)
- $^{12}\text{C}^{6+}$ 2MeV/u ($E_e=1.1\text{keV}$)

• Laser cooling

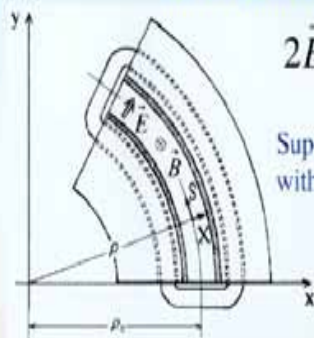


23, September, 2005

Aki

Lattice without Momentum Dispersion

(M. Ikegami et al. Phys. Rev. ST-AB. 7, 120101)



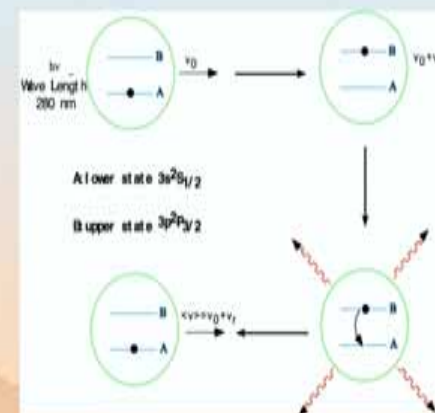
$$2\vec{E}(\rho_0) = -(\vec{v}_0 \times \vec{B})$$

Superposition of Electric Field
with Magnetic Field

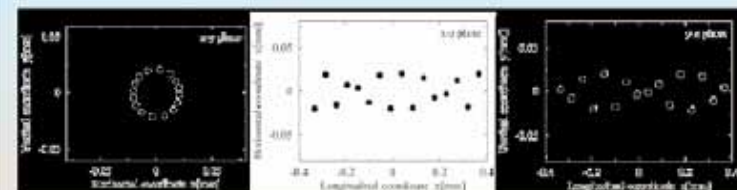
- 1] W. Hennelberg, Ann. D. Physik **19**, 335 (1934).
- 2] W.E. Millett, Phys. Rev. **74**, 1058 (1948).

Akira Noda, COOL05 at Brookhaven
Fig.

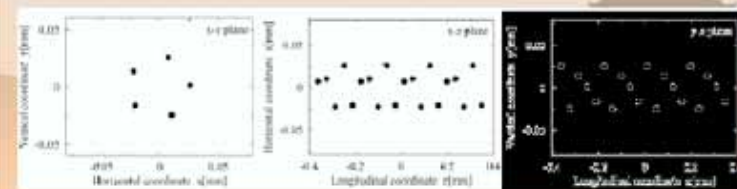
Principle of Laser Cooling (Longitudinal)



$\lambda=0.975$



$\lambda=1.22$



23, September, 2005

Akira Noda at COOL05 Eagle Ridge Inn, IL, USA

37



Thomas Jefferson National Accelerator Facility

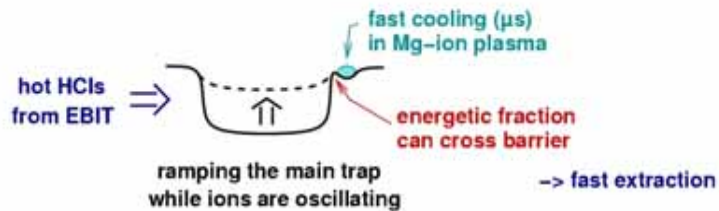




ion-ion cooling and stopping the idea

precision Penning-trap mass measurements of short-lived nuclei
require high charge states \rightarrow charge breeding
and cold ions \rightarrow fast cooling without charge exchange

\rightarrow fast cooling of $\sim 1\text{eV}$ HCLs in a continuously laser-cooled
Mg-ion cloud or crystal

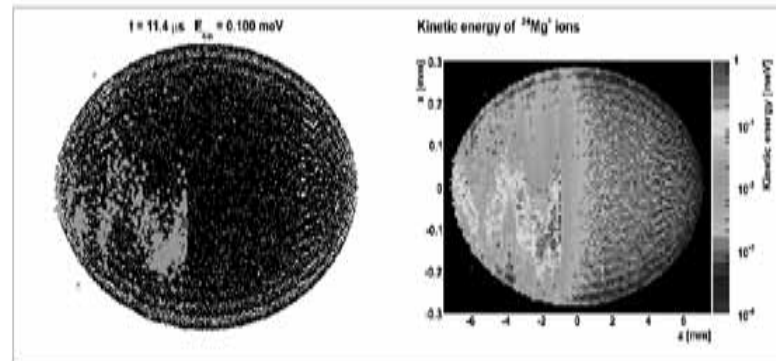


<http://www.hq.jlab.org/accel/beam/da/cooling.html>



ion-ion cooling and stopping MD simulation results

energy deposition can be compensated
by continuous laser cooling



green dots mark
Mg-ions above 0.1 MeV
 \rightarrow kicked out of the lattice

\rightarrow stopping of the HCL in $\sim 10 \mu\text{s}$

<http://www.hq.jlab.org/accel/beam/da/cooling.html>

F02: Laser cooling of relativistic heavy ion beams

U.Schramm LMU

Laser cooling of relativistic heavy ion beams

Why laser experiments under such 'extreme' conditions ?

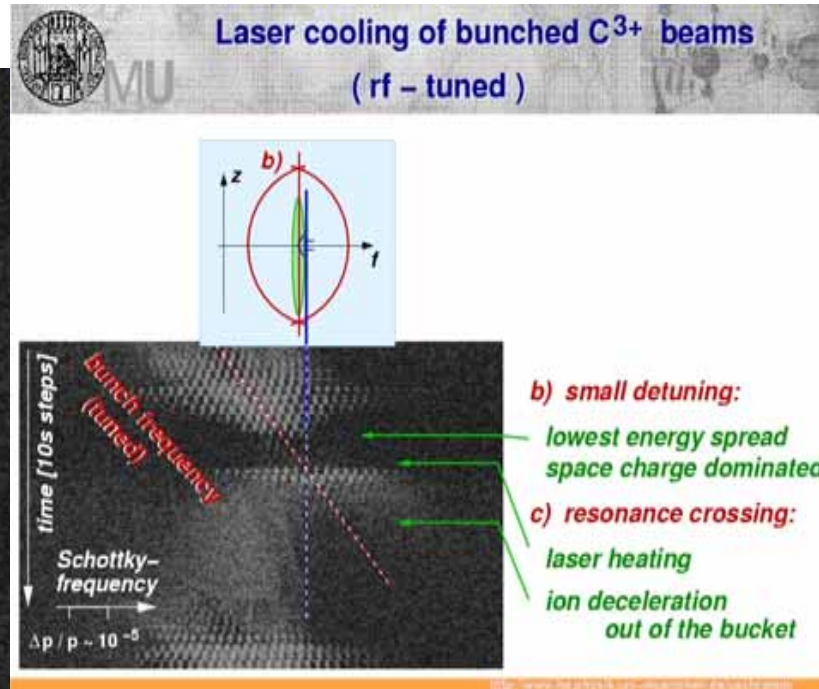
$$\omega_{out} \sim (2\gamma)^2 \omega_{in}$$

$$\omega_0 \sim (2\gamma) \omega_{in}$$

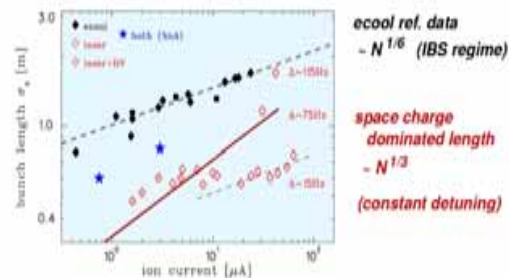
-> huge Doppler shift
and pulse shortening

-> laser spectroscopy of heavy few-electron systems

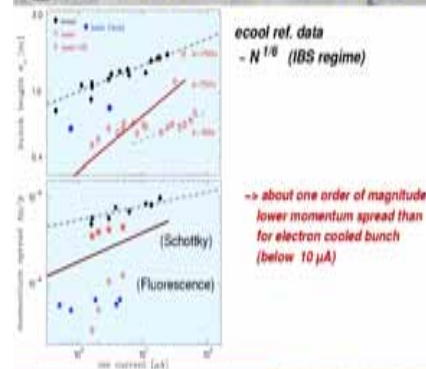
-> short pulse (high intensity) interaction studies



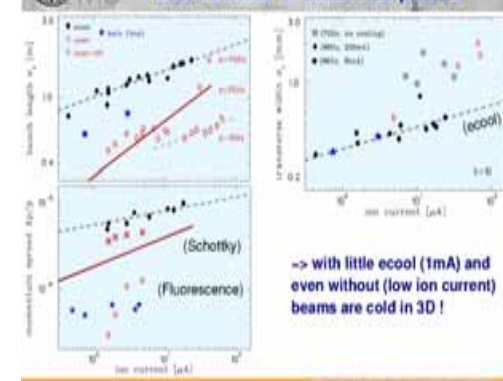
Laser cooling of bunched C^{3+} beams laser vs electron cooling - bunch length



Laser cooling of bunched C^{3+} beams laser vs ecool - momentum spread



Laser cooling of bunched C^{3+} beams laser vs ecool - transverse profiles



phase space manipulations



Thomas Jefferson National Accelerator Facility



M14 Transverse Echo Measurements in RHIC W.Fisher, BNL

Motivation

- IBS growth rate measurements usually done by observing the free expansion of bunches
 - Must be on time scale of interest [15min at injection, hrs at store]
 - Need precise emittance measurement [not easy transversely]
- Echo measurements are
 - Much faster (~1000 turns), allow parameter scans
 - Potentially very sensitive
 - Do not rely on precise emittance measurement

Transverse echoes – dipole moment simulation

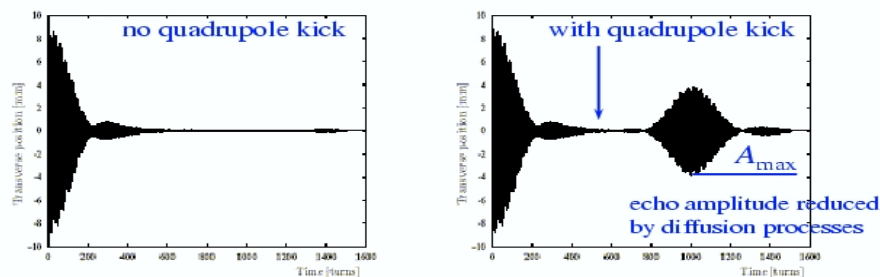


Figure 3: Left: The dipole moment of the distribution versus time after a dipole kick. Right: The same signal with an additional quadrupole kick at 500 turns after the dipole kick.

[W.Fischer, B. Parker, O. Brüning, "Transverse echos in RHIC", proceedings of the US-LHC Collaboration Meeting: Accelerator Physics Experiments for Future Hadron Colliders, BNL (2000).]

Transverse echoes – phase space simulation

US-LHC Collaboration Meeting: Accelerator Physics Experiments for Future Hadron Colliders, BNL, 2000

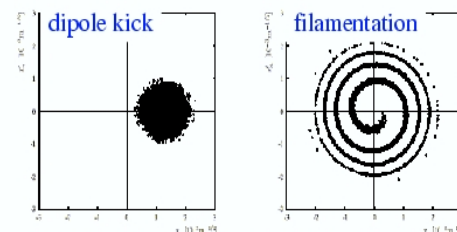
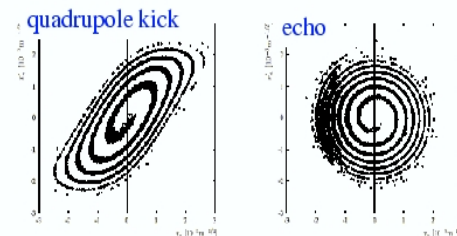


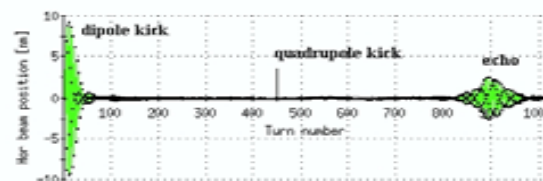
Figure 1: Left: Horizontal particle distribution in normalized phase space after the initial dipole offset. Right: The same distribution 500 turns later.

- 1-turn quadrupole kick is difficult
- echo-like signal was also observed with 2 dipole kicks of different strength (F. Ruggiero, SPS)



Summary – Transverse Echoes in RHIC

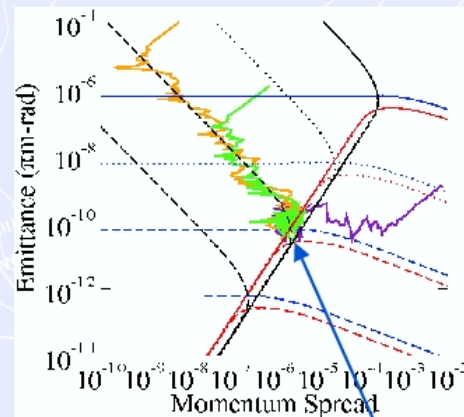
- Transverse echoes observed in RHIC with Au^{79+} , Cu^{29+} , p^+
 - Dipole kick with injection under angle
 - Air core quadrupole provides 1-turn kick
- Diffusion with p^+ stronger than with heavier ions (unexpected)
- Observed intensity dependent echoes with Au^{79+} , Cu^{29+} ,
→ were fitted to simulation results to extract diffusion rates



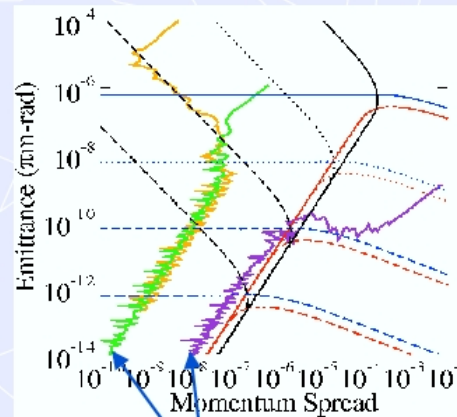
M15 Simulation of Beam Dynamics in Cooler Rings, A.Smirnov - JINR

Analytical and MD simulation of IBS for ESR

Equilibrium between ECOOL and IBS



Ordered state of ion beam



Equilibrium between
IBS and Cooling

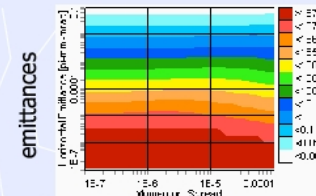
Ordered state

13

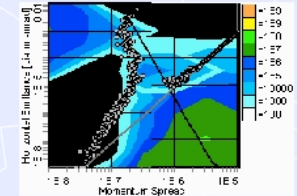
Ordered beam simulation for COSY

$N_p = 1e6$

IBS growth rates
(Martini model)

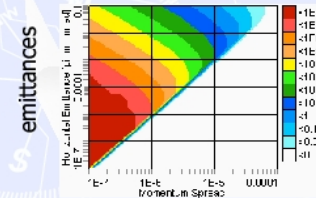


MD simulation

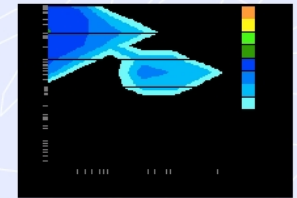


transverse

momentum spread

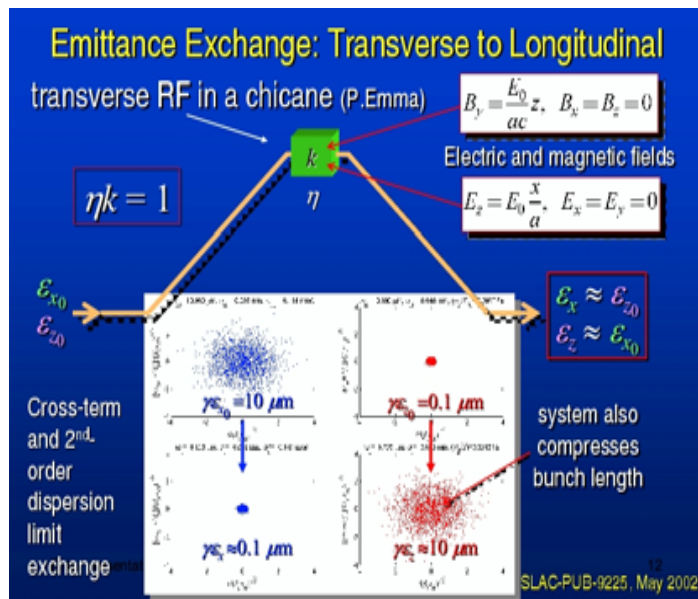


longitudinal

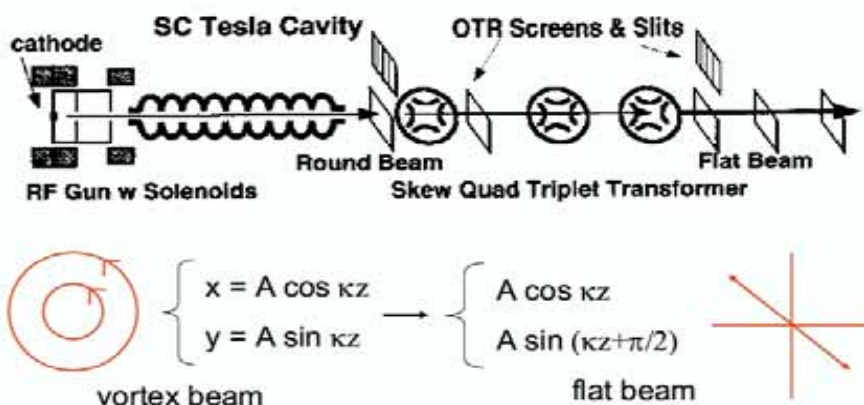


16

M10 Phase Space Manipulations, K.-J.Kim, ANL



Schematics of Flat Beam Experiment at FNPL



K.J.K., COOL05, 9/18-23/05

14

Minimum Achievable Pulse Length

(M. Borland)

Electron beam energy

$$\sigma_{x, \text{array}} = \frac{E}{V h \omega_0} \sqrt{\sigma_{y', \text{e}}^2 + \sigma_{y', \text{rad}}^2}$$

Deflecting rf voltage & frequency

Unchirped e-beam divergence (typ. 2~3 $\mu\text{-rad}$)

Divergence due to undulator (typ. ~5 $\mu\text{-rad}$)

For 6 MV, 2800MHz (h=8) deflecting system, get ~0.4 ps!

Normal APS bunch is 40 ps rms

K.J.K., COOL05, 9/18-23/05

35



Thomas Jefferson National Accelerator Facility



7. Conclusions

for

Transverse-Longitudinal Correlations: FEL

Performance and Emittance Exchange

- If conditioning can be achieved it would have a very large impact on FEL performance.
(Li-Hua Yu, Whittum).
- Conditioning without growth of effective emittance is possible in a symplectic system (Vinokorov, Wolski).
- It appears to be difficult (but maybe not impossible) to achieve the amount of conditioning likely to be required by real FELs (Kim, Emma, Wolski et al).
- Non-conventional (laser/wiggler (Zholents), laser backscattering (Schroeder), and laser-plasma (Wurtele and Penn) conditioning holds promise.
- Emittance transfer would benefit x-ray FELs (Kim)
- Emittance transfer from a large emittance to a small emittance is possible (Wei and Okamoto)
- Practical emittance transfer schemes have yet to be developed (but no one has even tried yet).

Laser-Wiggler Conditioner

Proposed by Sasha Zholents

Use a laser/wiggler rather than an rf cavity

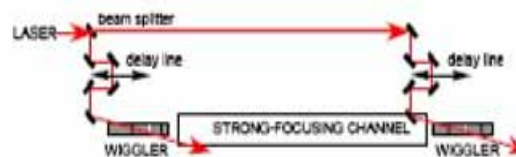
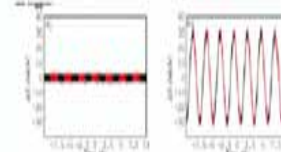


Figure 2. A schematic of the laser assisted conditioner.

Laser-Wiggler Conditioner (Cont)

- Some electrons gain energy and some lose energy. Only about 1/2 are conditioned.



Plasma Channel Conditioner

Work by Jonathan Wurtele, Gregg Penn, and myself.

Send a laser through a gas in a tube. Blow out all the electrons and make an ion channel. Send the high energy beam just behind the laser before the slow electrons return.

In the plasma channel $\beta = (2\gamma)^{1/2}c/\omega_p$
where $\omega_p = 6 \times 10^{12}(n(\text{cm}^{-3})/10^{16})^{1/2}$ and $\lambda_p = 2\pi c/\omega_p$

For example at $n = 10^{17} \text{ cm}^{-3}$ and 1 GeV, $\omega_p = 2 \times 10^{13} \text{ s}^{-1}$,
 $1/\omega_p = 50 \text{ fs}$, $\lambda_p = 100 \mu\text{m}$, and $\beta = 0.1 \text{ cm}$

Simulations, to follow, by Gregg Penn. Two cases (similar to Zholents and Emma and Stupakov [a FOFO channel at 100 MeV])

Clearly at 100 MeV only condition a small time slice.

rings



Thomas Jefferson National Accelerator Facility



P09: electron cooling for cold beam synchrotron for cancer therapy V.Vostrikov BINP

Electron Cooling for Cold Beam Synchrotron for Cancer Therapy

B.I. Grishanov, V.V. Parkhomchuk, S.A. Rastigeev, V.B. Reva, V.A. Vostrikov, BINP, Novosibirsk
Masayuki Kumada, NIRS, Chiba

Clinical spec: 2 fixed port (horizontal & 45 degree), 1 gantry
Type of particles: C energy 140-400 MeV/unit.
Average dose rate: 5 Gy/min
Field size: 15 cm x 15 cm
Dose uniformity: 4% of the prescribed dose over treatment field
Delivered dose accuracy: 2%
Irradiation method: Revised spot scanning system with synchronization of respiration

Electron Cooling is a key CBS Feature

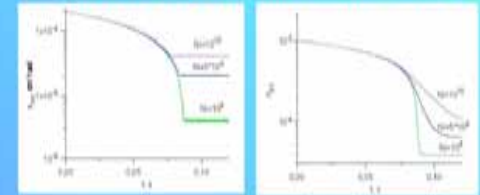
Storage of intense ion beam, 10^{10} per cycle
Decreasing of Aperture; MR and HEFT, Gantry
Slow extraction on recombination
Slow "pellet" extraction (up to 10^4 pellets)
Small aperture fast scanner
Precision scanning of beam energy

CBS electron cooler design based on EC-300 manufactured by BINP for IMEP, China

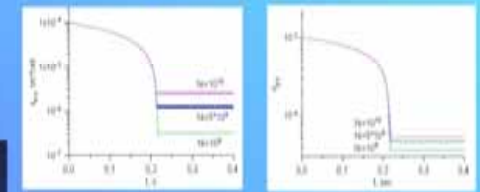
Electron Cooler Parameters

Length: 10.2 m
Cooling length: 7 m
Quality of the magnetic field: 10^{-4} or better
Power of magnetic system: 250 kW
SEB: 1.2 m \times 3 at standard pressure
Water: 500 L/min
Old cooling system
Vacuum: 10^{-5} - 10^{-6} torr

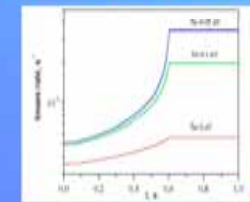
Storage & Cooling at Injection Energy 30 MeV/u



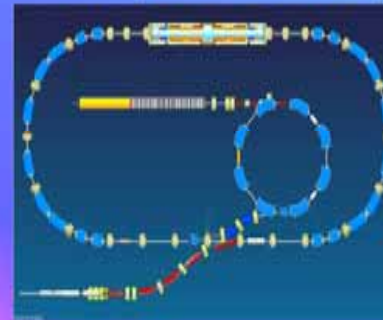
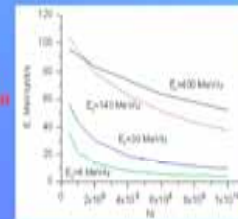
Cooling at Maximum Energy 400 MeV/u



Slow Extraction by Recombination



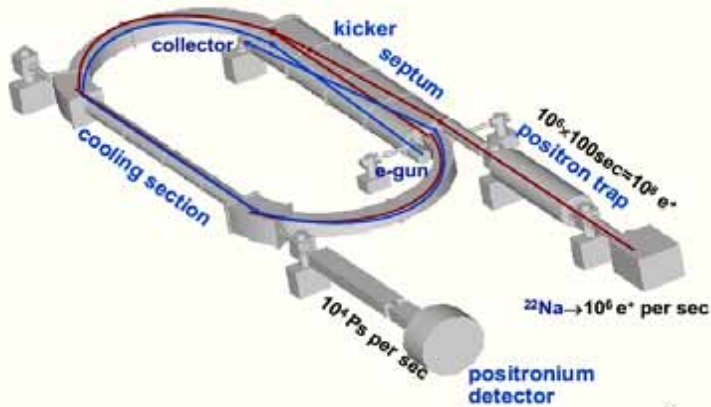
Precise Ion Energy Scanning by Electron Energy Change



Low aperture gantry



Design of the LEPTA



Helical quadrupole “stellarator windings”

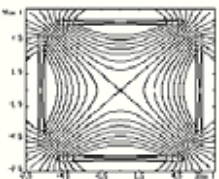


Quadrupole Length $L = 160 \text{ cm}$

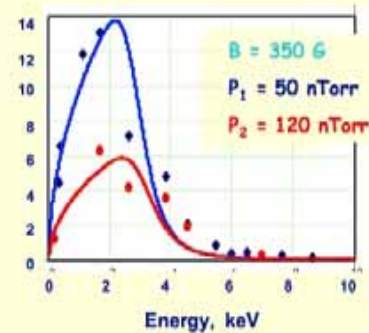
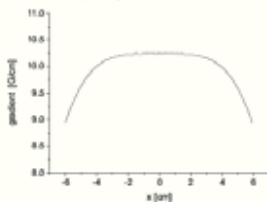
Helix step $h = 80 \text{ cm}$

$$G = \frac{2\pi NI}{c \cdot d^2}$$

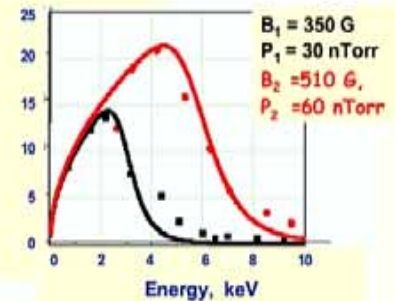
Cross section of the quadrupole is similar to Panofsky lens



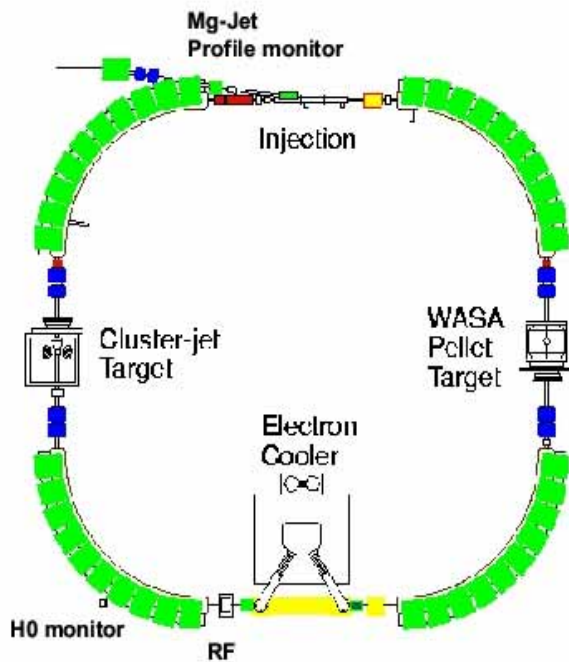
Uniform gradient magnetic field inside aperture



$\Delta B/B \sim 20\%$



The CELSIUS Ring

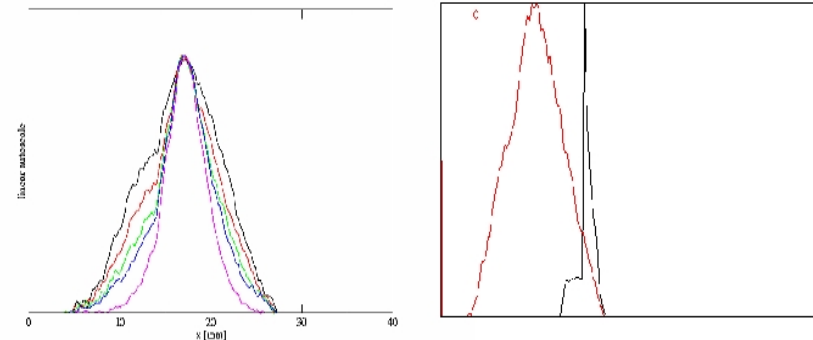


- Last CELSIUS run in June 2005
Now dismantled
- WASA to COSY, Jülich

Circumference	81.8 m
Length of cooling and injection straight sections	9.6 m
Length of target straight sections	9.3 m
Bending radius	7.0 m
Maximum rigidity	7.0 Tm
Maximum kinetic energy (protons)	1.36 GeV
Maximum kinetic energy per nucleon for ions with $Q/A = 1/2$	470 MeV

Transient cooling measurements

Transverse Mg-Jet profiles



0.3 s between profiles (total 1.5 s)

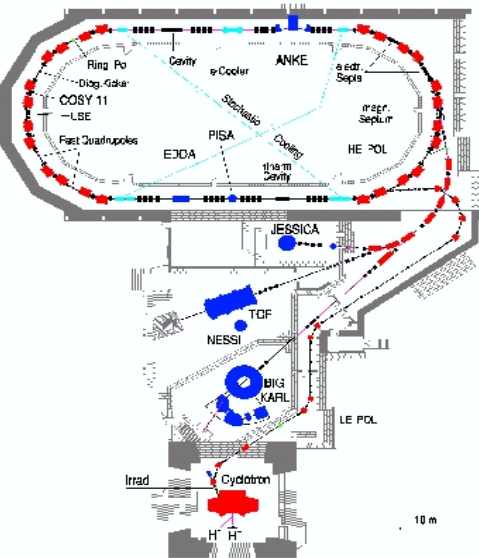
Time between frames 0.3 s. Total ~60 s

Cooling of core vs . tails

Electron current 10 mA and proton current 0.3 mA, $N_p = 1.7 \cdot 10^9$.

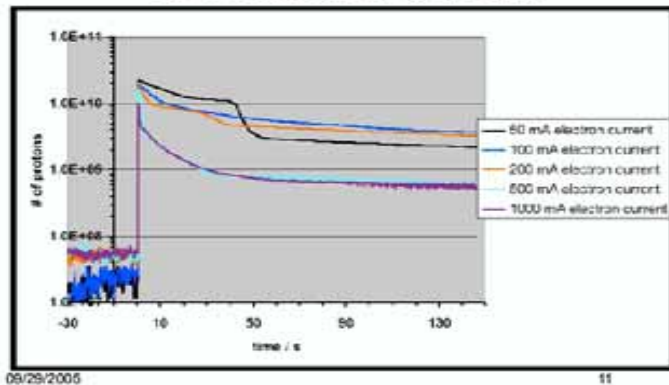
Can be used in comparisons of calculations with IBS models.

The Accelerator Facility

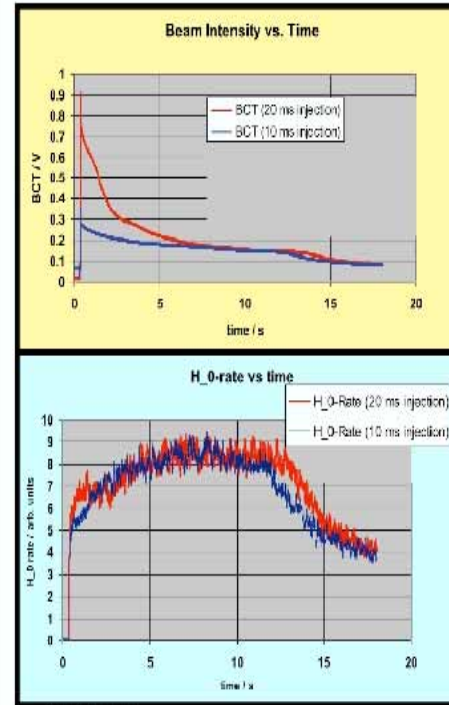


- COSY accelerates (polarized) protons and deuterons between 300 and 3700 MeV/c
- 4 internal and 3 external experimental areas
- Electron cooling at low energy
- Stochastic cooling at high energies

Proton intensity as function of time and electron current



Observation of initial losses

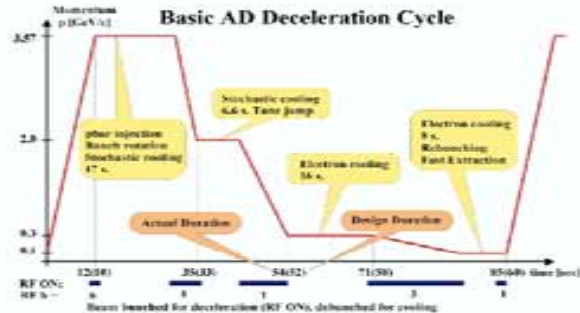


Initial losses disappear at smaller injected proton beam emittance

⇒ Protons outside the electron beam see a non-linear focussing by the electron beam

M08 Antiproton Decelerator

P. Belochitskii, CERN

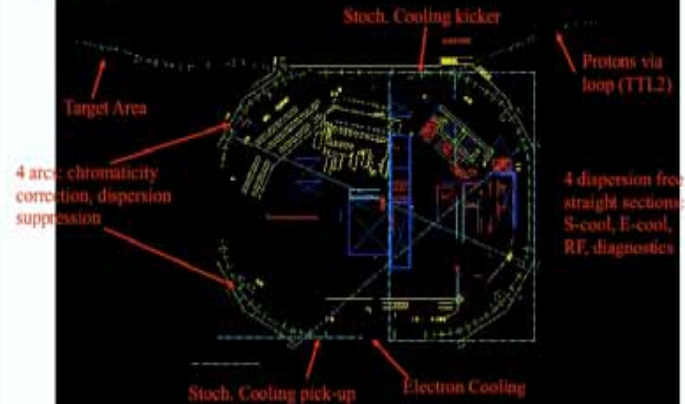


COOL05

P. Belochitskii 19 September 2005



AD Ring and Hall



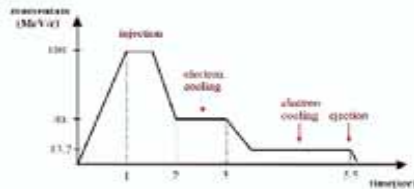
COOL05

P. Belochitskii 19 September 2005



Schematic view of ELENA cycle

- No electron cooling is performed at injection energy: beam is cooled already in AD. After injection beam is decelerated immediately.
- One intermediate cooling (at 40 MeV/c probably) is needed to avoid beam losses



COOL05

P. Belochitskii 19 September 2005



Requirements to ELENA:

- Compact machine located inside of AD Hall with minimum of reshuffle.
- Energy range from 5.3 MeV (AD extraction energy) down to 100 keV.
- Equipped with electron cooler to make beam phase space smaller in about two orders of magnitude with respect what we have today
- Machine assembling and commissioning has to be done without disturbing current AD operation.

COOL05

P. Belochitskii 19 September 2005



Thomas Jefferson National Accelerator Facility



M06 FAIR project

M.Steck, GSI

The New FAIR Accelerators

Goals:

High beam intensity
High beam energy
High beam quality

Synchrotrons

SIS100

SIS300

HESR

Storage Rings

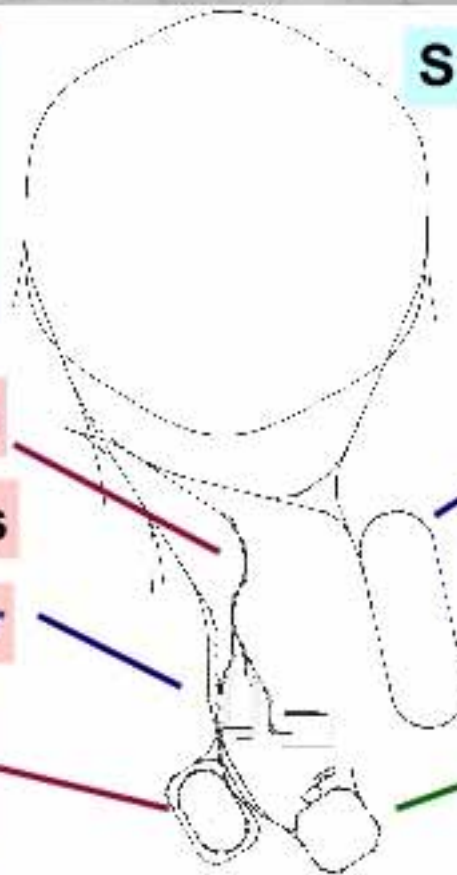
NESR

SuperFRS

Separators

pbar separator

CR-complex
(CR, RESR)



GSI

M. Steck, COOL05, September 19-23, 2005

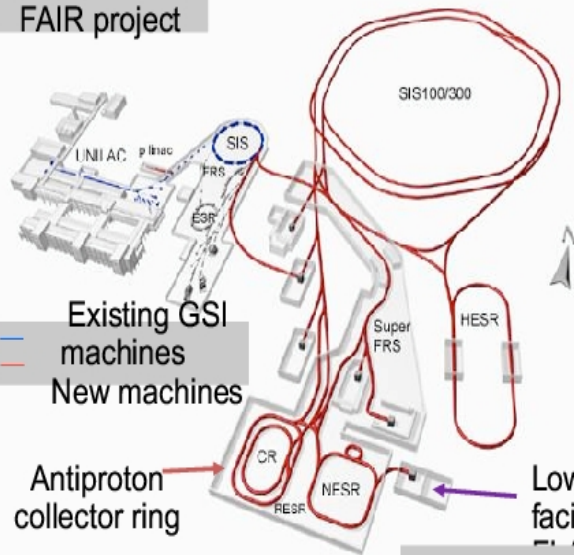
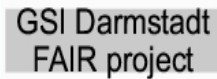


Thomas Jefferson National Accelerator Facility



W03: Heidelberg CSR, A.Wolf MPI-K

Stored antiproton beams at keV energies

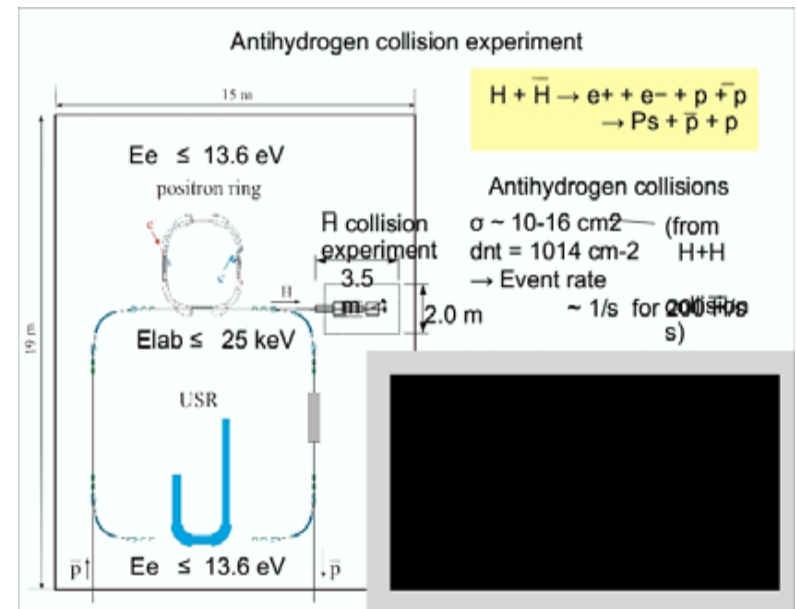


> 2010

Antiproton-
collector ring

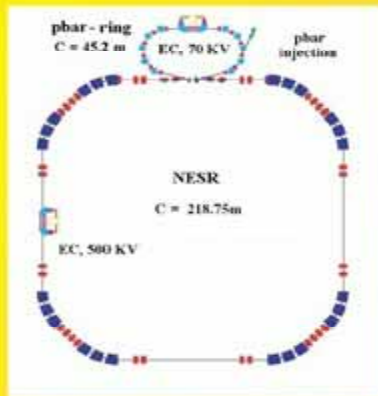
Low energy antiproton facility

30 MeV ... 300 keV: LSR (magnetic)
300 keV ... 20 keV: USR
(electrostatic)



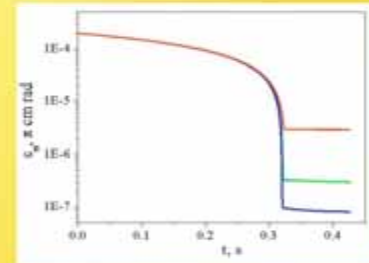
Antiproton - Ion Collider for FAIR Project

P.Beller¹, B.Franzke¹, P.Kienle^{2,4}, R.Kruecken², I.Koop³, V.Parkhomchuk³, Y.Shatunov³, A.Skrinsky³, V.Vostrikov³, E.Widmann⁴
¹GSI, Darmstadt, Germany; ²TUM, Munich, Germany; ³BINP, Novosibirsk, Russia; ⁴SMI, Vienna, Austria.

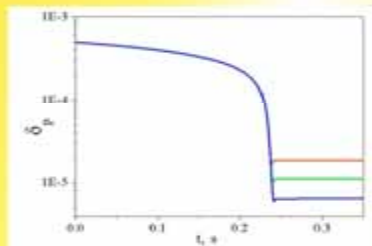
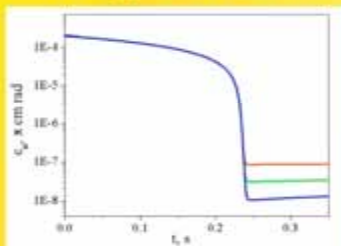


An antiproton-ion collider (AIC) is proposed to independently determine rms radii for protons and neutrons in stable and short lived nuclei by means of antiproton absorption at medium energies. The experiment makes use of the electron ion collider complex with appropriate modifications of the electron ring to store, cool and collide antiprotons of 30 MeV energy with 740A MeV ions in the NESR. Antiprotons are collected, cooled and slowed to 30 MeV. Hereafter the antiprotons are transferred to the electron storage ring using a new transfer line. Radioactive nuclei are produced by projectile fragmentation and projectile fission of 1.5A GeV primary beams and separated in the Super FRS. The separated beams are transferred to the collector ring (CR) and cooled at 740A MeV and transported via the RESR to NESR, in which especially short lived nuclei are accumulated continuously to increase the luminosity.

Pbar cooling in AIC, $N = 10^{10}, 10^9, 10^8$
 from top to bottom, $E = 30$ MeV



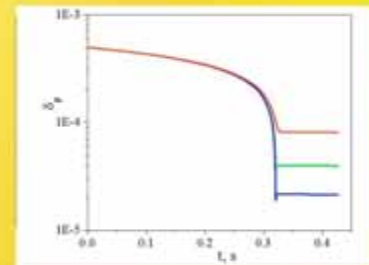
¹³²Sn⁵⁰⁺ ion beam cooling in NESR, $N = 10^7, 10^6, 10^5$
 Energy is 740 MeV/u



Main parameters of EC for AIC

Maximum electron energy	70 KeV
Maximum electron current	2 A
Electron beam diameter	5 - 20 mm
Magnet field in cooling section	0.2 T
Length of cooling section	3.5 m

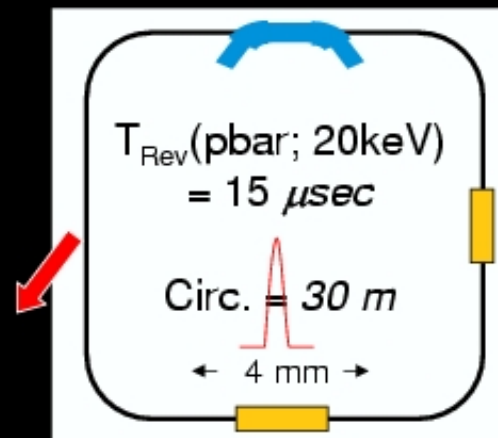
Design Luminosity $L = 10^{23} \text{ s}^{-1} \text{ cm}^{-2}$



USR - Main Goals



- Variable down to very low energies
 - 300 keV ~ 20 keV
- High luminosity for in-ring experiments
- Well defined extracted beams:
 - small emittance
 - small momentum spread
- Multi-User operation:
 - 2 straight lines for in-ring experiments
 - 1 extraction port
 - additional beam lines possible
- Central requirements
 - $\Delta t \sim 500$ nsec for injection into trap
 - $\Delta t \sim 2$ nsec / 10^4 ions for collision experiments



T04 Cooling at HESR, H.Stockhorst - FZJ/IKP

Cooling Scenario for the HESR

H. Stockhorst
Forschungszentrum Jülich GmbH
COOL 05, Eagle Ridge, Galena, IL USA
September 18th to 23rd, 2005

- HESR Layout
- Electron Cooling at Momenta $p \approx 8.9 \text{ GeV/c}$ for the High Resolution Mode
- Small Angle and Energy Scattering
- Stochastic Cooling with Internal Target for $p \approx 3.9 \text{ GeV/c}$ in the High Luminosity Mode

12.09.2005

H. Stockhorst



Longitudinal Stochastic Cooling Performance for Different Momenta in the HL mode

Transverse and Longitudinal Cooling

Including IBS+Target

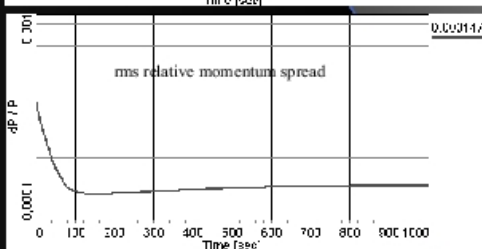
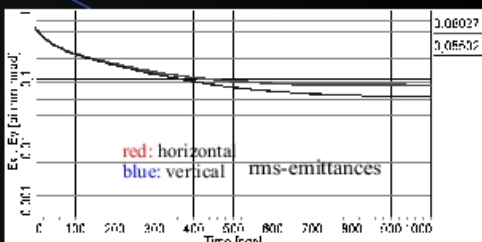
$p = 3.9 \text{ GeV/c}$

$$L = 2 \times 10^{32} \text{ cm}^{-2} \text{ s}^{-1}$$

$$N = 10^{11}$$

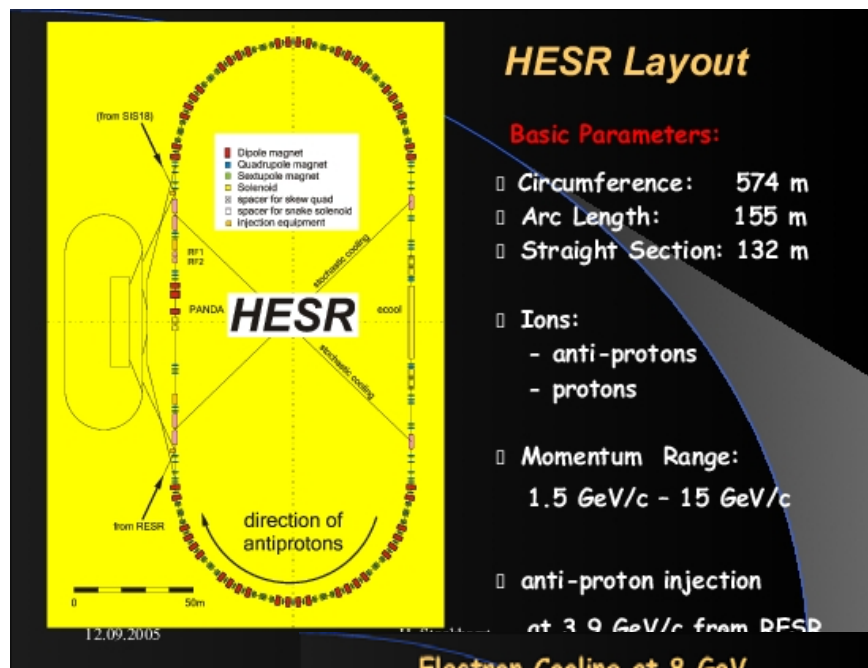
$$N_T = 4 \times 10^{15} \text{ atoms/cm}^2$$

12.09.2005



H. Stockhorst

18



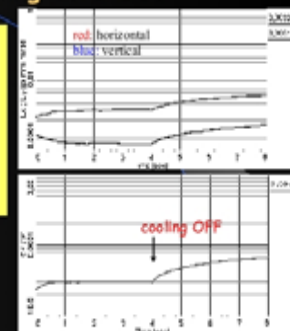
HESR Layout

Basic Parameters:

- Circumference: 574 m
- Arc Length: 155 m
- Straight Section: 132 m
- Ions:
 - anti-protons
 - protons
- Momentum Range: 1.5 GeV/c - 15 GeV/c
- anti-proton injection at 3.9 GeV/c from DESY

Electron Cooling at 8 GeV

Number of antiprotons:	10^{11}	
Initial rms emittance (H):	0.000843	mm mrad
Initial rms emittance (V):	0.000234	mm mrad
Initial rms relative momentum spread:	2.28×10^{-4}	
Rms-beam radius at cooler (H):	0.3	mm
Rms-beam radius at cooler (V):	0.2	mm
Revolution frequency:	119.40	kHz
Kinematic beta:	0.994	
Kinematic gamma:	19.526	
Frequency dip factor:	0.015	
Luminosity:	$2 \times 10^{31} \text{ cm}^{-2} \text{ s}^{-1}$	



- Electron cooling and target ON
- Equilibrium dominated by IBS
- rms-momentum spread with target and IBS: 3.0×10^{-5}

12.09.2005

H. Stockhorst

8



Thomas Jefferson National Accelerator Facility



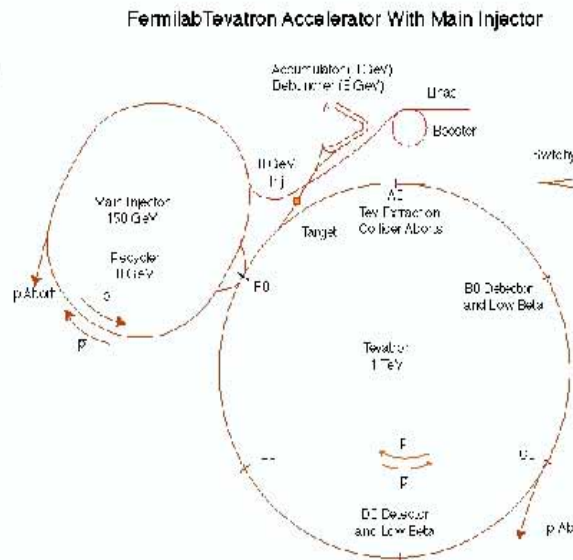
M07 antiproton cooling at FNAL

S.Nagaitsev, FNAL



Antiproton Production

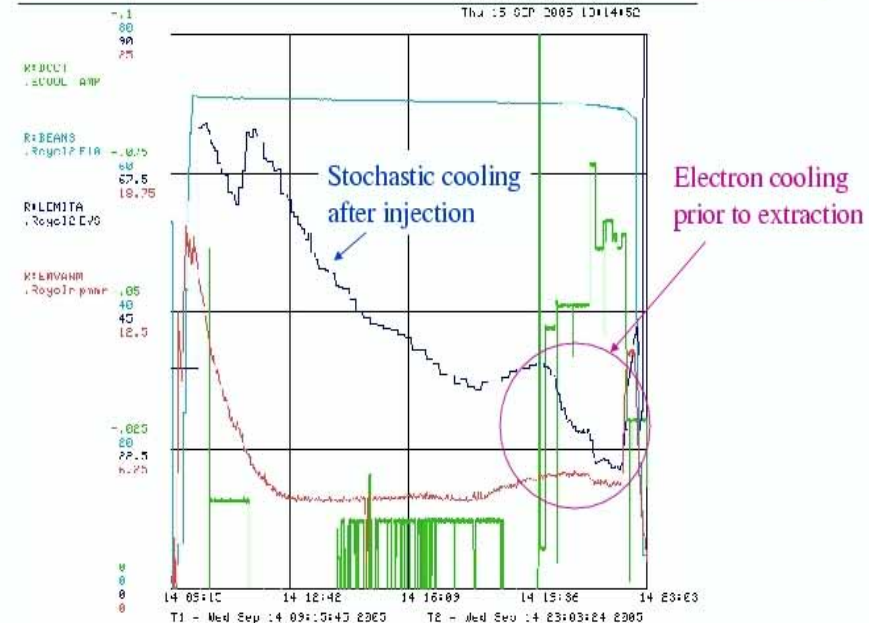
- 1×10^8 8-GeV pbars are collected every 2-4 seconds by striking 7×10^{12} 120-GeV protons on a Nickel target
- 8 GeV Pbars are focused with a lithium lens operating at a gradient of 760 Tesla/meter
- 30,000 pulses of 8 GeV Pbars are collected, stored and cooled in the Debuncher, Accumulator and Recycler Rings
 - The stochastic stacking and cooling increases the 6-D phase space density by a factor of 600×10^6
- 8 GeV Pbars are accelerated to 150 GeV in the Main Injector and to 980 GeV in the TEVATRON



Antiproton Cooling in the Fermilab Recycler Ring - Nagaitsev



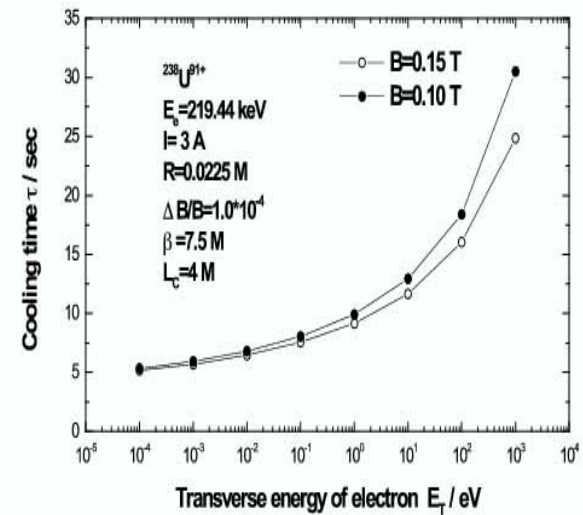
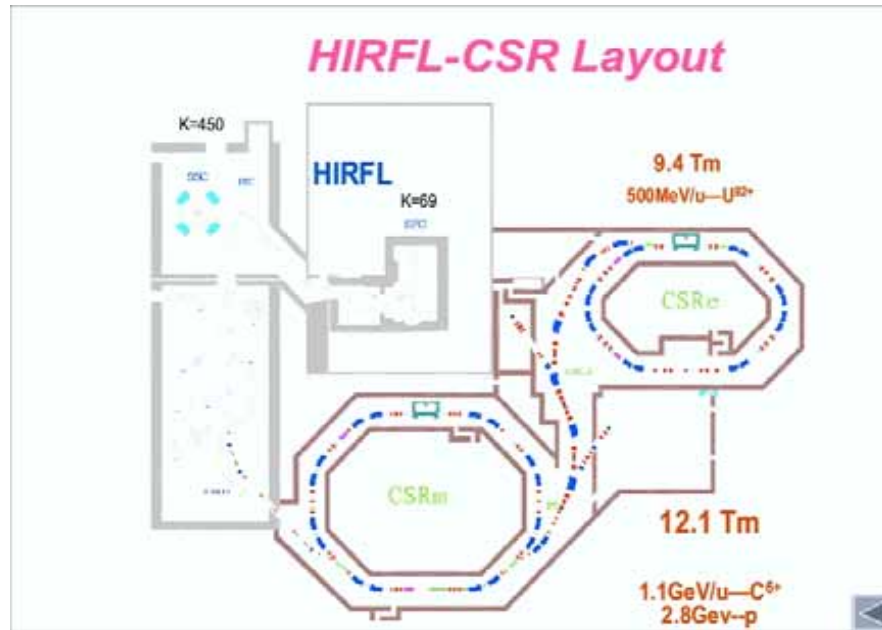
Electron cooling in operation



Antiproton Cooling in the Fermilab Recycler Ring - Nagaitsev

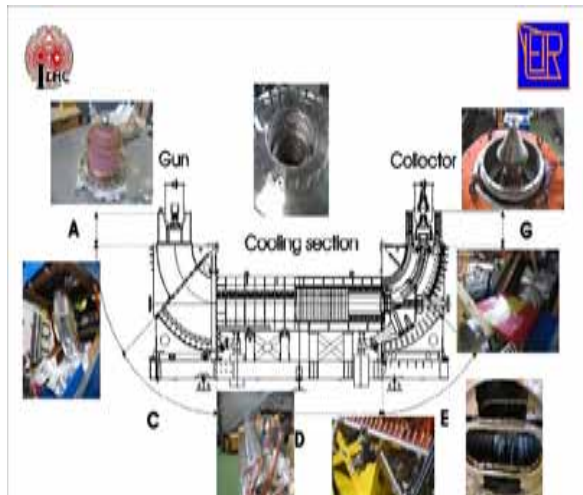


R03 HIRFL-CSR X.Yang IMP



Cooling time as a function of transverse energy of electron

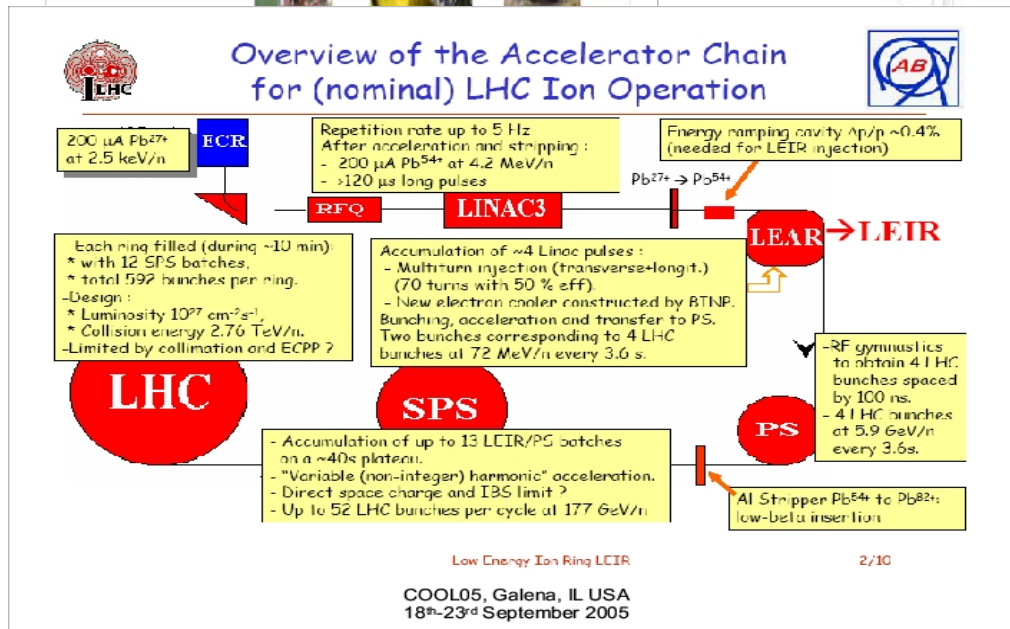
R02 LEIR cooler status G.Tranquille CERN



The Ions for LHC project

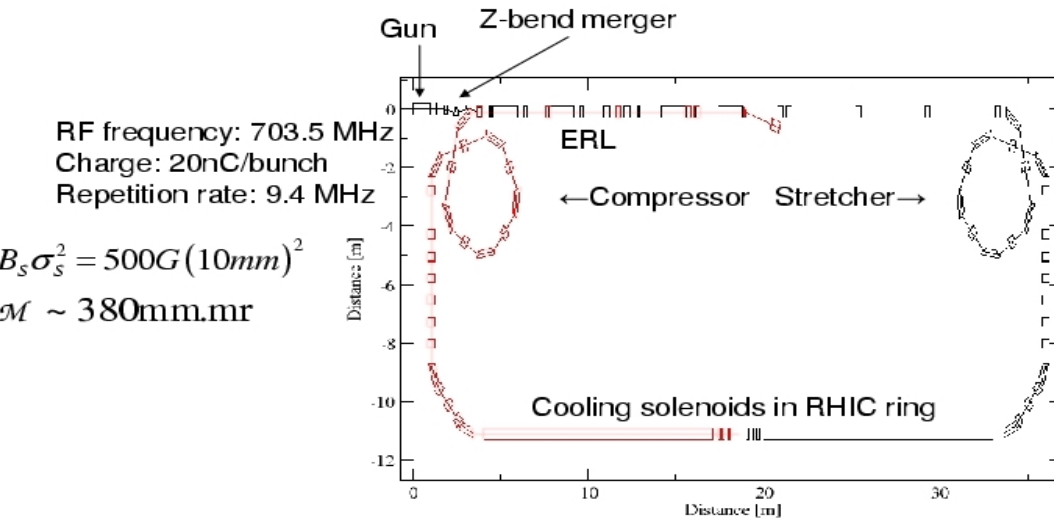


- LHC needs $L = 10^{27} \text{ cm}^{-2}\text{s}^{-1}$ at 2.7 TeV/n
- 592 bunches, $7 \cdot 10^7$ ions/bunch, $\epsilon = 1.5 \text{ } \mu\text{m}$, $\beta^* = 0.5\text{m}$
- Implies $9 \cdot 10^8$ ions with $\epsilon = 0.7 \text{ } \mu\text{m}$ every 3.6s in LEIR
- First run, early scheme, $L = 5 \cdot 10^{25} \text{ cm}^{-2}\text{s}^{-1}$ (60 bunches, $7 \cdot 10^7$ ions/bunch, $\beta^* = 1$) $\Rightarrow 2.25 \cdot 10^8$ ions in LEIR.



COOL05, Galena, IL USA
18th-23rd September 2005

Lattice for magnetized beam



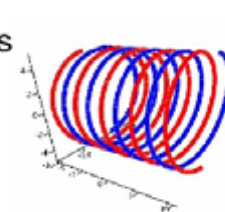
The use of a helical undulator

- Large coherent velocity can be achieved to reduce recombination.
- Small circle radius can be made with low field
- Undulator provides focusing of the electron beam

$$\theta = \frac{K}{\gamma} \approx \frac{93.4B\lambda}{\gamma}$$

$$r_0 = \frac{\theta\lambda}{2\pi} \quad L = \ln \frac{\rho_{max}}{r_0}$$

Take $\lambda=5cm$, $B=20$ Gauss, $R=5$ cm, $I=72$ Amp
Then $r_0=0.7 \mu m$, $\beta_w=180$ m

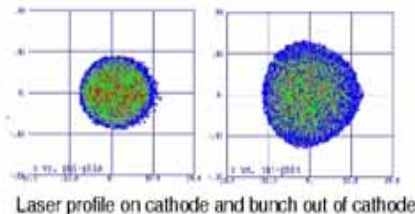


25 hours
recombination
Lifetime:
More than enough



Non-magnetized beam

- The combined use of ellipsoid bunch, high electric field and no magnetization results a good emittance



Charge/bunch (nC)	Maximum radius (mm)	rms radius (mm)
2.5	4	1.77
3.2	4	1.77
5	6	2.65

Bunch length: 16degrees (63ps) from head to tail.
Lunch phase: about 35deg.
Maximum field on axis: 30MV/m
Energy out of gun 4.7 MeV



<http://conferences.fnal.gov/cool05/Presentations/>



Thomas Jefferson National Accelerator Facility

